STRUCTURE/PROPERTY RELATIONSHIPS IN METHACRYLATE/DIMETHACRYLATE POLYMERS FOR DENTAL APPLICATIONS

By

JEREMY JOHN MEHLEM

A DISSERTATION PRESENTED TO THE GRADUATE SCHOOL
OF THE UNIVERSITY OF FLORIDA IN PARTIAL FULFILLMENT
OF THE REQUIREMENTS FOR THE DEGREE OF
DOCTOR OF PHILOSOPHY

UNIVERSITY OF FLORIDA

2001

[This dissertation is dedicated to all of those who gave their love and support during the writing of the dissertation, especially my wife Kacy.]

ACKNOWLEDGMENTS

I would like to thank my advisor and doctoral committee, Dr. Anthony Brennan, without whose enthusiasm, knowledge, and guidance none of this would be possible. I would also like to thank the members of the supervisory committee for their valuable input: Dr. Elliot Douglas, Dr. Christopher Batich, Dr. Ronald Baney, and Dr. Kenneth Wagener.

I cannot thank enough all of my colleagues who gave the support and collaboration necessary to make it through this onerous process: Mark Schwarz, Jennifer Russo, Jeanne Macdonald, Dr. Luxsamee Plangsangmas, Xiaomei Qian, Derek Lincoln, Arthur Gavrin, Jamie Rhodes, Lee Zhao, Dr. Brent Gila, Dr. Drew Amery, Bob Hadba, Dr. Chris Widenhouse, Dr. Rodrigo Orifice, Dr. James Marrotta, and Paul Martin. I would also like to thank the next generation of colleagues for bringing new ideas and perspectives to our discussions: Clayton Bohn, Adam Feinberg, Wade Wilkerson, Nikhil Kothurkar, Amy Gibson, Charles Seegert, Leslie Wilson, Brian Hatcher, Brendan Hauser, Bryan Cuevas, Josh Stopek, and all the other students, faculty, and staff that made my experience at the University of Florida memorable.

I cannot express enough gratitude to Dr. Jesse Arnold, Dr. Tom Miller and Dr. Mike Zamora for their guidance early in my career as a graduate student and their continued advice as I go into the workplace.

Special thanks goes out to Ms. Tonya Brevaldi for her help with NMR spectroscopy and Mrs. Jeanne Macdonald for her help with DSC measurements. I would

also like to thank Dr. C. Russell Bowers and his graduate student, Tony Zook, for all of their help making ^{129}xenon NMR measurements. I could not have completed the work without their collaboration.

I would be remiss not to recognize the aid that the program assistants provide. I would also like to thank Dr. Peter Ifju for his help in making modulus measurement on our standards and his impromptu mentoring at our board meetings.

I must acknowledge the Center for the Development of Alternatives to Dental Amalgam at the University of Florida, especially Mr. Ben Lee in the dental biomaterials laboratory and the NIH-NIDR (grant no. 2-P50-DE 09307) for funding my research and allowing me the opportunity to attend and present my work at national conferences.
I would like to thank my parents and family for supporting my continued education.
Last, but not least, I would like to thank my wife, Kacy, for her love and support through the last years of my education.

TABLE OF CONTENTS

page

LIST OF TABLES

LIST OF FIGURES

Abstract of Dissertation Presented to the Graduate School
of the University of Florida in Partial Fulfillment of the
Requirements for the Degree of Doctor of Philosophy

STRUCTURE/PROPERTY RELATIONSHIPS IN METHACRYLATE/DIMETHACRYLATE POLYMERS FOR DENTAL APPLICATIONS

By

Jeremy John Mehlem

May, 2001

Chair: Anthony B. Brennan
Major Department: Materials Science and Engineering

Since its invention Bis-GMA or one of its analogs has been the main component of the polymer portion of composites for dental restorations. The need for dilution of Bis-GMA and its analogs to optimize its properties has long been recognized. Bis-GMA is a highly viscous monomer. This high viscosity leads to early vitrification, which limits conversion during cure. This viscosity also limits filler loading. Vitrification at low conversions leads to heterogeneous systems composed of low and high cross-link density phases. The low cross-link density phases behave as defects in the system; therefore, if the amount of low cross-link density phases in the system can be reduced and a more uniform network structure can be achieved, then the mechanical properties of the resin can be improved. Since the increase in viscosity during cure causes vitrification, it is logical that a system with a low initial viscosity will delay the onset of vitrification. Reactive diluents such as triethylene glycol dimethacrylate (TEGDMA) are effective at

lower levels. However, large amounts negatively affect matrix properties by increasing polymerization shrinkage and water sorption. Shrinkage has been cited as one of the main deficiencies in dental composites. The goal of this project is to improve upon standard viscosity modifying comonomers such as triethylene glycol dimethacrylate. The comonomers that were explored were phenyloxyethyl methacrylate, cyclohexyl methacrylate, and tert-butylcylcohexyl methacrylate. Multicomponent systems based on analogs of ethylene glycol dimethacrylates with different length ethyl glycol chains were also examined. The substitution of monomethacrylates for TEGDMA as a comonomer resulted in enhanced or negligible affects on the mechanical properties of Bis-MEPP based polymer systems while reducing polymerization shrinkage.

^{129}Xenon NMR and TappingMode™ AFM were used to characterize the heterogeneity of dimethacrylates systems during their cure cycle as well as in their final state. Using these methods the size of the high and low cross-link density phase was examined and determined to be on the order of 50-150 nanometers.

Model compounds based on phenylethyl methacrylate were formulated to determine how of nadic methyl anhydride and maleic anhydride incorporate into dimethacrylate resin systems.

CHAPTER 1
INTRODUCTION

Since the discovery of the toxicity of mercury vapor, even in small amounts, there has been a large push in the dental industry for alternatives to dental amalgam materials. This need led to the introduction of polymer-based composites as restorative dental materials. Most polymer-based composites are composed of dimethacrylate polymers and inorganic fillers. Polymer-based composites have many redeeming qualities such as ease of use, high aesthetic appeal, and, of course, a less toxic alternative to mercury-based amalgams. Polymer-based composites are not without their drawbacks. The shrinkage that occurs upon polymerization is still cited as one of the major reasons for the failure of dental composites in the oral environment. This shrinkage results in stresses that cause defects with the composite matrix and debonding from the tooth restoration interface, resulting in poor marginal adaptation, marginal leakage, and subsequent recurrent decay. Most modern restorative materials are visible light-cured composites based on high molar mass monomers such as 2,2'-bis(4-(2-hydroxy-3-methacryloyloxyprop-1-oxy) phenyl)propane (Bis-GMA), in reference to its precursor materials bis-phenol A and glycidyl methacrylate, 2,2-bis-(4-methacryloylethoxyphenyl) propane (Bis-MEPP), sometimes referred to as ethoxylated Bis-GMA, and urethane dimethacrylates. The need for dilution of Bis-GMA and its analogs to optimize its properties has long been recognized. Bis-GMA is a highly viscous monomer (2980 Pa•s [1]), which leads to early vitrification, limited conversion during cure, and limited filler loading. Vitrification is defined as the point where the glass transition temperature of the reacting system reaches

the reaction temperature. Polymerization becomes diffusion limited at the vitrification point. Vitrification at low conversions leads to heterogeneous systems composed of low molar mass phases and highly cross-linked phases. The lower molar mass or low cross-link density phases behave as defects in the system. The mechanical properties of the polymer can be improved, if the volume fraction of the low molar mass or the low cross-link density material of the system can be reduced. IF the increase in viscosity during cure causes vitrification, it is logical that a system with a low initial viscosity will delay the onset of vitrification. This hypothesis is supported by the relationship between initial viscosity and degree of conversion[2-4]. Reactive diluents such as triethylene glycol dimethacrylate (TEGDMA) are effective at lower levels, but large amounts negatively affect matrix properties by increasing polymerization shrinkage and water sorption. The polymerization shrinkage of poly (TEGDMA) is 11.9 % and it water uptake is 6.0 weight percent. The polymerization shrinkage and water uptake of poly (Bis-GMA) are 6.4 % and 3.05 weight percent, respectively[5]. Excessive polymerization shrinkage results in tensile stresses in matrix materials adjacent to the glass filler. These stresses lower mechanical properties, i.e., modulus, stress at break. However, the lower viscosity achieved with the addition of reactive diluents also allows higher glass loadings, which improves mechanical properties and reduces the shrinkage in the overall system.

From this point in this work the term "light-cured" will be used to refer to light-initiated polymerization of the vinyl bonds. In light-cured systems the polymerization is initiated by radicals that are formed upon exposure to light and subsequently react with the vinyl bonds. The first light-cured systems were based on compounds that were activated in the UV region. More modern systems use compounds that are activated in

the blue region. The actual polymerization process is similar to a chemically initiated polymerization except for one very important aspect, i.e, light-cured systems do not require mixing, which is very significant clinically.

To date the three primary approaches for reducing polymerization shrinkage have been ring opening polymerizations, swellable clays, and monomers with higher specific volumes. All of these methods have their drawbacks [6-8].

Many dimethacrylates form heterogeneous structures that are characterized by areas of highly cross-linked polymer, which surround or contain areas of low cross-link density. This is a result of the evolution of structure during cure. Kinetic gelation modeling indicates that this heterogeneity has its roots early in the polymerization process and manifests itself in the form of isolated branched molecules with large numbers of pendant double bonds [9]. Modeling based on percolation theory also predicts the formation of these molecules [10]. These molecules, sometimes referred to as microgels, have been isolated and detected with dynamic light scattering [11]. Polymerization continues preferentially within and around these microgels. These molecules ultimately grow together resulting in the trapping of radicals and unreacted material. As a polymer network forms, the onset of vitrification limits monomer diffusion, the mobility of pendant groups, and the degree of conversion. The pendant groups and monomers act as defects. These structures along with the limited amount of active chains in the network restrict the mechanical and physical properties of these materials.

The goal of this work is to examine viscosity modifying comonomer systems based on monomethacrylates, or multicomponent analogs of ethylene glycol

dimethacrylate that will reduce the polymerization shrinkage and improve or negligibly affect mechanical properties of Bis-MEPP based polymers when compared to the standard comonomer TEGDMA. The specific aims of this work are as follows: Aim 1: To test the hypothesis that monofunctional methacrylates with a cyclic or aromatic pendent group can reduce polymerization shrinkage while improving or negligibly affecting mechanical properties. Aim 2: To test the hypothesis that heterogeneity can be reduced in polymers designed with the same glass transition temperature by having a lower viscosity monomer system. Aim 3: To test the hypothesis that multicomponent diluent systems based on analogs of triethylene glycol dimethacrylate with a range of molar masses can lower viscosity more effectively than triethylene glycol dimethacrylate. The multicomponent system will maintain the same weight average molar mass as triethylene glycol dimethacrylate. Aim 4: To test the hypothesis that norbornene monomers that react to form high glass transition temperature polymers can be incorporated into dental polymers. Aim 5: To test the hypothesis that ^{129}xenon NMR and TappingMode™ Atomic Force Microscopy with phase mapping can be used to characterize the size and distribution of heterogeneity in dimethacrylate polymers and how it changes with conversion.

CHAPTER 2
BACKGROUND

History of Dental Restorative Materials

The direct placement of filling material is a common dental procedure. Polymer-ceramic composite restorations are a favorite with patients for aesthetic reasons as well as ease of handling [12]. The shortcomings of the original polymer-based restorations have driven the evolution of dental materials to their current state.

The first polymer-based fillings were acrylates [13]. They were used from about 1945 until 1960, but were discarded because of their inadequate mechanical properties, large dimensional changes with temperature, large volumetric shrinkage during curing, and low stain resistance.

In 1962 Bowen developed the first Bis-GMA- based composite system (Figure 2.1). His work resulted in a molecule with the strong mechanical properties and low shrinkage of epoxies. The molecule also maintained the fast reaction capability of methacrylates [14]. Much of the research since then has evolved around modifications to this basic structure. Polymerization in these systems was initiated by a benzoyl peroxide/tertiary amine combination. Unfortunately, this initiator system's effectiveness was inhibited by the presence of water. Light-cured systems solved this problem as well as allowing dentists to work with materials that have not already begun to cure [12]. In addition, the chance of incorporating air into the composite system by mixing is eliminated. This reduces the number of voids in the restoration [15]. In general, light-

cured systems cure faster than chemically cured systems [16]. The physical and mechanical properties of light-cured systems are better than self-cured [16]. The control of setting time and color matching are easier compared to self-cured composites [17]. The ultraviolet light systems used initially were discarded for visible-light systems. Visible light has better depth of cure than UV as well as the ability to penetrate a layer of enamel, which UV light does not [16].

Components of Dental Composites

Dental composites consist of three essential components: a cross-linked polymeric matrix, a high volume fraction of particulate silicate reinforcing phase, and a bonding agent to promote matrix-filler adhesion [5].

Matrix materials are usually based on a combination of dimethacrylates, one acting as the base material such as a urethane dimethacrylate, Bis-GMA, or its ethoxylated version and another acting as reactive diluent to increase the extent cure as well as lower viscosity so higher glass loadings can be achieved. The viscosity of matrix portion of commercial composites is typically1000 to 2000 centipoise (cP) [18]. Taylor et al. have evaluated the role of the particle reinforcement volume fraction for an extensive range of Bis-GMA–type polymer matrices [18]. It was determined that lower viscosity matrices can accept more filler while maintaining workability. Maximum filler loading is dependent on the properties of the filler to a larger extent than matrix viscosity. An average 4.6 weight percent additional reinforcement could be used in 1000 cp solutions compared with 2000 cp solutions. The plasticity of the different matrices formulated to the same viscosity and then loaded with the same amount of filler varied depending on the chemical structure. The differences were more pronounced at lower

filler loadings were plasticity varied as much as 100percent. The authors refrain from hypothesizing about this phenomenon; one could speculate that the interaction between different chemical functionalities of the matrix materials and the filler may be one possible factor. Reactive diluents such as triethylene glycol dimethacrylate (TEGDMA) are effective at lower levels, but large amounts negatively affect matrix properties by increasing polymerization shrinkage and water absorption [19]. The polymerization shrinkage of poly (TEGDMA) is 11.9 percent and it water uptake is 6.0 weight percent. The polymerization shrinkage and water uptake of poly (Bis-GMA) are 6.4 percent and 3.05 weight percent, respectively[5].

Filler particles act as the reinforcing phase of the composite as well as reducing the overall shrinkage of the system upon polymerization. As long as bonding between the filler and the matrix and the quantity of the matrix is sufficient to fill the spaces between the filler particles, increased filler content tends to improve mechanical properties [5]. Filler particles are usually based on silicates such as zirconium glass, yiterbium trifluouride, quartz and bariumborosilicate. The filler materials have been developed for stability in the oral environment, aesthetics, and radiopacity. The average diameter of the filler particles in traditional composites is about 8 to 30μm, while modern composites' average particle size is in the range of 0.7 to 3.6μm [20]. Colloidal silica as small as 0.04μm has also been used as filler. Due to the silica's large surface area, i.e., 300 to 600 m^2/g, small filler particles increase the viscosity of the composite system they are added to, which limits the total volume fraction that can be added [21]. Willems et al. showed that the amount of filler in commercial materials ranged from 48.2 to 58.1 volume percent [22].

The mechanical strength of the composite is significantly enhanced by the use of a coupling agent applied to the filler. A coupling agent must chemically bond to the reinforcement phase and it must promote wetting by the matrix. However, the long term stability of the composite is strongly dependent upon hydrolytic stability of the interfacial bonds between the reinforcement phase, coupling agent, and matrix polymer [14]. A coupling agent should also be capable of forming covalent bonds with both the matrix and the filler. A typical coupling agent is γ-methacryloyloxypropyltrimethoxysilane (MPS). The silane end is capable of bonding with the filler particle and the methacrylate end is capable of forming bonds with the network polymer.

Areas for Improvement

Current composite filling materials have also been used for the restoration of posterior teeth, but they have not been as successful in this application as for the anterior teeth [5]. The main areas for improvement in composite restorations are the following: (1) polymerization shrinkage, which results in poor marginal adaptation, internal stresses and stress on the tooth; (2) water sorption, which has undesirable effects on dimensional and mechanical properties as well as on fillers and filler matrix bonding; (3) thermal conductivity and mismatch of CTE with tooth; (4) mechanical properties such as flexure and tensile strength as well as modulus; (5) abrasion resistance; (6) adhesion of matrix to filler particle as well as matrix to tooth structure and filler to teeth; and (7) radiopacity of filler material [5, 21, 23].

Network Structure

It seems that dimethacrylate networks are not uniformly cross-linked. Instead they resemble the porridge microstructure first attributed by Houwink to Bakelite [5]. More

scientifically stated, dimethacrylates are a heterogeneous structure that is characterized by areas of highly cross-linked polymer, which surround or contain areas of low cross-link density. This is a result of the evolution of structure during cure. Kinetic gelation and 2-D percolation modeling indicates that this heterogeneity has its roots early in the polymerization process and manifests in the form of isolated branched molecules with large numbers of pendant double bonds [9, 10]. Polymerization continues preferentially within and around these molecules. These molecules ultimately grow together to form the network structure. As a polymer network forms, the onset of vitrification limits monomer diffusion, the mobility of pendant groups, and the degree of conversion. The vitrification results in areas of low cross-link density that act as defects. These structures along with the limited amount of active chains in the network restrict the mechanical and physical properties of these materials.

The heterogeneity of dimethacrylate polymers has been demonstrated experimentally using such techniques as dielectric spectroscopy [24, 25], dynamic mechanical spectroscopy [26-28], extraction and swelling experiments [29-31], photochromic [32], charge-recombination luminescence [33], paramagnetic probes [34], CP/MAS NMR ^{13}C spectroscopy [9, 35] and electron microscopy [36]. There is still a need for further characterization of the heterogeneity in dimethacrylates, especially the size and distribution of the low and high cross-link density regions.

Chiu and Lee have isolated prepolymer molecules in ethylene glycol dimethacrylate systems [11]. The molecules isolated early in the polymerization had a bimodal molar mass distribution (0.4% conversion), i.e., 12 to 18 nm and 35 to 51 nm, which was measured by dynamic small angle light scattering (SALS). The number of

small particles was 3.55 greater than the larger particles, whose structure is comprised of clusters of the small particles. Further along in the polymerization the ratio of small particles to the larger particles decreased to 2.12, while the average particle size of both only increased slightly. At gelation (14.2% conversion), the particle size increased considerably. The sizes ranged from 17 to 25 nm and 71 to 173 nm for the small and large particles, respectively. The isolated particles had vinyl bond conversions ranging from 60-70 percent as by FTIR spectroscopy indicating that microgel particles are formed.

Lange et al. [33] have extended the work on micro-gelled particles using charge-recombination luminescence to identify vitrification. Samples cured above the polymer's Tg dropped to a baseline value of 2,000 counts during cure and never increased. Samples cured at temperatures below the polymer's Tg showed charge-recombination intensities (20,000 counts) indicating vitrification from the onset of cure and never dropped to the baseline values seen in the sample cured above its Tg. An epoxy recombination luminescence spectrum was provided for the comparison of condensation polymers with chain growth polymers. The initial portion of an epoxy spectrum mirrored the behavior of the dimethacrylate sample cured above its Tg. The intensities increased as vitrification point of epoxy was reached. This study provides evidence for the argument that vitrification is micro-scale as well as a macro-scale phenomena.

One of the problems in examining visible light-cured (VLC) systems is that radicals are trapped in the microstructure. Techniques that add energy to these systems and enhance mobility allow further reactions that can alter the network structure and skew results. Kannurapatti et al. [27] have used "living radical" polymerization based on

iniferters to avoid this problem. The iniferter polymerization proceeds while the system is exposed to light. When the light is shut off the reaction ceases, and the structure is frozen in either by vitrification or gelation. Dielectric measurements made on poly (Bis-GMA/TEGDMA) and poly (EGDMA) [25, 37] reacted with the iniferter system indicate an environment with a larger distribution of mobilities. High frequency relaxations present are attributed to pools of monomers. Similar relaxations were reported in earlier work with triethylene dimethacrylate/methyl acrylate polymers [24].

Similar work concerning the nature of networks formed by dimethacrylates performed by Simon, et al. [9] elucidated the structures of dimethacrylate polymers by cross-polarized proton-enhanced magic angle spinning ^{13}carbon nuclear magnetic resonance (CPPEMAS ^{13}C NMR) in conjunction with normal ^{13}C NMR. The CPPEMAS technique observes unsaturated groups where isotropic motion is constrained, i.e., unreacted chain ends attached to the network structure. The ^{13}C NMR technique observes unconstrained motions, i.e., pools of unreacted monomer. Various results were obtained depending on the length and flexibility of the ethylene glycol chain. Systems based on tertrakis(ethylene glycol) dimethacrylate reacted to form a network composed of only 2 percent pendant double bonds while those based on ethylene glycol dimethacrylate were composed of 18 percent pendant double bonds and unconstrained monomer. The EGDMA systems showed evidence of pools of unreacted monomer. Kinetic gelation models were also used to help interpret the results. In simulations of ethylene glycol dimethacrylate polymerizations, gelation models predicted the formation of small highly branched molecules early in the cure cycle. The model also predicted the growth and eventual coalescence of these molecules resulting in regions of trapped

monomer. The number of particles was shown to increase from the initiation until approximately 5 percent conversion. After 5 percent conversion, the number of particles decreases corresponding with an increase in the average size of the particles. This indicates that coalescence of these particles is the dominant mechanism of polymerization after 5 percent conversion.

The presence of "Globular Formations" was identified using transmission electron microscopy in phenol-formaldehyde resins [36]. The globular formations appeared as light and dark regions in the micrograph. The size of dark phases, regions of higher density, was determined to be 400 to 600 Å. Epoxy, silicone, diallyl phthalate, and phenol-formaldehyde samples were also examined by creating replicates of their fracture surfaces. The surfaces were examined with scanning electron microscopy. All of the samples had globular formations that were on the order of 400 to 900 Å. The globular structures were rare in the silcone resins when compared to the epoxy, diallyl phthalate, and phenol-formaldehyde resins. The identification of the globular phase from the replicates of the fracture surfaces should be taken with caution. It is possible the globular phases, which appear as bumps in the micrographs, may be artifacts of the fracture process.

Bis-GMA Analogs and Modifications

Bis-GMA has frequently been modified using the hydroxyl group located on the side chain of the molecule. Holter et al. have undertaken a systematic approach to modifying Bis-GMA by esterification of the hydroxyl groups with varying molar mass aliphatic and aromatic acids [1]. Viscosity and volumetric shrinkage were shown to decrease with increasing aliphatic chain length. Unfortunately, modulus was also shown

to decrease. The aromatic acids were compared with and without an oxy-spacer group. The mechanical properties were enhanced by the presence of the oxy-spacer, but the viscosity increased. Other studies have shown similar trends in viscosity and cure shrinkage by modifying the hydroxyl group of Bis-GMA with dimethylsiloxy and dimethylisopropylsiloxy side groups [38]. No mechanical properties were reported for these systems. It should be noted when hydroxyl groups are replaced, the system viscosities drop one to two orders of magnitude.

Several works have been published in which the interior propane group of Bis-GMA has been replaced by various chemical species [39, 40]. The central propane group was replaced with a group containing fluorine and phosphorus atoms with benzene rings. Viscosity increased with the stiffness of the central groups. Water uptake decreased in fluorine-containing polymers and increased in phosphorus containing polymers.

Stansbury et al. have extended the work in semi fluorinated monomers by synthesizing a wide variety of fluorinated monomers based on Bis-GMA analogs as well as a series of urethane-linked multifunctional fluorinated oligomers [40]. The presence of fluorine reduced water uptake. The oligomer-based systems have a dry breaking strength equal to the Bis-GMA baseline and a comparatively low water uptake. It is interesting to note that the highly fluorinated monomers and oligomers had poor wetting characteristics of silanated glass filler. The phenomenon is attributed to the relatively low hydrophilicity of the matrix materials. The issues of possible reaction kinetics differences were not addressed.

Shoba et al. have synthesized a series of novel dimethacrylates based on diphenols with one or two cyclic groups as the central structure (Figure 2.2) [4]. The

monomers were designed with a variation of straight and flexed structures. All of the monomers have the same side chains, which contained methacrylate groups with propoxy spacers. The flexed molecules have lower viscosities than the straight molecules. The bicyclic monomers have higher viscosities than single-ringed structures. This is due to the bicyclic rings making the molecule a stiffer straighter structure.

In separate papers Sandner et al. and Kawaguchi et al. have reported on high molar mass analogs of Bis-GMA [38, 41]. Both papers reported a reduction in shrinkage for the higher molar mass polymers. Mechanical properties were variable depending on the number of hydroxyl groups in the structure and segmental mobility. Table 2.2 contains the mechanical properties of various aromatic dimethacrylate polymers.

Chowdhury et al. showed that binary mixtures of urethane-based monomers with three and four methacryl groups have improved compressive and diametral tensile properties and increased modulus as measured by micro-indentation compared to a 60/40 weight percent Bis-GMA/TEGDMA system. Lower amounts of residual monomer were also reported [42].

Mitra has also explored multifunctional methacrylate monomers [43]. Triisocyanato-isocyanurates were used as starting materials in a synthesis that resulted in trifunctional ethylenically unsaturated carbamoyl isocyanurates. Increases in both compressive and diametral tensile properties were reported for composites based on these molecules.

Oligomers have been created based on poly (isopropylidenediphenol) (BPA)[44]. Ethoxylation and methacrylation of the BPA oligomer form these so-called multimethacrylates. The multimethacrylates are compatible with TEGDMA. A system

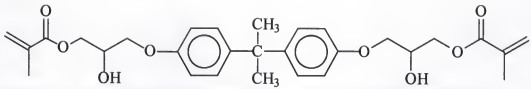

Figure 2.1: The structure of 2,2-bis(4-(2-hydroxy-3-methacryloyloxyprop-1-oxy)phenol)propane (Bis-GMA)

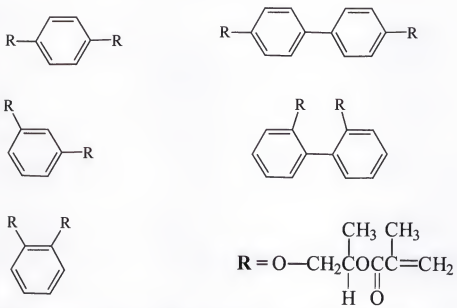

Figure 2.2: Dimethacrylates synthesized from various diphenols

composed purely of multimethacrylates had a polymerization shrinkage of 9.2 percent compared to 10.6 for a Bis-GMA system. The compressive strengths are higher (477.6 MPa) in the multi-methacrylate systems than the Bis-GMA/ TEGDMA systems (375.6 MPa) while the diametral tensile strengths are lower (32.8 MPa) compared to Bis-GMA/TEGDMA systems (26.4 MPa). No data was presented on the viscosity of these monomers.

Monomethacrylates

Some of the earliest work with diluents examined a series of mono, di, and tri functional methacrylate monomers with a range of molar masses. The diluent monomers were incorporated into Bis-GMA-based composites cured with benzoyl peroxide/N, N-dimethyl-p-toluidine [45]. Similar mechanical properties were obtained with mono, di, and trifunctional monomers. Mechanical properties were more affected by the molar mass of the monomers than their functionality. Tensile and compressive strength decreased with the increasing length of the linear pendant group on the methacrylates. Although methyl methacrylate/Bis-GMA systems showed excellent mechanical properties, methyl methacrylate's low molar mass caused excess shrinkage upon polymerization. Estimates or measurement of the glass transition in these polymers might provide more insight into the results seen in this work.

Later work with heterocyclic methacrylates demonstrated that high molar mass monofuctional methacrylates could be incorporated with positive effects on mechanical properties [46-48]. Tetrahydrofurfuryl methacrylate (THFMA)/Bis-GMA mixtures in the volume percent ratio of 5/95, heat cured at 80°C, were reported to have modulus as high as 4.8 GPa derived from flexure testing [46]. Bis-GMA tested in the same manner

was reported to have a modulus of 3.6 GPa. The authors attribute the increase to the smaller diluent molecules occupying free volume spaces within the main polymer network, thus enhancing the molecular interactions in the polymer. The addition of larger amounts of THFMA resulted in lower modulus and flexure strength values varying from approximately 80 to 100 MPa. Unfortunately, the statistical significance of these mechanical properties tests was not presented. Other work on the same systems showed that THFMA did not have significant effects (Newman-Keuls test at $\alpha = 0.01$) on the mechanical properties of Bis-GMA-based polymers when added in portions up to 30 weight percent [47]. The difference is attributed to varying properties of the Bis-GMA monomer due to different isomer compositions. The standard deviation of the strength values was approximately 20 percent and none of the values from the different compositions were significantly different at an α=0.01. These results suggest the need for better testing methods to evaluate the mechanical properties of these materials. Fracture toughness measurements would also provide more insight about the strength of these materials with less noise due to sample preparation. The monomers tetrahydrofurfuryl methacrylate (THFMA), hydroxypropyl methacrylate (HPMA), and isobornyl methacrylate (IBMA) were compared to ethylene glycol dimethacrylate (EGDMA) and triethylene glycol dimethacrylate (TEGDMA) as alternate diluents in heat cured (70°C) Bis-GMA-based polymers. All the monomers reduced polymerization shrinkage and increased mechanical properties in the dry state. Equivalent properties were maintained in the wet state when compared to Bis-MEPP/TEGDMA polymers. HPMA and THFMA were effective viscosity modifiers while IBMA was not. Flexure strength was not reported in this study. It is interesting to note that homopolymers of

IBMA are extremely brittle (10 MPa average flexure strength and 0.71 percent strain to failure) compared to those of THFMA, which had an average flexure strength of 94 MPa and a 6.88 percent strain to failure [49]. Flexure strength values and glass transition temperatures of the cured systems would provide insight into the effects of these monomers on network structure and formation. The mechanical properties and glass transition temperatures of the homopolymers formed from the diluent monomers are also valuable information when interpreting the effects of these monomers. The understanding of the effects of these molecules on Bis-GMA type polymers is in its infancy and further analysis is needed. The incorporation of alternate methacrylate monomers with higher molar mass and variable glass transition temperatures into light-cured systems would add to the understanding of these effects.

Polymerization Shrinkage

Methacrylates exhibit a volume reduction, from 12 to 22 percent [50, 51] or 22.5 ml/mol [52], during polymerization which is associated with two phenomena: (1) the change in intermolecular distances of 3 to 4 angstroms to primary covalent bonds lengths that are 1.5 angstroms [6]; and (2) the increased packing density of polymer chains compared to the packing density of monomer molecules [1]. Many restoration failures are associated with this volume contraction. The problems that result are stresses that are large enough to cause defects within the matrix and debonding at the restoration/tooth interface, which undermines the performance of the restoration [7]. The problem of shrinkage has been addressed in many ways. The addition of inorganic reinforcement phase is commonly used to lower the overall shrinkage in composites by reducing the volume fraction organic materials present [23]. Many different sizes of filler as well as

mixtures of several different sizes, referred to as hybrids, have been used to maximize the amount of filler incorporation.

Liu et al. have developed an ammonia-modified/hydrated mineral montmorillonite (NH3/MMT) filler [6]. The exotherm of cure vaporizes the ammonia, which swells the filler and offsets polymerization shrinkage. This system results in zero shrinkage with small additions of filler (4 weight percent). However, NH3/MMT requires large volumes of polymerizing material to create a sufficient exotherm to drive the expansion reaction (60-80°C), which is more than a sufficient amount of heat to damage tissue. The mechanical properties were not affected drastically due to the small volume fraction of the filler. An SEM examination in the same study revealed no porosity. However, the electron beam degraded the sample rapidly, which makes these results suspect. It was claimed that reduction in volumetric shrinkage was due to the gas that evolved during the reaction and was trapped in the filler particles. There is no study available that addresses the issue of long-term gas release and its effect on the porosity of the polymer. However, one might suspect that the diffusion of the gas from the network could enhance diffusion into the pores by fluids. This presence of the fluid would reduce the integrity of the composite.

Another common approach has been to increase the specific molar mass of the monomers used in the system. Several groups have used this approach with urethane dimethacrylates [41, 42]. The same approach has been used in the synthesis of higher molar mass analogs of Bis-GMA [38, 41]. Culbertson et al. has formulated higher molar mass multi methacrylates based on an oligomer chain of bis-phenol A molecules [44]. Bowen has also developed a molecule based on beta-cyclodextrin [53]. Shobha et al.

created Bis-GMA analogs with bent structures as well as varying degrees of stiffness [4]. The stiffer, straighter structures had the least shrinkage.

In an attempt to control the density of chain packing, several studies have modified the structure of Bis-GMA through the hydroxyl groups [1, 54]. Kalachandra replaced the hydroxyl groups with trimethyl and isopropylsiloxyl groups [54]. The bulky isopropyl group reduced shrinkage to a greater extent. No mechanical testing was done. In a more systematic and in-depth study, Holter esterified the hydroxyl groups with a series of aliphatic and aromatic acids [1]. Polymerization shrinkage and modulus trends are shown in Table 2.1. The aromatic acid-modified Bis-GMA molecule had comparable reductions in shrinkage, but less reduction in modulus. This was especially true where a flexible oxy-spacer group is used. This work indicates that shrinkage may be reduced without drastic losses in mechanical properties using structure-property relationships.

Liquid crystal molecules have also been studied in an attempt to minimize polymerization shrinkage [55]. The ordered nematic structure is denser than a typical monomer solution and the order-to-disorder transition that occurs during curing results in a less dense system. The nematic state also results in lower viscosities; therefore, higher molar mass monomers can be used further increasing the system's potential for offsetting shrinkage. The use of acrylates brings up concerns of toxicity, but future work is planned with methacrylates.

High molar mass analogs of Bis-GMA monomers can only reduce polymerization shrinkage. A monomer that expands upon polymerization is necessary to have a system that expands or has no volume change on polymerization. Stansbury and Byerley et al. were the first to attempt to develop spiro orthocarbonates (SOC) for incorporation into

dental monomers to offset polymerization shrinkage [7, 56]. Spiro orthocarbonates offset shrinkage by a double ring-opening free-radical polymerization mechanism. The first SOCs developed were crystalline and not compatible with monomer systems. Stansbury and Byerley et al. have attempted to rectify these problems in their early work. Byerley et al. has developed a series of stereoisomeric alicyclic spiro orthocarbonates, which expand between 3.9 and 3.5 percent upon polymerization. Low molar mass polymers were produced by a light-initiated cationic polymerization of the experimental monomers. All of these monomers, none of which were tested in dental monomers, are crystalline at room temperature, which would most likely decrease their solubility in dental monomer systems. Stansbury has taken the concept of SOCs and synthesized monomers with unsaturated functional groups that should allow the incorporation of the monomers with free radical-type systems. The systems were cured using photo, chemical, and dual cure mechanisms. Diametral tensile strength (DTS) values of

Table 2.1: Volumetric shrinkage values and modulus values for Bis-GMA molecules esterified with various-length aliphatic acids. The number next to C represents the number of carbon atoms in the aliphatic chain

Compound	Volumetric shrinkage (%)	Modulus (MPa)
Bis-GMA	4.3	2100
Bis-GMA-C2	4.7	1500
Bis-GMA-C6	5.0	220
Bis-GMA-C11	3.9	-
Bis-GMA-C18	2.6	-

Source: Holter et al. [1]

44.4 ± 2.1, 45.1 ± 4.6, and 50.4 ± 2.8 (MPa) were reported for 100 percent Bis-MEPP, 65/35 weight percent mixture of Bis-MEPP and 1,6 hexanediol dimethacrylate, and 68/32 weight percent mixture of Bis-MEPP and SOC monomers. This result may be misleading because the SOC molecules may be acting as a plasticizer. Some compositions were not stable and underwent polymerization during storage while others did not polymerize fully [7, 56]. There was also a lower offset of polymerization shrinkage than expected, which is attributed to an alternate ring opening polymerization system. Reaction kinetics and volume control under non ideal curing conditions are also limiting factors in these systems.

SOC molecules were incorporated into epoxy resins in later work based on the initial work of Byerley et al. [57, 58]. The use of polyols was explored to catalyze the polymerization. The systems were initiated with onium salt initiators and 2-chlorothioxanthen-9-one (CTX). The addition of SOCs to the composition caused an increase in cure times over the baseline epoxy resins. The fastest cure time reported for a mixture that contained a SOC was 48 minutes. The introduction of polyols reduced the cure times; however, no studies were presented with both polyols and SOCs present. It is possible that the polyols will open the SOC prematurely.

The advent of low toxicity onium light cure initiators has generated renewed interest in epoxy resins for dental applications. Tilbrook et al. have addressed the problems of water uptake in epoxy-polyol mixtures by varying the ratio of epoxy groups to polyol groups. The samples were cured using a camphorquinone/4-octyloxy-phenyl-phenyl iodonium hexafluoroantimonate system. The camphorquinone results in a system that is sensitive in the blue light regime commonly used in dental composites. The

polymerization shrinkage for epoxy systems formulated ranged from 3.8 to 5.4 percent. The water uptake ranged from 5.2 to 7.7 weight percent. Unfortunately the resins with the lowest amounts of shrinkage also had the greatest amount of water uptake. Baseline Bis-GMA/TEGDMA systems had less water uptake and higher shrinkage upon polymerization. The epoxy formulations showed higher biaxial flexure strengths than Bis-GMA/TEGDMA systems and modulus values were also higher for some formulations. All samples were tested in the dry state. The uptake of water will affect the properties of materials. Comparisons of these materials in the wet state should be made before further recommendation is made for implementation of the materials in composite restorations. The heat rise in the epoxy samples during cure might also be an issue. It was also noted that some samples had curing times in excess of 60 seconds. This time would not be acceptable to clinicians. An interpenetrating network of methacrylates and epoxies might take advantage of the favorable properties of both systems.

Mosner et al. have synthesized three series of radical ring opening monomers [59]. The synthesized molecules include SOC molecules with substituted unsaturated groups, as well as bicyclic 2-methylene-1,3,-dioxepane (BMDOE) derivatives, and 1,1-bis-substituted 2 vinylcyclopropanes. IR data showed that the SOC molecules polymerized through the unsaturated group. The ring opening mechanism was not utilized and no offset of shrinkage was seen. The BMDOE molecules synthesized were a mixture of liquid and crystalline monomers. Spectroscopic data indicated that ring opening takes place during polymerization. The crystalline molecules expanded upon polymerization. Some of the volume gain was attributed to the transition from the denser

crystalline state to the amorphous state during polymerization. Dental applications of these molecules are limited by their sensitivity to moisture and acid compounds. The BMDOE molecules react to form aliphatic polyesters that have low glass transition temperatures (27 to 37°C). The vinylcyclopropanes synthesized were able to form cross-linked networks when polymerized in bulk. Depending on the initial morphology, volume change during polymerization varied. The molecules that formed amorphous liquids shrank 3.9 and 7.0 percent, while the crystalline molecules expanded 1.0 percent.

Miyazaki et al. have synthesized methacrylates and acrylates that have SOC groups [60]. Heat curing resulted in a minimum shrinkage of 7.8 percent compared to 9.8 percent for Bis-GMA. Studies still need to be performed with a more suitable initiator system. The heat cure was performed at 120°C, which delays the onset of vitrification and allows higher amounts of conversion. Light initiation systems are used at room temperature. At these lower temperatures vitrification will limit the mobility of molecules and hence the conversion that can be obtained. The mechanical properties of a light-cured system will be significantly different than those of a heat-cured system.

Bowen has synthesized a methacrylated β-cylcoldextrin [53]. It is hoped that by housing monomer in the hydrophobic cavities of these molecules, polymerization shrinkage will be offset. If the monomer contained in the cavity diffuses out during polymerization and becomes an external chain segment, then the additional free volume created might help offset shrinkage. The issues of how the molecules will be placed into the cavity and controlling their diffusion properties have yet to be addressed.

Many approaches have been taken to minimize or offset the shrinkage that occurs upon polymerization. As yet, a non-shrinking system has not been introduced that meets

all the requirements for use in the mouth. Reduction of polymerization shrinkage has been obtained with molecules that have a larger molar mass than Bis-GMA. Ultimately these systems will offset polymerization shrinkage modestly and viscosity will become a limiting factor for large molar mass molecules. Liquid crystalline molecules show promise, but the toxicity of the current molecules and their ability to form a LC phase at lower temperatures are still issues. Ring open molecules must be employed to have zero shrinkage or an expanding system. Unfortunately, these molecules are hampered by slow reaction kinetics, moisture sensitivity, and crystallinity.

Anhydrides in Dental Materials

Numerous studies have evaluated the use of anhydrides as comonomers for both structural and adhesive purposes in dental materials [8, 61-66]; however, none have attempted to capture the ring opening as a mechanism for offsetting or reducing polymerization shrinkage. The anhydride functionality may also allow tailoring of mechanical properties through ionic interaction as well as a viable means to increase bonding to bone tissue.

A series of anhydrides were added as cross-linking agents to polymer composites based on UDMA, HEMA Bis-GMA, and TEGDMA [8]. It was hypothesized that monomers such as maleic anhydride introduced into dental materials containing hydroxy or amide groups would act as cross-linking agents. A cyclic anhydride can react with either of these functionalities and form an ester or amide linkage upon additional heating. This leaves the hydroxy group at the end of the carboxylic acid to react with a second amide or hydroxy functional group and form a di-ester or di-amide linkage. The best

results were found with anhydrides that contained unsaturated groups. It was suggested that the double bond makes it possible for these anhydrides to copolymerize with the other monomers. This seems counterintuitive, as polymerization with the network would lower the mobility of these species and the average functionality of these systems. The anhydride incorporation might also lower the cross-link density of these systems. In the case of maleic anhydride, for example, polymerization of the double bond may reduce the ring strain and hence the reactivity of the anhydride group [67]. Polymers based on UDMA and HEMA had more desirable properties. This is attributed to the greater reactivity of the amide groups with the anhydrides, hence a greater degree of cross-linking. A 20 percent increase in mechanical properties was reported for the combination of maleic anhydride and methacrylamide. There appears to be a synergistic effect between these two monomers. The authors provide no explanation for the observed effect. The results obtained in this work are interesting and suggest that the use of anhydrides as cross-linking agents may have some validity. Later studies done on selected anhydride containing systems from the initial work examined the relationship between wear and the quantity of remaining double bonds [63]. The effect of post cure heating on mechanical properties was also evaluated [62]. In vitro wear decreased with increased conversion of double bonds with the exception of the samples post cured at 37°C and 75°C. There was no difference in the quantity of remaining double bonds between these two samples; however, the wear rate was lower in the sample cured at 75°C. It was suggested that this is the result of cross-links formed by anhydride molecules. Clearly no spectroscopic evidence is provided about whether or not this is the mechanism responsible for the reduction in wear.

The ability of anhydrides to be incorporated into dental polymers was demonstrated with the model compound 2-phenylethyl methacrylate and propoxylated Bis-GMA/TEGDMA [68]. The ability of anhydrides to offset polymerization shrinkage was confirmed by post polymerization volume expansions observed after swelling in water as high as 2.0 percent. The hydrolysis was confirmed by a residual weight gain in dehydrated samples and FTIR observations.

One of the most important dental applications for functionalized monomers is their use as dentin adhesives [65]. Anhydrides are of interest in dentin bonding systems and bone cements because of their reported complexation with calcium cations. The addition of 4-methacryloyloxyethyl trimellitate anhydride (4-META) to standard MMA bone cements has been shown to increase adhesion to bone and hydroxyapatite [65, 66]. Increased bond strengths to dentin and enamel have been shown when 4-META and pyromellitic dimethacrylate (PMDM) were applied as coupling agents prior to bonding with composite polymers [61, 69]. Bond strength from 10.2 to 18.2 MPa were reported when PMDM and 4-META were used in conjunction with ferric oxalate solutions and N(p-tolyl)glycine glycidyl methacrylate (NTG-GMA) or N-phenylglycine glycidyl methacrylate (NPG-GMA) surface active monomers. The bond strengths reported for the composites used with the ferric oxalate ranged from 0.48 to 1.72 MPa. Shear bond strengths of composite to human dentine of 29.7 ± 11.8 MPa have been reported when the sodium salt of NTG-GMA was used as a bonding agent[70]. Maleic anhydride dissolved into standard dental monomers has also been studied as an adhesion promoter for Cr-Co alloys [64]. Unfortunately, initial improvements in the energy of adherence

were lost after storage in water for two months, most likely as a consequence of water adsorption.

Water Absorption

Water in dental materials induces swelling, leaches extractable material out of both the polymer and the filler, plasticizes polymers causing them to lose their mechanical properties, and degrades the bond between fillers and coupling agents. There are many variables that govern the uptake of water, and no one has been able to sort them all out yet. Hydrophilicity is related to the uptake of water. The hydrophilicity of a material seems to be based on how similar the polymer structure is to water. Polar materials are more hydrophilic. Kalachandra et al. have found a linear correlation between water uptake and weight percent oxygen (WPO)[71]. WPO is a more concrete way of defining hydrophilicity in polymers. Interestingly, the trend breaks down when there is a branch in the monomer that sterically hinders the polar sites from the water. Bis-GMA-type monomers also showed less water uptake than expected based on WPO. It was hypothesized that the reduction in water uptake is due to the formation of an intramolecular hydrogen bond between the carbonyl oxygen and the hydrogen of the secondary hydroxyl group. The intramolecular bond reduces water uptake by blocking the hydrophilic groups and acting as an additional cross-link.

The amount of free volume in the sample also has an effect on the amount of water taken up and hence the amount of swelling. Soderholm et al. have shown that polymers do not swell in a 1 to 1 ratio with the volume of water absorbed [72]. The lag in the swelling of the polymer was attributed to microcavities that accumulate water. The structure of the network formed clearly has an effect on water uptake. It has been shown

that there is a relationship between water uptake and degree of cross-linking [73]. As the dimethacrylate feed was increased into a PMMA polymer, so did the uptake of water. Although the cross-link density of the materials increased with dimethacrylate feed the number of pendant groups, trapped unreacted material, and regions of lower cross-link density also increase. This may account for the increase in water uptake. Simon et al. have proposed that solvent uptake occurs preferentially in regions of lower cross-link density [30]. In contrast to this theory, the water uptake of ethylene glycol methacrylate monomer is about 2percent less than its polymer. It might be possible that interaction between the various chemical groups prevents their interaction with water thus, lowering water uptake in the monomer systems. In the polymeric state mobility restrictions might prevent these interactions, therefore chemical groups might be more accessible to water molecules. As discussed earlier such an interaction was attributed to the lower than expected water uptake of Bis-GMA polymers. The physical phenomena underlying these results are difficult to ascertain.

Mechanical Properties

Adequate mechanical properties are necessary for a restoration to function properly. For example, a restoration with low modulus will readily deform elastically under stress. This deformation could result in failure of the tooth around the composite as well as increased leakage [21]. The restoration itself might also fail if it has low modulus or fracture strength. An understanding of the mechanisms that govern mechanical properties of filled and unfilled systems both wet and dry is important so improvements can be made in a systematic fashion rather than randomly.

Kawaguchi et al. have done extensive work relating the basic structure of dimethacrylates to their mechanical properties [41]. Nine aromatic dimethacrylates (Figures 2.3-2.5) were studied and their wet and dry mechanical properties were discussed. All of the monomers were mixed 50/50 by weight percent with triethylene glycol dimethacrylate (TEGDMA). Table 2.2 summarizes the results from the mechanical properties tests. Water sorption data is also included.

Table 2.2: Mechanical properties and water sorption of various unfilled dimethacrylate polymers wet and dry

Monomer Composition		Flexure Strength* (MPa)	Elastic Modulus* (GPa)	Amount of Water ($\mu g/mm^3$)
Bis-GMA/	Dry	149.1±7.3	3.53±0.05	58.9±0.03
TEGDMA	Wet	99.7±4.6	2.15±0.06	
Bis-GMA-F/	Dry	156.7±6.6	3.74±0.09	55.4±0.04
TEGDMA	Wet	119.6±6.6	2.87±0.07	
Bis-GMA-C/	Dry	101.1±2.6	2.51±0.05	62.3±0.02
TEGDMA	Wet	80.3±2.4	1.22±0.04	
Bis-GMA-Eph/	Dry	101.7±3.2	2.64±0.10	35.4±0.10
TEGDMA	Wet	61.4±1.3	1.50±0.05	
Bis-GMA-Ech/	Dry	113.4±3.2	2.85±0.11	40.2±0.04
TEGDMA	Wet	70.2±5.1	1.83±0.08	
Bis-MEPP/	Dry	170.3±7.3	2.96±0.06	20.5±0.04
TEGDMA	Wet	123.8±6.1	2.89±0.07	
Bis-MEEPP/	Dry	96.6±2.4	2.19±0.06	22.5±0.05
TEGDMA	Wet	93.8±1.5	1.31±0.02	
BisMPPP/	Dry	113.1±4.3	2.48±0.04	16.8±0.10
TEGDMA	Wet	107.6±3.4	2.33±0.04	
$BisME_{2.6}PP$/	Dry	120.7±4.6	2.72±0.05	18.2±0.02
TEGDMA	Wet	115.7±2.4	2.57 ±0.08	

*Measured by three-point bend testing on a universal testing machine
Source: Kawaguchi et al. [41]

One of the most obvious trends in this data is the loss of wet mechanical properties in the polymers with hydroxyl groups. The polymers without hydroxyl groups retain mechanical properties after soaking in water. This phenomenon is associated with plasticization by water and is supported by the correlation seen between water uptake and decrease in strength. Bis-GMA-EPh and -ECh are high molar mass analogs of Bis-GMA. Their mechanical properties are lower than those of Bis-GMA. The lower values of the mechanical properties are attributed to higher segmental mobility. It should also be noted that these two compounds are more hydrophobic than Bis-GMA, which resulted in less strength loss under wet conditions. The more hydrophobic nature of the molecules is due to the smaller amount of polar groups per molar mass. This also lowers modulus values. The fluorine-containing Bis-GMA polymers had excellent properties in both wet and dry states. Fluorine groups make the monomer more hydrophobic, which is seen in the lower uptake of water. The Bis-GMA-C monomer absorbed significantly more water than the -EPh and -ECh versions, yet maintained a similar amount of strength. More information is needed about the network structure of these monomers to hypothesize about these results. The non hydroxyl containing monomers all have good retention of strength when tested under wet conditions. Again, the mechanical properties can be related to segmental mobility, in this case, of the aliphatic side chains. The monomers with longer, more flexible side chains have lower mechanical properties. The addition of stiffer molecules does not always improve mechanical properties. TEGDMA, a more flexible and less viscous molecule than Bis-GMA, is added to all of the compositions discussed in this paper. The addition of TEGDMA allows further reaction of the system before the onset of vitrification.

Ferracane has shown that if enough TEGDMA is not present that the consumption of double bonds by polymerization or degree of conversion (DC) can be limited (Table 2.3). The stiffer, more viscous Bis-GMA molecules limit the network formation [3]

^{129}Xenon Nuclear Magnetic Resonance Spectroscopy

Xenon Nuclear Magnetic Resonance spectroscopy (NMR) has become an increasingly popular technique for sampling a wide variety of materials because of the sensitivity of ^{129}xenon's chemical shift to its environment. ^{129}Xenon, referred to as xenon from here forward, environmental sensitivity is due to its polarizable electron cloud. Xenon's relatively small size and chemical inertness also make it attractive as a probe molecule.

Table 2.3: Degree of conversion values for Bis-GMA/TEGDMA polymers systems obtained by Ferracane

Monomer (wt.%)	Catalyst (wt.%)	DC (%)
75/25	0.25 DMPT + 0.75 BPO + 0.01 BHT	60.1±1.9
75/25	0.31 DMPT + 0.75 BPO + 0.01 BHT	60.5±2.0
75/25	0.20 camphoroquinone + 0.75 DMAEM + 0.01 BHT	60.1±2.7
50/50	0.25 DMPT + 0.75 BPO + 0.01 BHT	69.4±1.3
50/50	0.20 camphoroquinone + 0.75 DMAEM + 0.01 BHT	71.5±0.9

Note: BPO = benzoyl peroxide, DMPT = N, N-dimethyl-p-toluidine, DMAPE = 4-N,N,-dimethylaminophenethyl alcohol, BHT = butylated hydroxytoluene (inhibitor), DMAEM = N,N-dimethylaminoethyl metharcrylate. The coefficient of variance for the modulus values is 7 percent. Source: Ferracane [3]

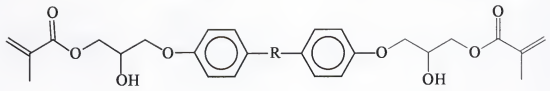

R = C(CF3)2 : Bis_GMA_F

:Bis_GMA_C

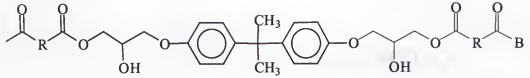

R =

: Bis_GMA_EPh

:Bis_GMA_ECh

B = 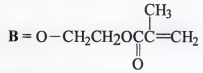

Figure 2.3: Bis-GMA analogs referred to in Table 2.2

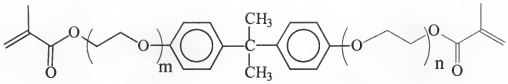

m = n = 1 : Bis_MEPP
m = n = 2 : Bis_MEEPP
m + n >= 2.6 : Bis_$ME_{2.6}$PP

Figure 2.4: Ethoxylated Bis-GMA molecules

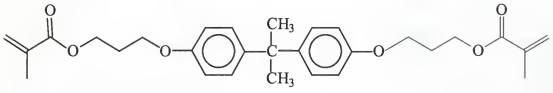

Figure 2.5: 2,2'-bis-(4-methacryloylpropoxyphenyl) propane (Bis-MPPP)

The nature of the chemical shift of xenon molecules has been assessed and the major portion of the shift is due to Van der Waals dispersion and repulsive interactions [74].

Initially xenon was used to examine the porous structure of solid materials such as zeolites, clathrates, and hydrates. The first applications of xenon NMR to polymers examined properties of the amorphous portions of bulk polymers. Sefcik was the first to report a xenon NMR signal in PVC. A broad signal, which is typical of polymers above their glass transition, was observed [75]. Stengle and Williamson later examined poly (ethylene) and poly (ethyl methacrylate) and elucidated that the xenon chemical shift is sensitive to the density of its solvent system, different amorphous environments with the same polymer, and glass transitions [76]. The sensitivity of xenon to the density of its solvent system was demonstrated using a series of N-alkanes. The chemical shift of xenon varied linearly with increasing molar mass of the alkanes. The shift ranged from 160 ppm for hexane to 200 ppm for LDPE. The increase in molar mass correlated with an increase in density. The densities in the systems ranged from 0.65 to 0.87 g/cm^3. The glass transition of poly (ethyl methacrylate) correlated to changes in line width and the chemical shift of the xenon NMR signal. A single peak was observed for LDPE while LLDPE showed a partially resolved doublet. The second peak indicates the presence of two different sub regions within the amorphous phase. Solubility within the crystalline phases of both polymers was assumed to be negligible. This is reasonable when the later work of Kentgens et al. showed that the signal to noise ratio decreased as the amount of crystallinity increased [77].

Kennedy identified 4 phases in EPMD rubber with xenon NMR[78]. The different peaks are associated with regions of different void space. Upon cross-linking

the peak that was furthest upfield, associated with the regions with the most void space, disappeared. The magnitude of the other peaks changed dramatically. This work illustrates the ability of xenon NMR to monitor changes in structure.

The line width of the xenon NMR signals is related to the distribution of absorption sites within a polymer and the frequency at which the xenon samples or exchanges between these sites. The three types of exchange are fast, slow, and intermediate [79]. The fast exchange occurs when the exchange rate of the xenon is rapid compared to the NMR time scale. Intermediate exchange occurs when the exchange time is on the order of the NMR time scale. Slow exchange is observed when the rate of exchange is slow compared to the NMR time scale. The NMR time scale is the time in which the NMR signal is collected. The length of sampling time is often dictated by the T2, spin-spin, relaxation times. Two-dimensional NMR can be used to confirm which type of exchange is taking place. Kentgen et al. performed such experiments with poly (ethylene) and poly (carbonate). The 2D poly (carbonate) spectra is round and almost 2000 Hz wide. The round shape indicates that the xenon NMR is sampling the different absorption sites in a slow exchange regime. Slow exchange is probably the case for most polymers below their glass transition temperature. Polymers such as poly (ethylene) have narrow line-widths on the order of 100 Hz. The narrow width is indicative of fast exchange. The chemical shifts of the different sites average and a narrow peak results. Kentgens et al. [77] tested poly (ethylene) at a range of temperatures and showed a dramatic increase in line width as the temperature of the β-relaxation temperature was approached. This supports the theory that narrow peaks in polymers above their glass transition are due to signal averaging. The mobility of polymer chains above their glass

transition is great. This allows for rapid xenon movement and thus fast exchange. Below their glass transition temperature the motion of polymer chains is curtailed, the diffusion of xenon gas is slowed and no averaging takes place, thus a broad peak is observed.

Xenon NMR has also seen limited use a means to study free volume in polymers. Chu et al. [80] have studied the relaxation of free volume in polymers below their glass transition temperature. The chemical shift of xenon continued to shift for several weeks after the polymer had been cooled below its Tg, indicating the free volume of the polymer continued to change. Morgan et al. have studied free volume distributions in dendritic and cross-linked polymer systems derived from poly (oxypropylene) diols and 2,4-toluene diisocyanate [81]. The xenon chemical shift increased linearly with increasing cross-link density. In variable temperature experiments signal intensity decreased as the cross-linked systems were cooled through their Tg. The decrease in free volume associated with the polymer's glass transition lowers the amount of absorbed xenon. The chemical shift of xenon was examined in dendritic structures in various generations. The chemical shift of xenon decreased linearly when compared to the number of chain ends normalized by the average molar mass of a chain. It is suggested that there is a relationship between generation number of the dendrimer and free volume. It is also noted that free volume measured is an average for each macromolecule and that there may be distribution of free volume within the molecule.

Xenon's most useful application may be as a tool determining miscibility in polymer blends and measuring the size of morphological features in polymers and polymer blends. It has been estimated that Xenon NMR techniques should be able to measure domain sizes from 0.1 to 25 micrometers [79]. Generally, if multiple phases are

present then multiple peaks will be observed in the NMR spectrum. This is due to the sensitivity of xenon to its chemical environment as discussed earlier. In the case of small domain sizes, a single peak can be observed due to rapid exchange between the domains. This problem can be addressed by using variable temperature experiments because the diffusion rate of xenon is temperature dependent [79].

Xenon has been used as a probe molecule in many polymer blends [82-89]. Browstein et al. were the first to study polymer blends using xenon NMR Two signals were observed in poly (styrene) poly (isoprene) blends [89]. The peaks were assigned based on linewidths. It was noted that the resonances were broader than in the pure materials. The broadening was attributed to the exhange of xenon between the two phases.

Walton et al. demonstrated that xenon NMR can be used as a tool to determine phase segregation in blends of poly (chloroprene) PC, poly (isoprene) PIP, and epoxidized poly (isoprene)[84]. Blends of PC/PIP, 50 percent epoxidized poly (isoprene)/PIP and 25 percent epoxidized poly (isoprene)/PIP, all known to be immiscible, showed two distinct peaks in the xenon NMR spectrum. The location of the peaks matched those of the pure polymers. A single resonance is observed in PC/50 percent epoxidized poly (isoprene) and PC/25 percent poly (isoprene) blends. A single resonance does not unequivocally indicate a miscible blend. It is possible for xenon to exchange rapidly between small domains. This would result in a signal that is an average of the signals from the two domains. Knowledge of the diffusion coefficients of xenon in these polymers yields an upper boundary on the domain size in which rapid exchange could take place. The possibility of miscibility was further examined by modeling the

signal based on rule of mixtures calculations. It was assumed that a miscible blend has a different signal than a signal from a blend that is the result of an average from the two separate phases. A signal that does not match these predictions is indicative of miscible polymer. The possibility of a chance match in the signal of the miscible blend and an average signal was ruled out using variable temperature experiments. This application demonstrates the usefulness of xenon NMR for determining phase segregation in polymers with similar glass transition temperatures. The miscibility of these blends could not be determined using DSC because of the similarity of their glass transition temperatures.

Walton et al. have used xenon NMR to study phase transitions in poly (isoprene and poly (butadiene) blends[88]. Phase segregation was detected beyond the limits of DSC. Sizes of the phases were estimated using the intermediate exchange assumptions and the xenon self-diffusion coefficient in poly (isoprene).

Mirabella and McFaddin examined a poly (propylene) ethylene-propylene rubber blend using xenon NMR[85]. A correlation was shown between peak location and domain size as measured by SEM. Calibration in this manner might allow domain size measurement in other blends of these polymers. The viable range of measurement with this technique is limited by xenon's rate of diffusion in these polymers because slow exchange must be maintained.

Tomaselli et al. have demonstrated the ability of two-dimensional NMR techniques to probe heterogeneous blends using fabricated lamellar structures. Two model systems were manufactured poly (styrene) or poly (vinyl chloride) and poly (vinyl methyl ether). The lamellar size for the PS-PMVE systems was 4 to 7 μm and 2 to 6 μm

for the PVC-PVME systems. Two-dimensional experiments were performed with various mixing times allowing the xenon molecules various amounts of time to move through the structures. The extent that xenon sampled the different environments was determined by examination of the cross-peaks. The ratio of the diagonal peaks to the cross-peaks was used to calculate an exchange rate constant. By assuming a lamellar size, a diffusion coefficient for the blend was determined using the exchange rate constant. There is a large amount of error due to the lamellar size assumption. It is also assumed that the rate of diffusion was similar for both polymers.

Schantz and Veeman used two-dimensional spectroscopy to examine heterogeneity in PEO/PMMA blends [87]. A two-dimensional spectrum demonstrated that the xenon sampled all the environments in a mixing time of 1 ms. Furthermore, two-dimensional experiments were forgone in favor of one-dimensional spectra in which exchange-average models were used to interpret data. The authors chose this approach because of the long times required for two-dimensional experiments and because the xenon was probing the system in the fast exchange regime. The models were based on the spectral parameters from the pure polymers. The exchange rate parameter was then adjusted so that the model spectra matched the experimental. Domain sizes were then estimated based on the exchange rate and an approximate diffusion coefficient. The uncertainty in the fitted values results in values ranging from 30 to 60 nm. This work demonstrates the ability of xenon NMR to measure domain sizes on the order of 50 nm. The need for accurate diffusion coefficients to determination of domain sizes in polymers is elucidated.

Xenon diffusion coefficients in polymers have been determined in several ways. Simpson et al. have measured xenon's self diffusion coefficient in poly (styrene) using microspheres of different and well controlled sizes. The rate of diffusion of the gas out of the spheres was then related to free induction decay of the signal of the absorbed xenon. The difference of length of the free induction in the xenon from the different size spheres is plotted. The result allows calculation of diffusion coefficients. This technique is dependent upon the ability to fabricate microspheres and that the absorbed xenon has a relatively narrow peak. Tomaselli et al. measured the average diffusion coefficients for two polymers in a similar way by manufacturing artificial lamellar structure and using two-dimension exchange experiments as mentioned earlier. Browstein et al. made also calculation of the diffusion coefficient in poly (styrene)/poly (isoprene) blends using calculated domain sizes and spectral line-widths[89]. It was also shown that the line width of the xenon NMR signal was related to the diffusion of the xenon from one phase to another. The effect of the interphase between the blocks was not considered.

Perhaps a more elegant technique of measuring the self-diffusion of xenon is the pulsed field gradient technique. Stejskal and Tanner developed this technique in 1965 using proton NMR [90]. Junker and Veeman have applied it to xenon in polymers using a stimulated echo sequence rather than a Hahn echo [86]. The stimulated echo sequence aids in signal collection, which is difficult with xenon absorbed in polymers due to its short T2, spin-spin, relaxation times. The diffusion coefficient of the elastomer ethylene-propylene-diene was shown to be approximately 20 times greater than that of poly (propylene). The pulsed diffusion technique is limited by the long times necessary to collect signals. The lengths of experiments in this study were on the order of 70 hours.

The long collection times are due to the short T2 times (3-8 ms), low signal to noise ratios, and long T1 times.

Dynamic Mechanical Spectroscopy

Dynamic mechanical spectroscopy (DMS) is a widely used technique for characterizing polymers but it has found limited applications in dental materials. Dental restorations experience a wide variety of temperatures in their service life. The ability of DMS to test properties at a variety of temperatures and provide information about network structure is desirable.

Some of the earliest reported analyses by DMS was performed by a torsion pendulum. The work evaluated the effect of different conditionings on various commercial composites [91]. Samples stored at 37°C in water had lower modulus and larger damping than samples stored at 37°C under dry conditions. Running the same sample twice showed that additional cure resulted from analysis at elevated temperatures.

Ferracane and Greener used DMS to examine the effects of the ratio of Bis-GMA to triethylene glycol dimethacrylate as well as the type of initiator system on thermomechanical properties [3]. This work demonstrated that the storage modulus at 11 hertz was lower over the temperature range tested (25-150°C) in polymers with lower degree of conversion; i.e., that modulus increases with increasing degree of conversion. Samples with higher degrees of conversion had higher glass transition temperatures. This work also indicated that some additional cure takes place during DMS testing at elevated temperatures.

Wilson and Turner have also performed DMS on dental polymers [92]. Their approach differs from that of other researchers in that Tg is reported at the significant loss

in storage modulus rather than where the tan δ plot is maximized. Two methods of polymerization were used: γ-radiation and photopolymerization. Bis-GMA and TEGDMA were the monomers used. The Tg values from the different interpretations and cures (Table 2.4) show that elastic modulus estimates are lower than the tan δ estimates. The photopolymerized samples are undercured as indicated by the Tg values. The modulus loss is related to a β-relaxation, which has been identified in other studies on Bis-GMA [93] type polymers as well as lower molar mass ethylene glycol dimethacrylates [28, 30]. The β-relaxation in dimethacrylates is insensitive to different frequencies with the error of measurement [93]. The molecular origins of β-relaxations in dimethacrylates are not well understood. A more in-depth discussion of this phenomenon will be given later in this work. Other work has shown that the Tg of similar materials range between 85°C and 130°C [3]. Similar samples that were cured at 80°C had glass transition temperatures that ranged from 151 to 195°C. The glass transition values obtained from the γ-radiation polymerized samples are extremely high and may be indicative of the properties of a network cured to its physical maximum. It is interesting to note that the glass transition of fully cured diethylene glycol methacrylate has been estimated at 500°C [27]. This indicates that gamma radiation produces a more uniformly cured matrix, but it is still not possible to link every pendent group into the network structure in order to reach a theoretically fully cured structure.

Wilson has examined the thermomechanical transitions in TEGDMA monomers cured with various dose levels (0.15-2.0 Mrad) of γ-radiation[94]. Four types of transitions that were identified: 1) associated with monomer in low dose samples (-60°C);

Table 2.4: Glass transition temperature estimates obtained by Wilson and Turner

Sample Type	Tan Delta Estimate (°C)*	Elastic Modulus Estimate* (°C)
γ-radiation cure of Bis-GMA	195	138
γ-radiation cure of TEGDMA	-	120
Photopolymerization of Bis-GMA(75%) / TEGDMA(25%) in air	48	-25
Photopolymerization of Bis-GMA(75%) / TEGDMA(25%) in Nitrogen	60	-25
Second run of photopolymerization in Nitrogen	120	20

*Values obtained with Autovibron in tensile mode at 11 Hz. and 2.5°C/min.
Source: Wilson and Turner [92]

2) associated with interactions between the oxyethylene groups (-10°C); 3) associated with additional polymerization of partially vitrified material because it occurs slightly above the curing temperature and a downturn in the length versus temperature curve is observed; and 4) associated with the glass transition temperature. At high dose levels transition 3, sometimes referred to as a β-relaxation, is no longer detectable. Others have detected this transition with dielectric relaxation techniques [24, 25].

Summary

Many approaches have been taken to minimize or offset the shrinkage that occurs upon polymerization. Currently, a non-shrinking system has not been introduced that meets all the requirements for use in the mouth. Reduction of polymerization shrinkage has been obtained with molecules that have a larger molar mass than Bis-GMA. Ultimately these systems will only offset polymerization shrinkage and viscosity will become a limiting factor for large molar mass molecules. Liquid crystalline molecules show promise, but the toxicity of the current molecules and their ability to form a LC phase at lower temperatures are still issues. In order to have zero shrinkage or an

expanding system, ring open molecules must be employed. Unfortunately, these molecules are hampered by slow reaction kinetics, moisture sensitivity, and crystallinity, which limits solubility in base monomers. There is still a need for reduced shrinkage in polymer composites for dental applications.

This work explored the use of viscosity modifying comonomers systems based on monomethacrylates, or multicomponent analogs of ethylene glycol dimethacrylate that reduced the polymerization shrinkage and improved or negligibly affected mechanical properties of Bis-MEPP-based polymers when compared to the standard comonomer TEGMDA. The monofunctional comonomers examined were cyclohexyl methacryalate (CHMA), 2-phenyloxyethyl methacrylate (PEMA), and tert-butylcyclohexyl methacrylate (t-BCHMA). The comonomers were selected because they have a range of viscosity modifying properties and their corresponding polymers have a range of glass transition temperatures. The relationship between initial viscosity and heterogeneity was explored by formulating monomers systems that cure to the same glass transition temperature but had different initial viscosities. The mechanical properties that were tested were tensile strength, fracture toughness, and modulus. The network structure of these polymers was evaluated using dynamic mechanical spectroscopy. These properties were examined at a range of comonomer molar concentrations.

The heterogeneous network structure of dimethacrylates has been studied extensively but many questions still remain. Much of the structure and organization detail that occurs during cure still remains inaccessible to direct observation. The size and distribution of the low and high cross-link density phases, heterogeneity, has still not been determined. Knowledge of the size and distribution of the heterogeneity is

important because it affects the structure and performance of cross-linked dimethacrylate polymers. Knowledge of these structures and how they form will allow the tailoring of monomer selection and cure cycles to improve properties. Xenon NMR and TappingMode™ Atomic Force Microscopy (AFM) were used to determine the size and distribution of heterogeneous structures in dimethacrylates. Fractured and microtomed surfaces were examined at the scale of 500 to 1000 nm and regions of low and high cross-link density were elucidated using the topographic and phase imaging capabilities of TappingMode™ AFM.

The efficiency of the incorporation of nadic methyl anhydride and maleic anhydride in methacrylate polymers was explored using the model compound 2-phenylethyl methacrylate. The polymers were examined with FTIR, DSC, and proton NMR to quantify the incorporation.

CHAPTER 3
ALTERNATE DILUENT SYSTEMS FOR BIS-GMA AND BIG-GMA ANALOGS

Relevant Background

The need for dilution of Bis-GMA and its analogs to optimize their properties has long been recognized. Bis-GMA, named for the starting products used to synthesize it (bis-phenol A and glycidyl methacrylate), is a highly viscous monomer (2980 Pa•s or 29800 cp [1]). This high viscosity leads to early vitrification, which limits conversion during cure. This viscosity also limits filler loading. Vitrification is defined as the process in which the glass transition temperature of the reacting system reaches the reaction temperature. Polymerization becomes diffusion limited at the vitrification point. Vitrification at low conversions and other reaction mechanisms leads to heterogeneous systems composed of low molar mass or low cross-link density phases and high molar mass or highly cross-linked phases. It has been proposed that the low cross-link density phases behave as defects [34]. Therefore, if the amount of low molar mass material of the system can be reduced, the mechanical properties of the resin can be improved. Since the increase in viscosity during cure causes vitrification, it is logical that a system with a low initial viscosity will delay the onset of vitrification. This hypothesis is supported by the relationship between initial viscosity and degree of conversion seen in the literature [2-4]. Reactive diluents such as triethylene glycol dimethacrylate (TEGDMA) are effective at lower levels, but large amounts negatively affect matrix properties by increasing polymerization shrinkage and water sorption. Shrinkage results in poor marginal adaptation of composite restorations, which can lead to reformation of the

cavity. Polymerization shrinkage also results in tensile stresses in matrix materials adjacent to the glass filler as well as intra-matrix stress. These stresses lower mechanical properties. The monomers studied in this work have a higher molar mass per methacrylate group than standard reactive diluents such as triethylene glycol dimethacrylate (TEGDMA). It has been observed that methacrylates with larger molar masses per methacrylate group have a lower theoretical shrinkage [51, 52]. Methacrylate monomers with cyclic pendant groups also have the ability to reduce the viscosity of Bis-GMA resins more effectively than TEGDMA [46-48]. This ability allows modifications in two ways: 1) lower amounts of diluent can be used, which results in less shrinkage; 2) resin mixtures with the same theoretical shrinkage that have a lower initial viscosity. Resin mixtures can also be designed that are a compromise between these two scenarios. If a material is failing through its weakest points then minimizing this structure should increase the strength of the material. The weakest point of the materials discussed in this work is the low cross-link density phase.

The monomers selected will also provide information about the β-relaxation that is present in dimethacrylates. The onset of β-relaxations seen in dimethacrylates in this work occurs at approximately 50°C. This relaxation is near oral temperature; therefore, understanding the molecular structures that cause it is important. Some work indicates that β-relaxations in dimethacrylate polymers are due to pendant methacrylates groups [26, 93]. Other studies attribute the relaxation to the precursors of larger scale cooperative motion of the glass transition and the beginnings of vitrification [95]. In radiation-cured dimethacrylate networks the β-transition has been identified as an artifact of cure temperature due to vitrification and trapped free radicals [94]. Although there is a β-relaxation associated with the pendant groups in methacrylates, their incorporation

may provide insight into the β-relaxation in dimethacrylates. The incorporation of monofuctional monomers should reduce the amount of partially reacted dimethacrylates. The magnitude of β-relaxation is affected by the size of the pendant group [96]. Substitution of methacrylates with smaller pendant groups for that of partially reacted dimethacrylates (pendant) should provide information about the β-relaxation. It is also interesting to note that the temperature of the β-relaxation in observed dimethacrylates is not sensitive to frequency, while the β-relaxation in methacrylates is sensitive to frequency. This suggests that the molecular mechanism of β-relaxations is different in dimethacrylate and methacrylates.

The monomers selected for this study take advantage of concepts developed in previous studies. Monofunctional methacrylates with cyclic structures in the pendant group can reduce shrinkage while maintaining mechanical properties [47, 48]. In this study monomers with higher molar masses than previous monomers and variable glass transition temperatures will be studied. These monomers are also more hydrophobic than previous monomer systems. These systems will be light-cured, while, samples in previous studies were heat-cured at 70°C. Initial viscosities may be a greater factor in the final properties when resins are light-cured at room temperature. The monomers (the Tg corresponds to the polymers formed by the monomers) that were used are cyclohexyl methacrylate (CHMA) (Tg = 83°C), t-butylcyclohexyl methacrylate (t-BCHMA) (Tg = 98°C), 2-phenyloxy ethyl methacrylate (PEMA)(Tg=54°C) (Figures 3:1-3.3);2,2'-bis-(4-methacryloyloxyethoxyphenyl) propane (Bis-MEPP) (Figure 2.4) was the base monomer.

Given two monomer systems that form polymers with the same glass transition temperature, the monomer systems with a lower viscosity will vitrify later and allow

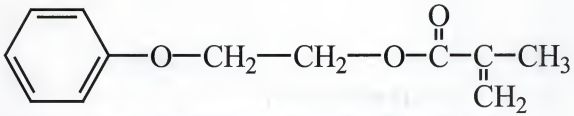

Figure 3.1: The structure of 2-phenyloxyethyl methacrylate (PEMA)

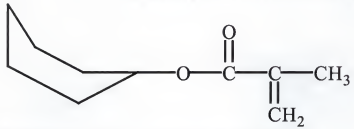

Figure 3.2: The structure of cyclohexyl methacrylate (CHMA)

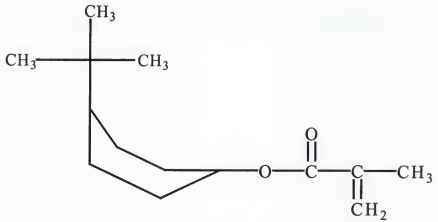

Figure 3.3: The structure of t-butylcyclohexyl methacrylate (t-BCHMA)

higher conversions. Whether the higher conversion will result in a polymer with a less heterogeneous structure will be explored in this work.

Polydisperse polymers have lower viscosities than their corresponding monodisperse systems [97]. A multicomponent diluent system with the same average molar mass as triethylene glycol dimethacrylate should result in a lower viscosity. The lower viscosity will allow increased conversion and improved mechanical properties. A multicomponent system may also allow the reduction of polymerization shrinkage through the use of a smaller amount of diluent to obtain an acceptable viscosity. The monomers used for the multicomponent diluent experiments were ethylene glycol dimethacrylate, diethylene glycol dimethacrylate, triethylene glycol dimethacrylate, and poly (ethylene glycol 400 g/mol, 600 g/mol, 1000 g/mol) dimethacrylate (Figure 3.4). Three mixtures will be created that have the same weight average molar mass as triethylene glycol dimethacrylate (TEGDMA). TEGDMA systems will also be formulated as a baseline. One mixture will contain all of the monomers mentioned. The second will contain all of the monomers except the 1000 molar mass monomer. The third will contain all of the monomers except for the 600 and 1000 molar mass monomers.

The hypotheses that are tested in this work are:

1. Monofuctional methacrylates with a cyclic or aromatic pendant group can reduce polymerization shrinkage while improving or negligibly affecting mechanical properties when compared to a Bis-MEPP/TEGDMA baseline system. The wet modulus of a 65/35 weight percent ratio Bis-MEPP/TEGDMA system is 2.6 ± 0.1 GPa and wet fracture toughness is 0.56 ± 0.10 MPa.m$^{0.5}$. An increase in modulus would be a modulus of 2.8 GPa or greater and no change would be modulus values ranging from 2.5

to 2.7 GPa. Similarly, an increase in fracture toughness would be values of 0.75 MPa.$m^{0.5}$ or greater and no change would be fracture toughness values ranging from 0.50 to 0.74 MPa.$m^{0.5}$. The percent shrinkage for the baseline Bis-MEPP/TEGDMA systems is 9.7 ± 0.4 and an improvement would be shrinkage values less than 9.0 percent. The viscosity of the baseline Bis-MEPP/TEGDMA systems would be 780 ± 20 centipoise an improvement would be values lower than 740 centipoise.

2. Heterogeneity can be reduced in polymers designed with the same glass transition temperatures by having a lower viscosity monomer system.
3. Blends of TEGDMA analogs are more effective at reducing the initial viscosity compared to TEGDMA alone.

Materials and Methods

All monomers diluted with acetone and passed over inhibitor removal columns obtained from Aldrich. The acetone was removed from the monomers by evaporation under vacuum. The t-BCHMA monomer was obtained with catalyst still present, which resulted in an orange color. The catalyst was titanium tetrabutoxide. The catalyst was removed by reacting it with water. The t-BCHMA monomer was extracted from the water/precipitate mixture with chloroform in a separation funnel. The chloroform was removed from the t-BCHMA monomer by evaporation under vacuum.

The initiator system that will be used for all systems is 0.5 weight percent camphoroquinone and 0.5 weight percent N,N-dimethyl-p-toluidine. Samples were cured using a UniXS twin Xenon strobe lamp light cure oven manufactured by Heraeus Kulzer. The resins or pastes were clamped between glass plates and polyethylene terephthalate

Table 3.1: Materials used

Materials	Abbreviation	Manufacturer
2,2'-bis-(4-methacryloylethoxyphenyl) propane	Bis-MEPP	Sartomer Co., Exton, PA, USA
cyclohexyl methacrylate	CHMA	Sartomer Co., Exton, PA, USA
tertiary-butylcyclohexyl methacrylate	t-BCHMA	Esstech, Essington, PA, USA
2-phenyloxyethyl methacrylate	PEMA	Sartomer Co., Exton, PA, USA
triethylene glycol dimethacrylate	TEGDMA	Sartomer Co., Exton, PA, USA
ethylene glycol dimethacrylate analogs up to 600 g/mol.	EGDMA, DEGDMA, TetraEGDM, EG(400), EG(600)	Sartomer Co., Exton, PA, USA
poly (1000) ethylene glycol dimethacrylate	EG(1000)	Polysciences, Warrington, PA, USA
Camphoroquinone	CQ	Aldrich Chemical Co., Milwaukee, WI, USA
N, N-dimethyl-para-toluidine	DMPT	Aldrich Chemical Co., Milwaukee, WI, USA

(PET) film with a piece of Tygon tubing as a spacer (Figure 3.5). The mold was then illuminated on both sides for 180 sec. The distance between the glass plates was checked at various points to make the plates parallel. This ensured uniform samples. DMS and flexure samples were then cut using a slow speed diamond saw. Tensile samples were made in a similar manner to the flexure and DMS samples except an aluminum mold made to ASTM type 5 dogbone specifications was clamped between the glass plates and PET film. All samples for mechanical properties and DMS testing in the wet state were prepared in the same manner. The cured samples were placed in ultrapure water (16-18 MΩ-cm) at 37°C for 1 month. The water was changed periodically to facilitate monomer leaching and to better simulate the oral environment. The dry samples were aged in a desiccator for 1 week after curing and then tested. The monofunctional

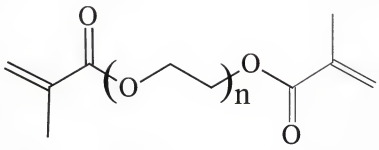

n=1 Ethylene glycol dimethacrylate
n=2 Diethylene glycol dimethacrylate
n=3 Tri " " "
n=4 Tetra" " "
n=9 Poly(400) ethylene glycol dimethacrlate
n=14 Poly(600) " " "
n=23 Poly(1000) " " "

Figure 3.4: The basic structure of poly (ethylene glycol dimethacrylate) analogs

monomers were added at 30, 40, 50, and 60 mol.% to the Bis-MEPP base monomer. The multicomponent diluent systems were added to the Bis-MEPP base monomer at 35 weight percent. The matched Tg systems were formulated to have a Tg of 135°C (denoted by the maximum in the tan δ peak at 1 Hz) using data from the previous systems. Table 3.2 contains the corresponding weight fractions of the resin formulations.

Table 3.2: Molar fractions, weight fractions, and viscosities of Bis-MEPP/CHMA, Bis-MEPP/t-BCHMA, and Bis-MEPP/PEMA resins

Resins	Molar fractions	Mass Fractions	Viscosity (cP)
Bis-MEPP/CHMA	70/30	87.7/12.3	2170 ± 10
	60/40	82.1/17.9	1330 ± 10
	50/50	75.3/24.7	880 ± 10
	40/60	67.1/32.9	460 ± 10
Bis-MEPP/PEMA	70/30	83.7/16.3	2030 ± 10
	60/40	76.7/23.3	1390 ± 10
	50/50	68.7/31.3	890 ± 10
	40/60	59.4/40.6	590 ± 10
Bis-MEPP/t-BCHMA	70/30	80.6/19.4	2640 ±10
	60/40	72.7/27.3	1640 ± 10
	50/50	64.0/36.0	990 ± 10
	40/60	54.3/45.7	600 ± 10

Flexure testing, for the measurement of the flexural modulus, was performed according to ASTM D790-81 three-point bend test procedure. An Instron 1122 fitted with an environmental chamber operating at 37°C was used. The three-point bend test fixture has a support span of 40 mm and load span of 20 mm. The cross-head speed used is 1 mm/min. The sample size was 2.5 mm x 2.7 mm x 45 mm.

The tensile breaking strength was measured according to ASTM standard D638-89 on the Instron 1122 fitted with an environmental chamber set at 37 ± 2°C. The samples, which were type five geometry, were held with pneumatic grips with a clamping

force of 70 psi (0.48 MPa). The cross-head speed was 0.05 inches/min (1.3 mm/min) corresponding with an elongation rate of 5 percent/min.

Flaws resulting from the manufacture of samples often influence strength in mechanical properties tests. To remove noise that results from sample manufacture and isolate materials properties, fracture toughness was measured using quantitative fractography. Fracture toughness is typically measured using methods such as single-edge notched, short rod, compact tension, or double torsion. These methods require particular sample preparation techniques and are often labor intensive to implement. Fracture toughness can be measured from the fracture surface of an ASTM dogbone when the fracture stress is known. The following equation was used to determine fracture toughness for brittle failures with edge flaws [98]:

$$K_{IC} = 1.24\sigma_f \{(ab)^{0.5}\}^{0.5}$$

Where: σ_f = fracture stress

a = depth of crack

b = half-width of crack

This equation is based on the assumption that failure-initiating crack can be modeled as an equivalent semicircular crack. The following equation was applied if yielding behavior was observed [98]:

$$(K_{IC})^2 = \{1.2\pi(\sigma_f)^2 c\} / [\phi^2 - \{0.212(\sigma_f)^2 / (\sigma_{ys})^2\}]$$

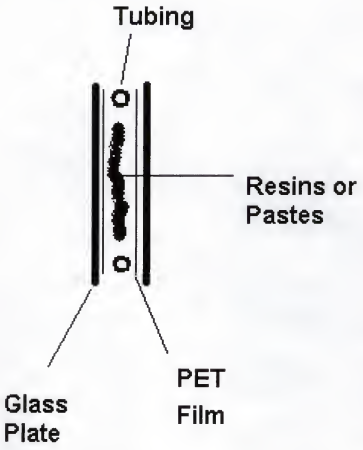

Figure 3.5: Schematic of mold used for sample manufacture. Source:[99]

Where: $c = (ab)^{0.5}$

$\phi = 1.57$

σ_{ys} = yield stress

This equation is based on the assumption that the radius of the plastic zone is small compared to the crack size and that the plastic deformation is occurring at the crack tip. These assumptions allow the application of linear elastic fracture mechanics. Fracture toughness was measured in both wet and dry samples. Similar equations were applied if corner flaws were observed:

$$K_{IC} = (1.12)^2 \frac{2}{\pi} \sigma_f \sqrt{\pi a}$$

The flaw sizes were determined using an Olympus optical microscope at 100 and 200 magnification. The depth and the half–width of the fracture initiating flaws were measured using a reticule. The magnitude of the length was calibrated using a standard glass scale at each magnification.

Dynamic Mechanical Spectroscopy was performed on one sample from each system. DMS imposes a sinusoidal strain on a sample over a range of temperatures and frequencies. It provides information about relaxation processes in polymers such as glass transitions and sub-glass transitions. The information is collected in the form of storage modulus (E'), loss modulus (E''), and the loss dispersion (tan δ) as a function of temperature and frequency. A Seiko DMS110 (double cantilever type) interfaced with a Seiko SDM5600H Rheostation was used to analyze the thermomechanical response in flexure mode. Measurements were taken at frequencies of 0.1, 0.5, 1, 5, and 10 Hz over the temperature range, -140°C to 200°C at a heating rate of 0.75°C/min in a nitrogen environment. The sample size used was approximately 2.5 mm x 10 mm x 40 mm.

Fourier Transform Infrared Spectroscopy was used to determine the degree of conversion in the various network polymer systems. The monomer samples were prepared by placing two drops of material between two sodium chloride (NaCl) crystals. The cured material samples were prepared for analysis by cryo-milling. The powders were mixed with IR grade KBr powder and pressed into thin pellets. Backgrounds were taken before every run with a blank crystal or KBr pellet. The spectra obtained represent 32 scans using a Nicolet 20SX FTIR. No baseline corrections were performed on the spectra. The degree of conversion or percent-unreacted double bonds was determined by comparing the peak areas of the vinyl group at 1637 cm^{-1} of the monomers and the cured polymers. Peak fitting software was used to draw baselines, deconvolute, and measure the areas of these peaks (PeakFit v4 by SPSS Inc.). The magnitude of these peaks is related to the path length of the radiation, the molar absorptivity, and the concentration of the chemical species. The aromatic peak at 1608 cm^{-1} is used as an internal reference peak to normalize the vinyl peak intensities in different spectra. The normalization makes the peak areas a function of the concentration of chemical species. The intensity of peak at 1608 cm^{-1} that is associated with aromatic bonds does not change during polymerization. The following equation was used to calculate the percent of unreacted double bonds (UDB)[100]:

$$UDB\ (\%) = (bc/ad)*100$$

Where: a = the vinyl absorbance peak at 1637 cm^{-1} of the resins or pastes

b = the aromatic absorbance at 1608 cm^{-1} of the resins or pastes

c = the vinyl absorbance at 1637 cm^{-1} of the cured materials

d = the aromatic absorbance at 1608 cm^{-1} of the cured materials

It should be noted that this technique only samples vinyl bonds. It is possible for molecules to exist without vinyl bonds due to consumption by termination and disproportionation that are not incorporated into the network structure. Termination in the free radical polymerization methyl methacrylate at 60°C occurs 79 percent by disproportionation and 21 percent by combination [101].

The viscosities of the various monomer mixtures were measured at 25°C with a Brookfield CAP2000 cone and plate viscometer. Shear rates ranging from 2667 to 6667s^{-1} were used to determine shear rate dependence of the viscosity. The two cone types used are: cone #1, which has a 0.45° slope angle and a radius 1.511 cm, and cone #2, which has a 0.45° slope angle and a radius of 1.200 cm.

The shrinkage of the monomer systems was calculated from differences in density between the monomers and cured polymer systems. The monomer densities were obtained by the average of 5 measurements from 25 ± 0.03 ml volumetric flasks. The densities of the cured samples were measured 5 times using the Mettler 33360 Density Determination Apparatus (ASTM D792-86).

Statistical analysis was performed using the Sigma Stat™ software package. Student's t-tests were used to statically compare the different sample sets.

Results and Discussion

Physical Properties

The viscosity of the Bis-MEPP/monofunctional diluent systems decreases, as expected, with increasing concentration of diluent monomers (Figure 3.6). At the 30 percent molar concentration the CHMA systems have a higher viscosity than the PEMA and t-BCHMA systems. At the higher mol.% of diluent, the viscosity of the Bis-

MEPP/CHMA is lower than the viscosity of the Bis-MEPP/PEMA systems. This indicates that differences in weight percent of diluent are a larger issue at lower concentrations (Table 3.2), which holds true for the t-BCHMA systems as well.

The monofunctional diluent will be compared to TEGDMA on a weight percent basis because of the large difference in weight fractions that would result from comparing resins formulated on a molar basis. The multicomponent diluent systems will be denoted with the following abbreviations: EG (400), EG (600), EG (1000). The abbreviations represent the multicomponent diluent systems EGDMA (400), EDGMA(600) and EGDMA(1000) described earlier in this work. A comparison of the diluent systems at 35 weight percent shows that CHMA is the most effective followed by PEMA diluent (Figure 3.7). This is due to its small molar mass. T-BCHMA is the only diluent that is not more effective on a per weight basis as indicated by comparison with TEGDMA in the Bis-MEEP system. Although the molar mass of t-BCHMA is smaller than that of TEGDMA its structure is more rigid and bulky as evidenced by higher viscosity of the Bis-MEPP/t-BCHMA systems. The ethylene glycol units in the backbone of the TEGDMA produce a more flexible structure, which lowers viscosity more effectively than stiff bulky structures. Isobornyl methacrylate, a high molar mass methacrylate with a bulky stiff ring pendant group, also reduced the viscosity less effectively than TEGDMA[48]. FTIR analysis indicated that t-BCHMA monomer contained 10.4 ± 6.1 percent non-reactive contaminates, which depending on their exact nature may decrease the t-BCHMA's ability to lower viscosity. There is no significant trend toward lower viscosity in the multicomponent systems composed of molecules with a greater range of molar masses. It seems that molar mass dispersity might only have significant effects in

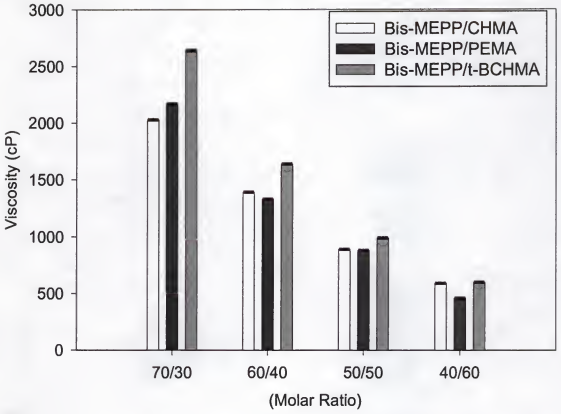

Figure 3.6: Viscosity measurements on Bis-MEPP/PEMA, Bis-MEPP/t-BCHMA, and Bis-MEPP/CHMA resins at 25°C

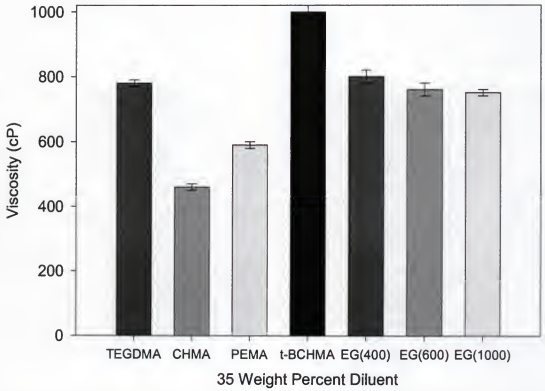

Figure 3.7: Viscosity measurements of various diluents in the Bis-MEPP-based resin systems diluted at approximately 35 weight percent

systems of greater molar mass.

Methacrylates have been shown to have shrinkage of 22.5 ml/mol per double [52] bond upon complete conversion of the double bonds to single bonds (Tables 3.3-3.7). Decreasing the molar concentration of methacrylate groups present in the monomer system can reduce the shrinkage that occurs upon polymerization. One way to reduce the molar concentration is to increase the specific volume of the monomers or the molar mass of the monomers with respect to the methacrylate groups. The discrepancy between the theoretical shrinkage and the measured shrinkages is due to the incomplete reaction of these systems.

Table 3.3: Predicted theoretical and measured shrinkage values for Bis-MEPP-based copolymer systems

Co-Monomer	35 wt.%. TEGDMA	33 wt.% CHMA	31 wt.%. PEMA
Molar Mass of comonomer* (g/mol)	286	168	206
# of moles of comonomer in 1ml of mixture	1.35×10^{-3}	2.07×10^{-3}	1.68×10^{-3}
# of moles of Bis-MEPP	1.59×10^{-3}	1.58×10^{-3}	1.68×10^{-3}
# number of moles C=C from co-monomer in 1ml of mixture	2.70×10^{-3}	2.07×10^{-3}	1.68×10^{-3}
# number of moles C=C from Bis-MEPP in 1ml of mixture	3.58×10^{-3}	4.14×10^{-3}	3.36×10^{-3}
Total # number of moles C=C in 1ml of mixture	6.38×10^{-3}	5.23×10^{-3}	5.04×10^{-3}
Theoretical volumetric shrinkage (%)	13.2	11.8	11.3
Measured volumetric shrinkage	9.7	9.0	8.7

*The molar mass of Bis-MEPP is 452 g/mol.

For example, the Bis-MEPP/t-BCHMA systems, which have the highest average specific volume per methacrylate group, display the least amount of shrinkage. The systems that shrink the most upon curing are the Bis-MEPP/EDGMA-type systems, which have the lowest specific volume per methacrylate group of all the systems examined in this study.

This corresponds with results reported in other work where monomers with larger specific volume per methacrylate groups displayed less polymerization shrinkage [47, 48, 50-52].

The percent shrinkage values within each system increase with increasing amount of diluent. This is expected in Bis-MEPP/CHMA and Bis-MEPP/PEMA systems because the molar mass per methacrylate group is smaller than that of the Bis-MEPP. In Bis-MEPP/t-BCHMA systems shrinkage also increases with increasing amounts of diluent.

Table 3.4: Physical properties of Bis-MEPP/PEMA systems

Composition (molar ratio)	Monomer density (g/cm^3)	Polymer density (g/cm^3)	Shrinkage (%)	Water uptake (wt.%)
70:30	1.113 ± 0.001	1.203 ± 0.001	8.1	0.5 ± 0.1
60:40	1.105 ± 0.001	1.197 ± 0.002	8.2	0.5 ± 0.1
50:50	1.100 ± 0.001	1.196 ± 0.002	8.7	0.3 ± 0.1
40:60	1.098 ± 0.002	1.193 ± 0.002	8.7	0.4 ± 0.1

The systems examined here are not taken to a high degree of conversion as FTIR experiments presented later in this work will show. The incomplete reaction results in smaller amounts of polymerization shrinkage than theoretically predicted.

Water uptake is lower in all of the monomethacrylate systems than the EGDMA-based systems. This is due to the lower polarity of the monomethacrylate systems. There is no difference in the water uptake within the error of measurement in the Bis-MEPP/PEMA systems. This is due to the similar structure of PEMA to Bis-MEPP. The water uptake experiments in the Bis-MEPP/CHMA systems have similar results to the

Table 3.5: Physical properties of Bis-MEPP/CHMA systems

Composition (molar ratio)	Monomer density (g/cm^2)	Polymer density (g/cm^2)	Shrinkage (%)	Water uptake (%)
70:30	1.097 ± 0.002	1.186 ± 0.001	8.0	0.7 ± 0.1
60:40	1.089 ± 0.002	1.180 ± 0.001	8.4	0.6 ± 0.1
50:50	1.078 ± 0.002	1.170 ± 0.001	8.6	0 5 ± 0.1
40:60	1.065 ± 0.002	1.161 ± 0.001	9.0	0.6 ± 0.1

Bis-MEPP/PEMA systems. There is also not much difference in the polarity of the structure of Bis-MEPP and CHMA. It has been shown that water uptake decreases in methacrylate-dimethacrylate polymers as the amount of methacrylate feed is increased [73]. This difference in the results seen in these systems and those examined in this work lies in sample preparation. The samples in the cited study were heat-cured to high conversion and then extracted prior to water uptake experiments. The samples in this work are light-cured at room temperature. This results in a larger amount of pendant groups and regions of low cross-link density material. It has been postulated that areas of low cross-link density take up solvents preferentially [30]. This preferential uptake is the mediating factor in the water uptake experiments. The Bis-MEPP/t-BCHMA systems have lower water uptake than the other systems. This could be due to the less polar structure of the t-BCHMA monomer. The lower value could also be due to loss of material while the samples are immersed in water. Bis-MEPP/t-BCHMA polymers lost an average of 8 weight percent in extraction studies performed with chloroform while the other polymers in this study had no detectable weight loss. No conclusions about the trend toward lower water absorption with increasing concentrations of t-BCHMA are possible due to leaching of materials during the hydration process.

Table 3.6: Physical properties of Bis-MEPP/t-BCHMA systems

Composition (molar ratio)	Monomer density (g/cm^2)	Polymer density (g/cm^2)	Shrinkage (%)	Water uptake (%)
70:30	1.081 ± 0.002	1.159 ± 0.002	7.2	0.3 ± 0.1
60:40	1.068 ± 0.002	1.147 ± 0.002	7.4	0.3 ± 0.1
50:50	1.052 ± 0.001	1.133 ± 0.002	7.7	0.2 ± 0.1
40:60	1.036 ± 0.001	1.118 ± 0.002	7.9	<0.1

Table 3.7: Physical properties of Bis-MEPP/EGDMA-type resins

Diluent system	Monomer density (g/cm^2)	Polymer density (g/cm^2)	Shrinkage (%)	Water uptake (%)
TEGDMA	1.097 ± 0.001	1.204 ± 0.002	9.7	1.0 ± 0.1
EGDMA(400)	1.098 ± 0.002	1.206 ± 0.002	9.7	1.0 ± 0.1
EGDMA(600)	1.097 ± 0.002	1.203 ± 0.002	9.6	1.0 ± 0.1
EGDMA(1000)	1.100 ± 0.001	1.205 ± 0.001	9.5	1.0 ± 0.1

The degree of conversion values obtained from the FTIR spectra correspond well with those seen in the literature (Tables 3.8 and 3.9) [3, 102-105]. Other studies using monomethacrylates have reported values for degree of conversion that were slightly lower when mixed at 54 mol.% with Bis-GMA resins [47, 48]. A true comparison is not possible between these systems and those used in this study because the Bis-GMA systems were heat-cured at 70°C for 8 hours in a nitrogen atmosphere. Cure under such conditions results in a different network structure because the elevated temperature delays vitrification and the nitrogen eliminates oxygen inhibition of the polymerization. The polymerization process is also different due to differences in the concentration of radicals when heat curing and light curing are used. The lower conversion in these systems is due to their high viscosity and the difference in the curing techniques mentioned earlier. The higher viscosity is a result of the hydroxyl groups on Bis-GMA

molecules and its slightly higher molar mass compared to Bis-MEPP. The viscosity of a Bis-GMA system diluted with 54 mol.% tetrahydrofurfuryl methacrylate was nearly 2000 cP [48]. Bis-MEPP resin formulated with similar mol.% of diluents had viscosities lower than 1000 cP.

The degree of conversion increases with higher concentrations of diluent (Table 3.8). The three factors that control the degree of conversion are viscosity of the initial monomer formulation, the Tg of polymer formed, and the average functionality of the system. All three of these factors are changed in ways that promote higher degrees of conversion by adding diluent, i.e., viscosity is lowered, average functionality is decreased, and the Tg of polymer formed is also decreased. Table 3.9 contains the degree of conversion values for the Bis-MEPP/EGDMA-type resins and the corresponding monomethacrylates with approximately the same weight percent diluent. At the same weight percent the Bis-MEPP/CHMA and Bis-MEPP/PEMA systems have a smaller average number of remaining vinyl bonds; however, the actual weight percent of the PEMA in the system is 31. A Bis-MEPP/PEMA system formulated with 35 weight percent would have a smaller quantity of remaining double bonds. The Bis-MEPP/t-BCHMA systems average value is lower than that of the Bis-MEPP/EDGMA-type systems; however, the error in measurement indicates that there is not a significant difference. The lower degree of conversion of the Bis-MEPP/t-BCHMA systems is due to the high viscosity of the monomer systems and the high Tg of the polymer system formed.

Table 3.8: Degree of conversion values based on percent vinyl bonds remaining in Bis-MEPP/PEMA, Bis-MEPP/CHMA, and Bis-MEPP/t-BCHMA systems

Molar Ratio	Bis-MEPP/PEMA	Bis-MEPP/CHMA	Bis-MEPP/ t-BCHMA
70/30	33.6 ± 3.9	36.0 ± 4.7	40.4 ± 2.6
60/40	23.7 ± 2.5	25.1 ± 3.1	31.8 ± 3.3
50/50	22.5 ± 3.2	24.3 ± 2.6	24.7 ± 3.5
40/60	18.1 ± 3.1	21.3 ± 3.6	22.3 ± 2.6

Table 3.9: Degree of conversion values based on percent vinyl bonds remaining in Bis-MEPP/EDGMA-type systems, and the Bis-MEPP/PEMA, Bis-MEPP/CHMA, and Bis-MEPP/t-BCHMA systems formulated to approximately 35 weight percent diluent

System	Percent remaining vinyl bonds
Bis-MEPP/TEGDMA	27.5 ± 4.4
Bis-MEPP/EGDMA(400)	25.3 ± 3.0
Bis-MEPP/TEGDMA(600)	27.9 ± 3.4
Bis-MEPP/TEGDMA(1000)	27.0 ± 4.2
Bis-MEPP/PEMA	22.5 ± 3.2
Bis-MEPP/CHMA	21.3 ± 3.6
Bis-MEPP/t-BCHMA	24.7 ± 3.5

The mechanical properties data is presented as a comparison of different comonomers grouped by mol.%. The Bis-MEPP/PEMA, Bis-MEPP/CHMA, and Bis-MEPP/t-BCHMA systems will also be compared to Bis-MEPP/TEGDMA-type systems with similar weight percent formulation. The mechanical properties of each system are grouped by the molar ratios of the monomer components of the polymers (Figures 3.8-3.10).

Flexure Testing

The flexure modulus values from the Bis-MEPP/PEMA, Bis-MEPP/t-BCHMA, and Bis-MEPP/CHMA polymers are grouped by mol.% formulation (Figure 3.8). There are no pervasive trends with the change in mol.% of diluents in the dry or wet state.

The average modulus of the Bis-MEPP/PEMA resins varies 0.2 GPa throughout the entire range of PEMA concentrations in both the wet and dry states. Student's t-tests found no significant difference ($P > 0.05$) in any of the groupings in the Bis-MEPP/PEMA series.

There are also no clear trends in the modulus of dry Bis-MEPP/CHMA systems. The 60/40 system seems to be anomalously low ($P < 0.05$). In the wet Bis-MEPP/CHMA set there is a significant increase in modulus ($P < 0.05$) as CHMA is added up to 50 mol.%. Further addition of CHMA past 50 mol.% does not result in an increase in modulus upon hydration. The 50/50 and 40/60 systems are not significantly different ($P < 0.05$). The increase in modulus corresponds with a decrease in water uptake. Examination of the dynamic mechanical spectra of the 70/30 Bis-MEPP/CHMA systems shows that the glass transition is lower than the 60/40 Bis-MEPP/CHMA system, while the magnitude of the tan δ maximum in the 70/30 system is less than the 60/40 system. This indicates that there is a large amount of low cross-link density material and pendant groups. The regions of low cross-link density and the increased water uptake result in the decreased modulus compared to the systems with larger amounts of diluent. Further discussion of the DMS is presented later in this work. The average values of modulus in the wet state were not significantly different from the dry state for all of the resins accept the 70/30 composition. The modulus of the 70/30 composition is significantly ($P < 0.05$) decreased in the wet condition.

There are no clear trends in Bis-MEPP/t-BCHMA systems in the wet or dry states. Pair-wise comparison of all of the dry compositions indicates that there is not a significant difference ($P > 0.05$). In the wet condition, the 60/40 composition is

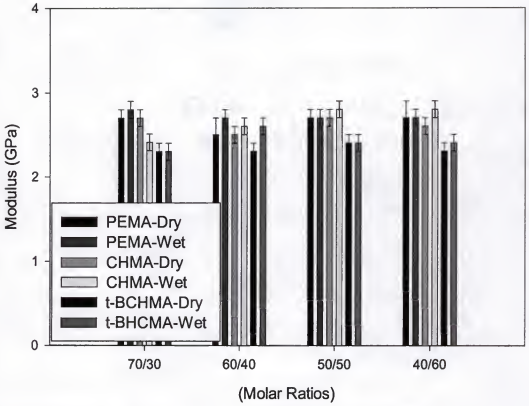

Figure 3.8: Flexure modulus values of wet and dry Bis-MEPP/CHMA, Bis-MEPP/PEMA, and Bis-MEPP/t-BCHMA polymers at 37°C. The legend represents the monomers used to diluent the Bis-MEPP monomer

significantly greater ($P < 0.05$) than the other compositions. Pair-wise comparison of the same systems in the wet and dry state shows that the wet modulus is significantly greater ($P < 0.05$) in the 60/40 composition.

Pair-wise comparison of the different polymer systems by mol.% formulation in the dry state indicates that the Bis-MEPP/t-BCHMA systems have significantly ($P < 0.05$) lower modulus than the Bis-MEPP/CHMA and Bis-MEPP/PEMA systems in all cases except the 60/40 systems where the Bis-MEPP/PEMA is not significantly different from the Bis-MEPP/t-BCHMA systems. There is not a significant ($P > 0.05$) difference between the Bis-MEPP/PEMA and Bis-MEPP/CHMA systems in any of the formulations. The addition of monomethacrylates results in an increase in the molar mass between cross-links as evidenced in the DMS plots present later in this work. The different methacrylates result in different glass transition temperatures even though the average functionality of the mol.% formulations are the same. The tan δ curves in the DMS have a shoulder on the low temperature side of the main relaxation. Correlation of the shoulder of tan δ curves with the E' plots shows the E' values drop concurrently with shoulder. It is thought that the shoulder in the tan δ curve, which is associated with a β-relaxation, is responsible for the similarity of the flexure modulus values. A more in-depth discussion of β-relaxations will be given later in this work.

The results of a pair-wise statistical comparison of the different polymer systems by mol.% formulation in the wet state are shown in Table 3.10. The Bis-MEPP/t-BCHMA systems have the lowest modulus values with the exception of the 60/40 mol.% system. Generally speaking the Bis-MEPP/t-BCHMA polymers have the highest glass transition temperature and their monomer systems have the highest viscosities. The

presence of contaminates also results in a reduction in the modulus of the Bis-MEPP/t-BCHMA systems.

Table 3.10: Pair-wise comparison of the modulus values of different polymer systems by mol.% formulation in the wet state using Student's t-test

Molar Ratio	Significantly different ($P < 0.05$)	Not Significantly Different ($P > 0.05$)
70/30	CHMA/PEMA, PEMA/t-BCHMA	CHMA/t-BCHMA
60/40		PEMA/t-BCHMA, CHMA/PEMA, CHMA/t-BCHMA
50/50	CHMA/t-BCHMA, PEMA/t-BCHMA	CHMA/PEMA
40/60	CHMA/t-BCHMA, PEMA/t-BCHMA	CHMA/PEMA

In the 70/30, 50/50, and 40/60 Bis-MEPP/t-BCHMA systems the modulus values are not significantly different ($P > 0.05$). There is a smaller amount of water uptake in these systems than in the 70/30 and 60/40 systems, but the water uptake values are suspect due to the possible loss of materials during the water treatment; therefore, differences in water uptake cannot be cited for the lack of modulus increase in the 70/30, 50/50, and 40/60 systems. It is likely that there is some limit at which the loss of extractable material no longer results in increased modulus. The 70/30, 50/50, and 40/60 systems have reached this limit with a final weight loss of 6.5, 8.5, and 11.0 percent, respectively, after extraction in chloroform.

The small range of modulus values observed in this work can be understood by examination of the dynamic mechanical spectrum of these polymers (Figures 3.11-3.21). There is a shoulder present on the low temperature side of the main relaxations in all the tan δ spectra. The samples were tested at 37°C, which is in close proximity to onset of

this relaxation. This relaxation is likely in great part due to the incomplete curing of these systems as well as β-relaxations common to the methacrylate family. Further discussion about the nature of β-relaxations will be given later in this work. The incomplete cure of the systems results in a large of amount of heterogeneity, regions of low and high cross-link density materials. The systems with a higher average functionality form more highly cross-linked polymers; however, they form a less uniform network structure with a great amounts of defective structures. This structure and the incomplete cure of the samples results in small variations in the modulus values. A small range of modulus variation (0.4 GPa) has also been reported in other monomethacrylates that were incorporated into Bis-GMA systems [47, 48]. In order to confirm that the low temperature shoulder is a contributing factor of the modulus values a 70/30 Bis-MEPP/PEMA sample was post cured at 140°C for 2 hours immediately after the initial light curing. The post cure resulted in a dramatic reduction in the shoulder associated with the β-relaxation and a slight increase in the glass transition temperature as well as an increase in the cross-link density (Figure 3.24). The modulus values at 37°C tested using the Instron and procedures described earlier were 3.0 ± 0.1 and 2.7 ± 0.1 GPa for the post cured and normally cured sample, respectively. Although, the β-relaxation is greatly reduced by the post cure at 140°C, it has not been completely removed. This indicates that there is an underlying mechanism for this relaxation as well as the one that is an artifact of cure temperature.

Understanding the results of flexure testing in the wet state as well as the changes in the modulus upon hydration requires knowledge of the processes that affect network structure during hydration. Hydration can increase modulus, decrease modulus, or have

no effect on modulus depending on the amount of water absorbed and how long the samples are soaked in water [5, 21, 23, 41]. The mechanisms responsible for these phenomena are plasticization by water and unreacted material, the leaching of materials from the system and physical and chemical aging. Swelling in water has also been shown to increase conversion [106, 107]. Dynamic mechanical spectroscopy results presented later in this work also indicate that additional polymerization or aging is occurring during hydration. Additional polymerization might also be occurring independently of water absorption. Diacrylates can continue to polymerize in the glassy state after the initial curing provided that the system has not vitrified or gelled to the level that diffusion is no longer reasonable [108]. The dry samples were tested one week after polymerization and the wet samples were tested one month after polymerization. The additional aging time of the wet samples may allow additional polymerization and physical aging to occur that would result in increased modulus values. In the Bis-MEPP/CHMA and Bis-MEPP/PEMA systems it is unlikely that leaching of materials is taking place in appreciable amounts because weight loss was not detected in extraction experiments performed in acetone and chloroform. The increase in the average modulus values at 37°C, although not significant in most cases, from the wet to dry state is a result of additional polymerization and physical aging. The effect water has on the additional polymerization and physical aging is difficult to discern. The concentration of water is small and may aid the previously mentioned processes or it might result in a loss of modulus due to plasticization. Testing samples dry aged from 1 month might give more insight into the role the water is playing.

In the Bis-MEPP/t-BCHMA system the 60/40 composition is notable because there is a significant increase ($P < 0.05$) in modulus in the wet state. A 5 percent weight

loss was observed in chloroform extraction of the 60/40 Bis-MEPP/t-BCHMA system. The loss of unreacted material coupled with the additional polymerization and physical aging are responsible for the observed results.

Fracture Toughness and Tensile Testing

The tensile strength data and fracture toughness data will be discussed simultaneously in this section. Caution should be used when interpreting tensile strength data because of the sensitivity of tensile strength to flaws induced by sample preparation. This is why fractographic analysis was used to interpret the strength properties of these materials. Tensile strength is an indicator of materials performance; however, it is not a materials property. It should also be noted that there was greater difficulty obtaining wet samples in which the flaws could be resolved than in the dry samples.

The tensile strength of dry Bis-MEPP/PEMA polymers decreases significantly with the addition of PEMA ($P < 0.05$) (Figure 3.9). The 40/60 dry systems displayed a slight yielding behavior. The average yield stress of the 40/60 set was 41 ± 2 MPa slightly higher than the average break stress, 38 ± 2 MPa. The yielding behavior is a result of the large molar mass between cross-links and the low glass transition temperature of the system as indicated by DMS (Figure 3.11). Fracture toughness (Figure 3.10) shows an increasing trend with the addition of PEMA; however, it is not significant ($P > 0.05$). This indicates that the tensile strength values may be a result of artifacts from sample preparation. There is not a significant difference ($P > 0.05$) in wet tensile strengths with the exception of the 70/30 system, which is significantly stronger ($P < 0.05$) than the other systems. There is not a significant difference ($P > 0.05$) between fracture toughness values in the wet state with the exception of the 40/60 system being significantly tougher ($P < 0.05$) than the 70/30 system. Again, the fracture toughness

results are different than tensile strength results. The difference in the trends is due to flaws resulting from sample preparation. The similarity of the strength values of this system can be attributed to the same factors that resulted in small variations in modulus for the Bis-MEPP/PEMA systems. As discussed earlier there is a β-relaxation in the dynamic mechanical spectra of these polymers that correlates with a decrease in modulus values. The β-relaxation is stronger in the samples with higher cross-link densities. The β-relaxation has been associated with a loose defective interlayer [34, 94] and regions of higher mobility [26] that are a result of vitrification. Although the cross-link density is higher in systems with less PEMA, it seems that the networks formed are less homogeneous than the networks formed when more PEMA is present. The less homogeneous network structure is indicated by the presence of the shoulder in the systems with less PEMA and also the larger full-width half maximums of the tan δ peaks (Figure 3.11 and Table 3.11). The samples with higher concentrations of PEMA have a more uniform network structure. The heterogeneity of the higher cross-link density systems results in moderation of the strength properties of the systems; hence, the similar values of fracture toughness and tensile strength for all of the systems. The difference in the fracture toughness of the 70/30 and 40/60 Bis-MEPP/PEMA systems in the wet state may be a result of the weakening of the 70/30 systems due to preferential swelling in the regions of lower cross-link density. This mechanism has been proposed for the loss in fracture toughness of tetraethylene glycol dimethacrylates swelling in water [30]. Comparison of the wet and dry samples of the same mol.% formulations indicates that all the wet polymers have significantly higher ($P < 0.05$) tensile strengths than their dry counterparts. Again the fracture toughness values contrast the tensile strength values. There is no significant difference ($P > 0.05$) between fracture toughness of the wet and

dry Bis-MEPP/PEMA samples. The wet state of the 70/30 system appears to have quite a bit lower fracture toughness than the dry state, but the scatter on the measurement is large. The mechanisms discussed previously in this work that affect the modulus of these systems when they are hydrated also affect their strength properties. The additional polymerization and relief of residual stress that occurs over time in these samples is influenced by the presence of water. It is difficult to say if the presence of water enhances the addition polymerization and relief of residual stress or if it results in a reduction in properties compared to a system aged for a similar amount of time without water present.

The 50/50 and 60/40 wet Bis-MEPP/CHMA systems have significantly ($P < 0.05$) higher tensile strengths than the corresponding dry systems (Figure 3.9). There is no significant difference between tensile strengths of the wet and dry state of the 70/30 and the 40/60 systems ($P < 0.05$). There is no significant difference ($P > 0.05$) in the tensile strength values of the different mol.% formulations within the wet and dry states of the Bis-MEPP/CHMA system. There is no significant difference ($P < 0.05$) in the fracture toughness values for any of the Bis-MEPP/CHMA systems wet or dry or by pair-wise comparison of wet and dry systems with the same mol.% formulation. The same arguments presented for the Bis-MEPP/PEMA systems can be applied to the Bis-MEPP/CHMA systems. Examination of the DMS plots of these systems shows a shoulder located on the low temperature side of tan δ peak in the higher cross-link density systems. The shoulder is not as pronounced in the shoulder in the Bis-MEPP/PEMA systems but its onset is near the same temperature. The lack of resolution is likely due to the increased width of the main portion of the tan δ in the Bis-MEPP/CHMA systems (Table 3.11).

The tensile strength in the Bis-MEPP/t-BCHMA systems decreases with increasing concentration in the dry state with the exception of the 70/30 formulation. In the wet state there is a decreasing trend with the addition of t-BCHMA. Table 3.9 contains the results of statistics comparing the formulations in the wet state, the formulations in the dry state, and the pair-wise comparison of the formulations in the wet and dry state. The fracture toughness behavior is similar to the tensile strength behavior: additions of t-BCHMA greater than 40 mol.% result in a decrease in strength in the wet and dry state. The decrease is not significant between any of the systems in the dry state ($P > 0.05$). The 70/30 and 60/40 Bis-MEPP/t-BCHMA systems are significantly stronger ($P < 0.05$) than the 40/60 systems in the wet state. Pair-wise comparison of the wet and dry states of systems with the same mol.% formulations

Table 3.11: Student's t-tests comparing tensile strengths of the various Bis-MEPP/t-BCHMA formulations in the wet and dry state and the same formulation in its wet and dry state

Significantly different ($P < 0.05$)	Not Significantly Different ($P > 0.05$)
70/30w vs. 40/60w, 60/40d vs. 40/60d, 70/30d vs. 40/60d, 50/50d vs. 40/60d 40/60w vs. 40/60d	70/30w vs. 70/30d, 60/40d vs. 50/50d, 70/30w vs. 50/50w, 70/30w vs. 60/40w, 60/40d vs. 70/30d, 60/40d vs. 40/60w, 60/40w vs. 60/40d, 60/40w vs. 40/60w, 60/40w vs. 50/50w, 50/50w vs. 40/60w, 50/50w vs. 50/50d

indicates that there is not a significant ($P > 0.05$) difference in fracture toughness between any of the systems. As mentioned earlier, extraction studies resulted in weight loss in the Bis-MEPP/t-BCHMA systems and FTIR studies indicated that approximately 10.4 ± 6.1 percent of the vinyl bonds were reacted in the t-BCHMA monomer. The DMS spectra of

the Bis-MEPP/t-BCHMA systems indicate similar network structure to the Bis-MEPP/PEMA and Bis-MEPP/CHMA systems, the shoulder on the low temperature side of the tan δ peak. The high viscosity and Tg of the systems with low concentrations t-BCHMA result in early vitrification and a heterogeneous network structure. As mentioned earlier, additional polymerization and the relief of residual stress of the samples results in improvement of the fracture toughness and tensile strength. This mechanism is more prominent in samples with lower concentrations of t-BCHMA. The water uptake in these samples is also low; therefore, little reduction in properties results from its presence. In these samples, leaching of unreacted materials during hydration can also be considered as a mechanism that will improve properties. In the 70/30 and 60/40 Bis-MEPP/t-BCHMA systems the concentrations of unreacted materials are small and its removal results in improvement in mechanical properties along with the factors mentioned previously in the Bis-MEPP/CHMA and Bis-MEPP/PEMA systems. In the 50/50 and 40/60 Bis-MEPP/t-BCHMA systems the leaching of unreacted material is great enough that the beneficial results of removing the material are minimized. As mentioned earlier, water uptake values are difficult to interpret because of the possible weight loss during hydration. The large amount of unreacted materials in the 50/50 and 40/60 Bis-MEPP/t-BCHMA systems results in the reduction of their mechanical properties when compared to the 70/30 and 60/40 Bis-MEPP/t-BCHMA systems as well as lower average values when the wet state is compared to the dry state.

The tensile strength and fracture toughness properties in the dry state are significantly lower ($P < 0.05$) in the Bis-MEPP/t-BCHMA systems than either the Bis-MEPP/CHMA or the Bis-MEPP/PEMA systems with the exception of the fracture toughness in 60/40 Bis-MEPP/CHMA and Bis-MEPP/t-BCHMA systems, which was not

significantly different ($P > 0.05$). The lack of significance in this system is due to the large scatter in the Bis-MEPP/CHMA systems and the small number of samples in the Bis-MEPP/t-BCHMA system. The low toughness and strength values of the Bis-MEPP/t-BCHMA systems can be attributed to presences of low molar mass materials due to contaminates as discussed earlier, as well as the high viscosity of the monomer systems and the high Tg of the polymer. The high viscosities and Tg result in early vitrification. The cross-link density is also lower in the Bis-MEPP/t-BCHMA systems than the Bis-MEPP/PEMA or Bis-MEPP/t-BCHMA, as indicated by the height of the tan δ peaks. Although the factors such as viscosity, Tg, and cross-link density all play a roll in the properties of the Bis-MEPP/t-BCHMA systems, their true properties are masked by the presence of contaminants and it is possible the difference in the strength properties is purely a result of the contaminants. There is a significant difference between the 40/60 Bis-MEPP/CHMA and Bis-MEPP/PEMA systems ($P < 0.05$). The decrease in fracture toughness in the Bis-MEPP/CHMA systems is due to its more heterogeneous network structure. The Tg, as indicated by DMS, of the 40/60 Bis-MEPP/CHMA systems is higher than that of the Bis-MEPP/PEMA system by 20°C. It is likely that these factors as well as other differences in microstructures formed during polymerization result in a more heterogeneous network structure. This is indicated by the larger width of the tan δ peak of CHMA.

The comparison of the wet state of different systems by formulations shows that Bis-MEPP/t-BCHMA systems have significantly ($P < 0.05$) lower tensile strengths than Bis-MEPP/CHMA and Bis-MEPP/PEMA systems. There is not a significant difference ($P > 0.05$) in the tensile strength values in any of the formulations of the Bis-MEPP/PEMA and Bis-MEPP/CHMA systems. Table 3.11 contains the results of the

statistical comparison of the fracture toughness values of the different systems in the wet state. The lack of significant difference in the wet state is partially due to the large scatter in the fracture toughness values and the small number of samples in some of the sets. The low fracture toughness in 50/50 and 40/60 Bis-MEPP/t-BCHMA systems can be attributed to the high viscosity of the monomers systems, Tg of the polymer formed, low cross-link density, and contaminates as discussed earlier. The presence of low molar mass materials is confirmed by the high amounts of extractable materials in these systems. In the 70/30 and 60/40 Bis-MEPP/t-BCHMA systems the leaching of the unreacted material resulted in some increase in the fracture toughness during the hydration period. Additional polymerization and the relief of residual stress are factors

Table 3.12: Student's t-tests comparing wet fracture toughness values of the various formulations in the wet state

Molar Ratio	Significantly different ($P < 0.05$)	Not Significantly Different ($P > 0.05$)
70/30		PEMA/t-BCHMA, CHMA/t-BCHMA, CHMA/PEMA
60/40	CHMA/t-BCHMA	PEMA/t-BCHMA, CHMA/PEMA
50/50	CHMA/t-BCHMA, PEMA/t-BCHMA	CHMA/PEMA
40/60	CHMA/t-BCHMA, PEMA/t-BCHMA	CHMA/PEMA

that may increase the fracture toughness. The similarity in the results of all the Bis-MEPP/PEMA and Bis-MEPP/CHMA polymers can be attributed to the heterogeneous network structures. The areas of low cross-link density are dictating the properties in both systems, which results in little difference in the tensile and fracture properties. Water uptake is not a factor because it is within the error of measurement for all of the

systems except the Bis-MEPP/t-BCHMA system, which is lower, but the values are suspect due to leaching of material during hydration.

Dynamic Mechanical Spectroscopy

Dynamic mechanical spectroscopy was used to determine the glass transition and β-transition temperatures of the network polymers as well as the change in modulus with temperature. Modulus information is important because of the range of temperatures experienced by dental restorations. The area of the tan delta peak is an indication of the heterogeneity of the networks formed. The width of tan delta peak is a measure of the distribution of environments seen by the polymer chains. The height of the tan delta peak is an indication of the average molar mass between cross-links. Table 3.13 contains a summary of the peaks statistics for the tan δ peaks of all the dry polymers tested in this work. The glass transition temperatures are reported as the temperature at which the maximum in tan δ occurs. As might be expected when comparing the mol.% formulations of the different systems, the Bis-MEPP/t-BCHMA systems generally have the highest glass transition temperatures and the Bis-MEPP/PEMA systems have the lowest. This can be related to the glass transition of the homopolymers formed by monomethacrylates. The homopolymer of t-BCHMA has a higher glass transition temperature due to its stiff bulky structure; therefore, the polymers it forms with Bis-MEPP have higher glass transitions temperature than the Bis-MEPP/PEMA systems. The homopolymer PEMA has lower glass transition temperature due to its more flexible structure; hence, the polymers formed with Bis-MEPP have lower glass transition temperature than either the Bis-MEPP/PEMA or the Bis-MEPP/CHMA polymers. Similar arguments can be made for the Bis-MEPP/CHMA polymers. The glass transition

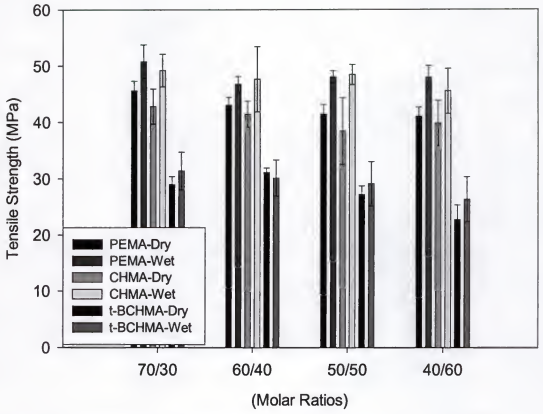

Figure 3.9: Tensile strength values of wet and dry Bis-MEPP/PEMA, Bis-MEPP/CHMA, and Bis-MEPP/t-BCHMA polymers at 37°C

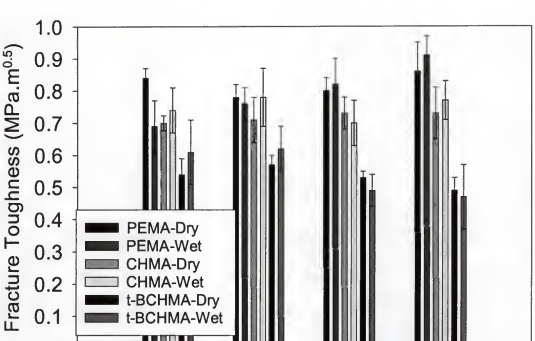

Figure 3.10: Fracture toughness values of wet and dry Bis-MEPP/PEMA, Bis-MEPP/CHMA, and Bis-MEPP/t-BCHMA polymers at 37°C

temperature of the Bis-MEPP/t-BCHMA polymers might also be slightly low due to the contamination discussed earlier. This would account for the similarity in the glass transition temperatures of the 40/60 systems in the Bis-MEPP/CHMA and Bis-MEPP/t-BCHMA systems. The glass transition temperatures of the Bis-MEPP/EDGMA-type polymers are higher than all of the Bis-MEPP/t-BCHMA, Bis-MEPP/CHMA, and Bis-MEPP/PEMA systems because of their low molar mass between cross-links as indicated by the tan δ max values, which are half the magnitude of the highest cross-link density monomethacrylate systems. The maximums in tan δ increase with increasing concentration of monomethacrylate. The values for the same mol.% formulation are similar in the Bis-MEPP/CHMA and Bis-MEPP/PEMA systems. The values for the Bis-MEPP/t-BCHMA systems are generally higher. This may be due to the larger viscosity and glass transition temperatures of the Bis-MEPP/t-BCHMA systems, resulting in early vitrification. The early vitrification would limit the amount of cross-links and result in larger max tan δ values. The contamination in the Bis-MEPP/t-BCHMA systems also results in a reduction in the cross-link density of the systems. The full width at half max (FWHM), which is an indicator the heterogeneity of the network structure, decreases with increasing concentration of monomethacrylates. The FWHM was not reported for the Bis-MEPP/EDGMA systems because the main relaxation is not resolved enough from the β-relaxation to measure the values. The width of the peaks appears to be much broader than the monomethacrylate systems. The FWHM values of the Bis-MEPP/PEMA systems are generally the lowest as might be expected due to the low glass transition temperature and similar viscosities to the systems with the same mol.% formulations. The FWHM values of the Bis-MEPP/t-BCHMA polymers are larger than the corresponding Bis-MEPP/PEMA systems, which is expected based on the glass transition

temperatures and viscosities of the Bis-MEPP/t-BCHMA systems; however, the FHHM values are lower than the Bis-MEPP/CHMA systems. The FWHM values of the Bis-MEPP/CHMA system would be expected to be larger than the Bis-MEPP/PEMA systems, based on the fact the Bis-MEPP/CHMA systems form high Tg polymers at similar formulations. Based on the same argument it might be expected that the FWHM values of the Bis-MEPP/CHMA systems would be smaller than the corresponding Bis-MEPP/t-BCHMA systems, but they are not. The FWHM for the Bis-MEPP/CHMA polymers is exceptionally large and are likely a result of the specific details of network formation that will be discussed in-depth later in this work.

As might be expected, the glass transition, as indicated by the maximum in the tan δ, decreases with increasing amounts of PEMA in the Bis-MEPP/PEMA polymers (Figure 3.11). There is a corresponding decrease in the rubbery modulus values and increase in the magnitude of the tan δ peak with increasing concentrations of PEMA, both of which correspond to a decrease in cross-link density. This is expected due to the reduction in the average functionality of the system and thus the cross-link density, as larger amounts of PEMA are added. There is a notable shoulder on the lower temperature side of the tan δ peak. The shoulder is most prominent in the samples with lower concentrations of the PEMA. The elastic moduli (E') decrease concurrently with the shoulders. These shoulders have been attributed to a β-relaxation in dimethacrylate polymers.

As mentioned earlier β-relaxations in dimethacrylates have been attributed to a number of different physical phenomena. Some have attributed β-relaxations in dimethacrylates to unreacted pendant groups [26]. β-relaxations in methacrylates have

Table 3.13: Statistics on tan δ plots and glass transition activations energies for polymers in the dry state at 1 Hertz

System	FWHM (°C)	Tan δ Max	Glass Transition Temperature (°C)
Bis-MEPP/ PEMA			
70/30	63	0.29	139
60/40	51	0.34	127
50/50	44	0.39	123
40/60	38	0.47	114
Bis-MEPP/ CHMA			
70/30	86	0.28	136
60/40	71	0.31	142
50/50	67	0.37	138
40/60	62	0.41	134
Bis-MEPP/ t-BCHMA			
70/30	65	0.33	149
60/40	55	0.38	148
50/50	54	0.45	142
40/60	51	0.53	135
Bis-MEPP/ TEDGMA	N/A	0.16	172
Bis-MEPP/ EDGMA(400)	N/A	0.14	170
Bis-MEPP/ EDGMA(600)	N/A	0.14	167
Bis-MEPP/ EDGMA(1000)	N/A	0.12	170

been associated with pendant groups; however, β-relaxations in methacrylates are sensitive to frequency[96]. As mentioned earlier, β-relaxations in this work and in other work on [93] dimethacrylates are not sensitive to frequency. β-Relaxations in the ethylene glycol dimethacrylate-type polymers have been attributed to the beginnings of vitrification [24, 95] and larger scale cooperative motions and localized oxyethylene chain motions coupled to the acrylate chain, the precursors of larger scale cooperative motions responsible for glass transitions. β-relaxations occur in glassy ethylene glycol

dimethacrylates in the range of 20 to 30°C[30]. The β-relaxations studied in this work occur at approximately 80°C and the polymers do not have a true oxyethylene structure. The presence of the bis-phenol-A group may stiffen the oxyethylene chain and result in the β-relaxation occurring at a higher temperature. Clarke has also reported similar transitions in Bis-GMA-type polymers [93]. The α and β relaxations in the study by Clarke follow the same trends with frequency as those in this study. The only difference is the relaxations in Clarke's study occur at higher temperatures. The difference is due to variation in the sample preparation methods. The samples in the study by Clarke were heat-cured at 80°C for 3 hours. The samples in this study were prepared by light-initiated cure at room temperature. Clarke argued that these peaks could not be regarded as a relaxation process because they are independent of frequency. The mechanism proposed of cooperative motion and the beginnings of vitrification proposed earlier may account for the β-relaxations' insensitivity to frequency. Wilson has identified β-relaxations in triethylene glycol dimethacrylate in various stages of cure by γ-radiation [94]. The reactions were detected at approximately 40°C and were accompanied by a decrease in sample length. The decrease in sample length was attributed to additional polymerization. The relaxations were attributed to partially vitrified materials that are an artifact of the curing temperature. Studies in which tetra ethylene glycol dimethacrylates were cured initially at 55°C and then post cured at 155°C have reported β-relaxations in the range of 20 to 30°C. This suggests that the β-relaxation is not entirely an artifact of the polymerization temperature. The onset of the β-relaxation occurs at virtually the same temperature in the Bis-MEPP/t-BCHMA, Bis-MEPP/PEMA, and Bis-MEPP/CHMA systems in this work. It is likely that the Bis-MEPP/t-BCHMA, Bis-

MEPP/PEMA, and Bis-MEPP/CHMA samples achieve similar temperatures during their cure cycle. This suggests that the β-relaxations observed in this work are related to the temperature obtained during the cure cycle of these polymers. Several other factors also suggest that these relaxations are related to partially vitrified materials: 1) the apparent insensitivity of the β-relaxation to the concentration of monomethacrylate, i.e., the lack of resolution when the temperature at which the α-transition is decreased by the addition of monomer. This suggests that as the Tg of the polymers is brought down near the temperature of the β-relaxation that the mechanism for the transition is same and 2) the dramatic change in the β-relaxation in the post cured samples (Figure 3.24) shows that in these systems this relaxation is in large part due to a loose defective structure that is an artifact of the cure. The small shoulder left after the post cure indicates there is a relaxation present that can be attributed to β-relaxations common to the methacrylate family.

The tan δ peaks indicate that the location of the glass transition shifts with frequency in the dry 70/30 mol.% Bis-MEPP/PEMA systems (Figure 3.12); however, the temperature that the β-relaxations occur at is not sensitive to frequency within the error of measurement. The magnitude of the β-relaxation decreases with increasing frequency, while the magnitude of the α-relaxation increases with increasing frequency. This may be due to the coupling of the β-relaxation with the α-relaxation. Examination of the E" spectra confirm that the β-relaxation is not sensitive to frequency.

The glass transition temperature, as indicated by the maximum in the tan δ peak, is lower in the wet systems compared to their dry analogs (Figure 3.13). The hydration of the polymers result in a merging of the α and β relaxations (Figure 3.13). As discussed

earlier hydration and aging have been shown to increase conversion in dimethacrylates. Polymerization has also been shown to continue in the vitreous state. If the β-relaxation is associated with the beginnings of vitrification and hydration and aging result in additional polymerization then the temperature at which the β-relaxation occurs would increase during hydration. The main relaxation (α) is associated with a more fully vitrified state that additional polymerization is unlikely to occur in during hydration; hence, hydration results in a decrease in the temperature of the main relaxations due to plasticization. These changes result in the merger of the relaxation in the tan δ plots.

Many of the same features of the Bis-MEPP/PEMA systems are seen in the E' and tan δ plots of the Bis-MEPP/CHMA polymers (Figure 3.14). One notable difference is in the 70/30 systems. The glass transition as indicated by the maximum in the tan δ peak is at a lower temperature than the 60/40 resin systems. This is due to the large amount of pendant groups and low cross-link density material plasticizing this system. This phenomenon is not present in the 70/30 Bis-MEPP/PEMA systems because of the larger weight percent of PEMA at the 70/30 molar ratio. The Tg of 70/30 Bis-MEPP/PEMA polymer is 139°C while the Tg of the 70/30 Bis-MEPP/CHMA is 136°C. The β-relaxations of the Bis-MEPP/CHMA polymers are much less pronounced than those of the Bis-MEPP/PEMA polymers. As discussed earlier the onset of the relaxation begins at the same temperature in both systems but the Bis-MEPP/PEMA systems have a slight plateau region. The magnitude of the tan δ curves in the Bis-MEPP/CHMA polymers increase in a more continuous manner. The main relaxation blends more with the β-relaxation in Bis-MEPP/CHMA. This less resolved shoulder is largely due to the

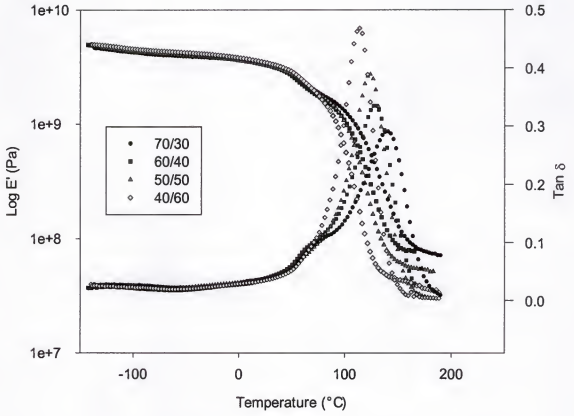

Figure 3.11: Log E' and tan δ response of dry Bis-MEPP/PEMA polymers at 1 hertz

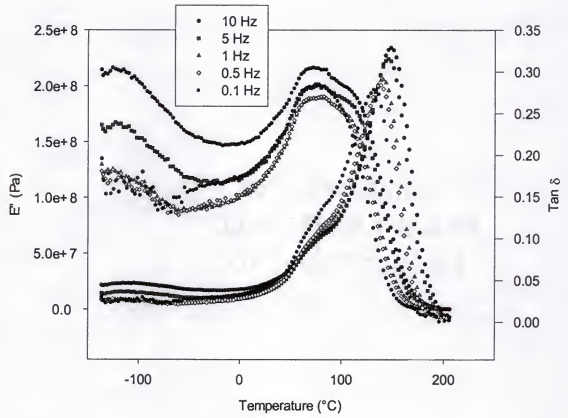

Figure 3.12: Log E' and tan δ response of dry 70/30 Bis-MEPP/PEMA polymers at various frequencies

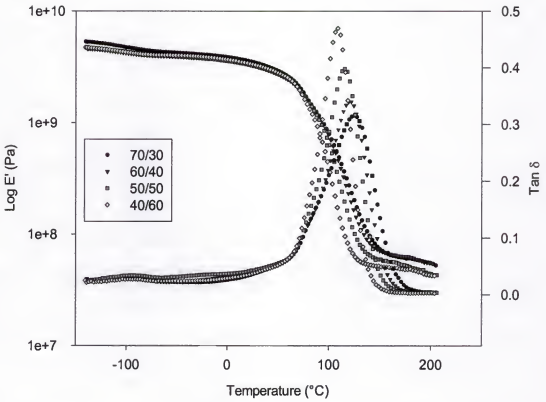

Figure 3.13: Log E' and tan δ response of wet Bis-MEPP/PEMA polymers at 1 hertz

broader width of the main relaxation peak. The onset of the α-relaxation occurs at a lower temperature in the Bis-MEPP/CHMA polymers than the Bis-MEPP/PEMA polymers. The half max widths of the Bis-MEPP/CHMA systems are generally wider than those of the Bis-MEPP/t-BCHMA and Bis-MEPP/CHMA systems. Differences in the glass transitions, monomer viscosity, and the specifics of network formation may account for the broadening. A more in-depth discussion of the peaks widths will be given later in this work. There is also a sub-Tg relaxation or γ-relaxation present at approximately –80°C in the Bis-MEPP/CHMA polymers. This relaxation has been assigned to chair-to-chair configuration changes in the cyclohexane group in poly (cyclohexyl methacrylate) [109]. The increase in the magnitude of the relaxation with increasing concentration of CHMA corroborates this hypothesis. The sub-Tg relaxation is also seen in the E" plots shown in Figure 3.16. As seen with the Bis-MEPP/PEMA systems, the β-relaxations are not affected by frequency (Figure 3.16). The E" plots confirm that the temperature at which the β-relaxations occur is not sensitive to frequency. It is also interesting to note that the maximums in the E" plots occur at the temperature of the β-relaxations. The merging of the shoulder associated with the β-relaxation and the main peak can be attributed to the insensitivity of the β-relaxation to frequency compared to the α transition.

The trends of the DMS spectra of the wet Bis-MEPP/CHMA polymers (Figure 3.15) are similar to those of the dry Bis-MEPP/CHMA resins. The glass transition temperatures decrease with increasing amounts of CHMA. The glass transition temperatures are lower than those of the corresponding dry resins. The β-relaxations in both the Bis-MEPP/CHMA and Bis-MEPP/PEMA are not as prominent in the wet

systems as they are in the dry systems. Again the merging of the shoulder with the main peak can be attributed to the same phenomena that cause the merger of the shoulder and the main peak in the Bis-MEPP/PEMA systems. The sub-Tg relaxation is still present in wet Bis-MEPP/CHMA polymers.

The dry Bis-MEPP/t-BCHMA spectra display the same general trends as both the Bis-MEPP/CHMA and the Bis-MEPP/t-BCHMA systems (Figure 3.17). The temperature at which the glass transition occurs decreases with increasing concentration of the t-BCHMA and the magnitude of the maximum associated with the glass transitions increases. The increase in the magnitude is attributed to a decrease in the cross-link density or a larger molar mass between cross-links. The beginnings of the rubbery plateau region of the E' also indicate an increase in the molar mass between cross-links with increasing amounts of t-BCHMA. The tan δ plots have a shoulder on the low temperature side of the main peaks that is more prominent in the formulations with low concentrations of t-BCHMA. The shoulder is associated with a β-relaxation that can be attributed to the same network structures that caused the relaxations in the Bis-MEPP/PEMA and Bis-MEPP/CHMA polymers. There is also very little change in the Tg values of the 70/30 and 60/40 formulations. The small amount of change is due to pendant groups and contaminants plasticizing the systems. As seen with the Bis-MEPP/PEMA and Bis-MEPP/CHMA systems, the storage moduli (E') decrease correspondingly with the shoulders in the tan δ peaks. Hydration of the Bis-MEPP/t-BCHMA (Figure 3.18) systems results in the same phenomena in the tan δ peaks seen in the Bis-MEPP/PEMA and Bis-MEPP/CHMA systems, which can be attributed to

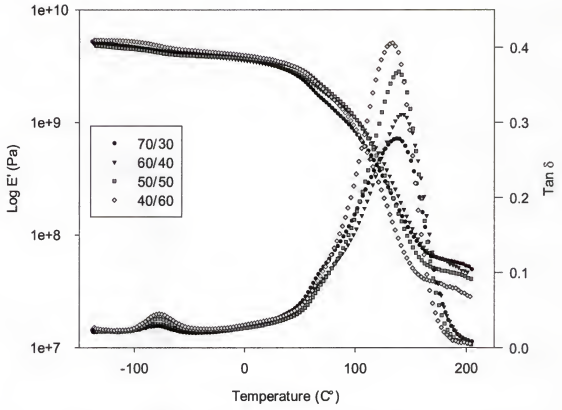

Figure 3.14: Log E' and tan δ response of dry Bis-MEPP/CHMA polymers at 1 hertz

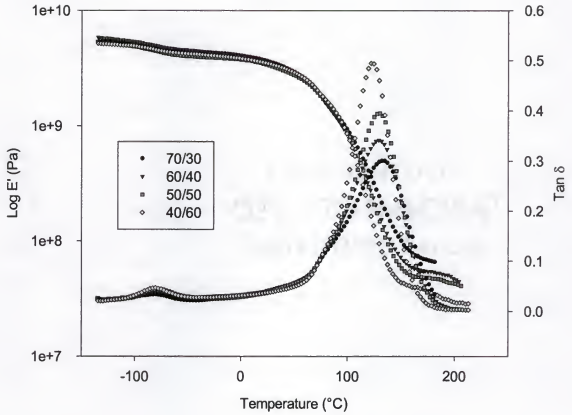

Figure 3.15: Log E' and tan δ response of wet Bis-MEPP/CHMA polymers at 1 hertz.

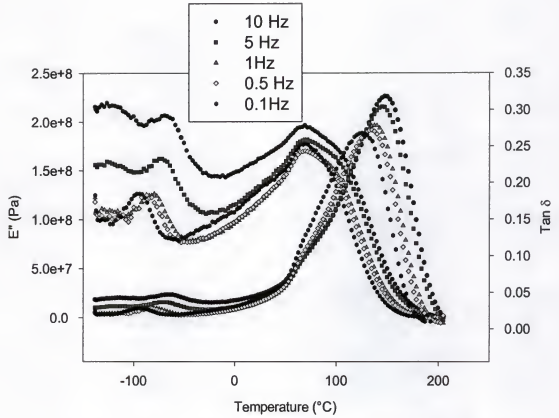

Figure 3.16: Log E' and tan δ response of dry 70/30 Bis-MEPP/CHMA polymers at various frequencies

additional polymerization associated with aging and hydration as well as plasticization of the structures associated with the main relaxations. Examination of the different frequencies of the DMS (not shown) plots showed behavior similar to the Bis-MEPP/CHMA and Bis-MEPP/PEMA systems.

The DMS of the Bis-MEPP/EDGMA type systems in the dry state (Figure 3.19) shows Show many of the same features seen in the monomethacrylate systems: the main peaks, the shoulder and the decrease in storage modulus corresponding with the shoulder in the tan δ peak. One notable difference is the relative size of the shoulders associated with the β-relaxations. The shoulder appears large when compared to the magnitude of the main peak; however its magnitude is similar to the shoulders in the other systems. The small magnitude of the main peak makes the shoulder appear larger. There is also a broad relaxation present at approximately –100°C. Relaxations in this temperature range have been attributed to the presence of moisture in the polymer (-90°C) and localized motions in the oxy-ethylene chains (-130°C) [95]. The relaxation is broad and covers the temperature range from –140 to –80°C in the dry state. The relaxation appears more prominent in the wet state, indicating that it may in fact be due to moisture. Other work on dehydrated Bis-MEPP/TEGDMA resins also show a broad low temperature relaxation [99] that occur in the same temperature range as those seen in the dry. It is likely that both relaxations due to moisture and oxy-ethylene chain mobility are occurring but cannot be resolved. There is also a slow increase in magnitude of the tan δ from approximately –50°C to the onset of the β-relaxation. It is difficult to attribute increase to one physical phenomenon. It is an indication of the overall heterogeneity of the

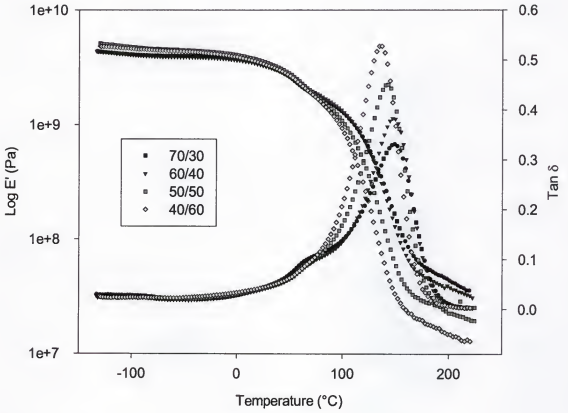

Figure 3.17: Log E' and tan δ response of dry Bis-MEPP/t-BCHMA polymers at 1 hertz.

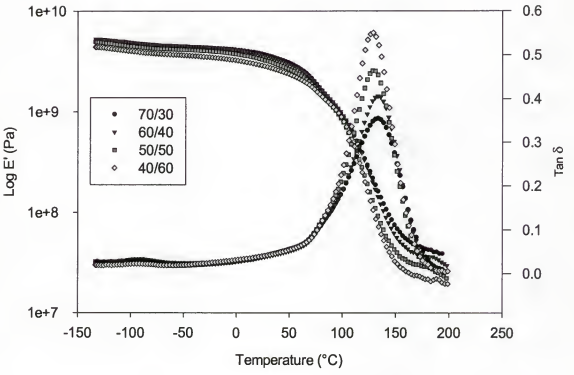

Figure 3.18: Log E' and tan δ response of wet Bis-MEPP/t-BCHMA polymers at 1 hertz

systems formed and distribution of mobility in the network. The height of the tan δ decreases from the TEGDMA to the EG(1000) series. This is due to the smaller N average molar mass between cross-links associated with the increasing range of molar mass units in the diluent mixture. Similar behavior to the monomethacrylate systems is seen in the wet state of the Bis-MEPP/EDGMA-systems (Figure 3.20). The main relaxation decreases in temperature and the β-relaxation increases in temperature. The β-relaxation is more resolved in these systems than the monomethacrylate systems because the main relaxation occurs at a higher temperature. The multifrequency (not shown) plots also show similar behavior to the monomethacrylate systems.

Bis-MEPP/CHMA, Bis-MEPP/t-BCHMA, and Bis-MEPP/PEMA polymers were formulated to the same glass transition temperature to isolate the effect of the viscosity of the monomer systems (Figure 3.21). It is difficult to draw conclusions about the effect of monomer viscosity on heterogeneity when comparing systems that have different glass transition temperatures because vitrification is related to the Tg of the polymer system forming. A polymer system with a high Tg is likely to vitrify sooner than one with a low Tg. The viscosities were 1710 ± 20, 460 ± 10, and 600 ± 10 cp for the Bis-MEPP/PEMA, Bis-MEPP/CHMA, and Bis-MEPP/t-BCHMA systems, respectively. The widths of the tan δ peaks at half max were 59, 62, and 51°C for the Bis-MEPP/PEMA, Bis-MEPP/CHMA and Bis-MEPP/t-BCHMA systems, respectively. There appears to be no correlation between the viscosity of the monomer systems and the width of the tan δ peaks. The Bis-MEPP/CHMA system has the lowest viscosity of the formulated polymers yet it has the largest peaks width. The width of the Bis-MEPP/t-BCHMA

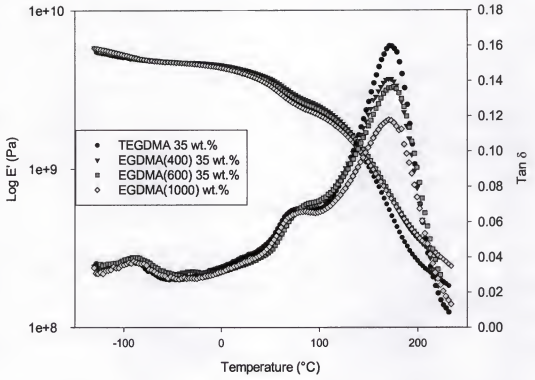

Figure 3.19: Log E' and tan δ response of dry Bis-MEPP/EDGMA type polymers at 1 hertz

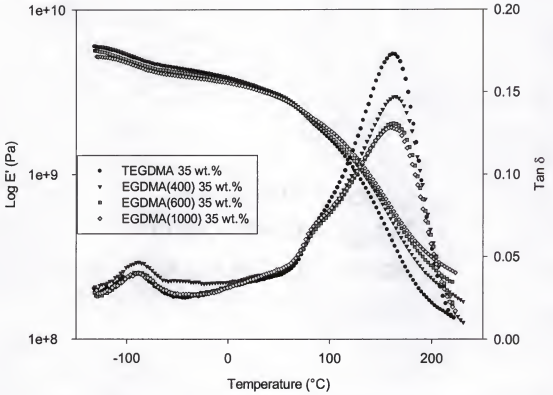

Figure 3.20: Log E' and tan δ response of wet Bis-MEPP/EDGMA type polymers at 1 hertz

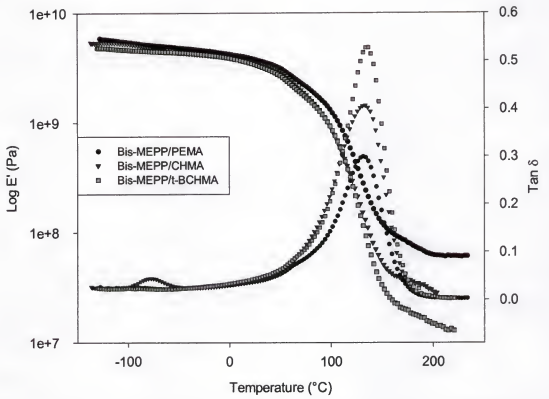

Figure 3.21: Log E' and tan δ response of dry Bis-MEPP/PEMA, Bis-MEPP/CHMA, and Bis-MEPP/t-BCHMA polymers formulated to a Tg of 135°C

system is narrower than the Bis-MEPP/PEMA systems. This is more in line with the expectation that a lower monomer viscosity and a larger molar mass between cross-links will result in a more homogeneous structure; hence, a narrow peak width. The origins of the large peak widths in the Bis-MEPP/CHMA system may be due to such factors as isomers of the CHMA, which are in turn due to its synthesis and specific structural sequences that form during polymerization, i.e., alternating type copolymers, linear segments composed of CHMA units, tacticity, etc. All of these structures are not detectable using any of the techniques in this work so their possible existence and affect on the DMS plots can only be speculated. The possibility of different isomers forming during the synthesis of these systems cannot be discounted; however, their effect would be expected to be pervasive in the all of the systems. Although the specific synthetic techniques of the CHMA and t-BCHMA monomers are not known, the techniques might be similar. Based on this similarity we might expect a similar response of the tan δ curves if the isomers were the cause of the broad line widths. Differences in tacticity might also result in a broader tan δ peak. Again, we might expect similar results in the Bis-MEPP/t-BCHMA and Bis-MEPP/CHMA due to the similar structure; however, the effect of tacticity cannot be ruled out. Dielectric relaxation studies on polymers composed of TEGDMA and methyl acrylate suggest that linear segments of methyl acrylate are formed in the network structure [24]. Similarly, CHMA might form linear segments. CHMA is the smallest of the three monomers and may have the highest mobility, allowing it to diffuse through the partially reacted network and form linear chains of poly (CHMA). The PEMA and t-BCHMA monomers are larger than CHMA and may have more restricted diffusion through the partially reacted network, thus resulting in smaller regions of linear polymer. The lower viscosity of the Bis-

MEPP/CHMA systems when equal masses of the monomethacrylate diluent are compared suggests that CHMA has a higher mobility than PEMA or t-BCHMA; however, no specific data about the relative diffusivity of the these monomers in Bis-MEPP systems is available so these claims cannot be substantiated. Although no claims can be made that clearly explain the unexpectedly wide tan δ peaks width seen in the Bis-MEPP/CHMA systems, the formation of linear segments of poly (CHMA) seems to be the most plausible.

Master curves were made for the Bis-MEPP/PEMA and Bis-MEPP/CHMA systems (Figure 3.22) to obtain additional information about the network structure of these polymers (Table 3.14). The modulus of the Bis-MEPP/CHMA system decreases to smaller values at lower frequencies compared to the Bis-MEPP/PEMA systems. This is due to the lower cross-link density of the Bis-MEPP/CHMA system compared to the Bis-MEPP/PEMA system. The shift factors (Figure 3.23) of the Bis-MEPP/PEMA and Bis-MEPP/CHMA systems are similar in the range of the reference temperature (Table 3.14). The shift factors deviate at temperatures higher and lower than the reference temperature. At 60°C above the reference temperature the shift factors of the Bis-MEPP/CHMA and Bis-MEPP/PEMA systems differ by less than 1, while at 60°C below the temperature the factors differ by almost 5. The C1 and C2 parameters of the WLF equation listed below can be related to the fractional free volume at Tg (f_g) and the

$$\log a_t = \frac{-C_1(T-T_g)}{C_2+T-T_g}$$

thermal coefficient of expansion of the fraction free volume above Tg (α_f). C_1 is identified with $B/2.303f_g$, and C_2 is identified with f_g/α_f [110]. The values for C_1 only vary slightly because the free volume of different polymers in the glassy state does not vary greatly. The smaller C_1 value of Bis-MEPP/PEMA indicates that it has a greater free volume at Tg. The larger C_2 value of the Bis-MEPP/PEMA system indicates that it has a smaller coefficient of thermal expansion. This smaller coefficient is due to its higher cross-link density. The master curves, tan δ, and shift factor plots give insight into the network structure beyond a simple measurement of the glass transition temperature. These results indicate that it is possible to formulate systems that have the same glass-transition temperature with different monomer systems. How the systems behave over a range of temperatures and frequencies is not purely a function of the glass transitions temperature. The details of the network formation such as cross-link density, specific chemical structures, and the distribution of mobilities in different phases dictate the response of the materials over a range of temperature and frequency.

Table 3.14: WLF parameters used to obtain the master curve fits for the Bis-MEPP/PEMA and Bis-MEPP/CHMA systems formulated to a glass transition temperature of 135°C

Polymer	C_1	C_2	Reference temperature (T_r)	Glass transition temperature (T_g)
Bis-MEPP/CHMA	30	175	60	80
Bis-MEPP/PEMA	22	125	60	80

Comparison of Alternate Comonomer Systems by Weight to Triethylene Glycol Dimethacrylate

Triethylene glycol dimethacrylate is considered a baseline or standard of comparison for comonomers in Bis-GMA type systems. This section will compare the mechanical properties of the monomethacrylate and multicomponent ethylene glycol dimethacrylate-based comonomer systems that were formulated at the weight percent ratio of approximately 65/35 Bis-MEPP/comonomer. The Bis-MEPP/EGDMA-type systems will be compared to themselves and the monofunctional monomers will be compared to TEGDMA in the wet state and the dry state.

Flexure Testing

There is not a significant difference between any of the systems based on EGDMA-type comonomer systems ($P > 0.05$) (Figure 3.25) except the EG(600) and EG(1000) systems in the wet state. This is due to the similarity in structure of all these monomer systems. It was originally hoped that formulating multicomponent diluent systems based on ethylene glycol units with a range of molar mass would lower viscosity more effectively than a TEGDMA system. The viscosity values were similar in all the multicomponent systems (Figure 3.6); hence, the properties of these systems are generally similar. There is a slight increase in cross-link densities within the increase in molar mass dispersity as indicated by DMS presented earlier in this work; however, the differences were not great enough to result in significant changes in mechanical properties. Similarly, the lack of difference between the wet and dry modulus can be attributed to the effects of aging in water. As mentioned earlier, aging samples in water has been shown to have little effect on, increase, or decrease modulus depending on the hydrophilicity of the systems in question and the hydration conditions [21, 41, 106]. The

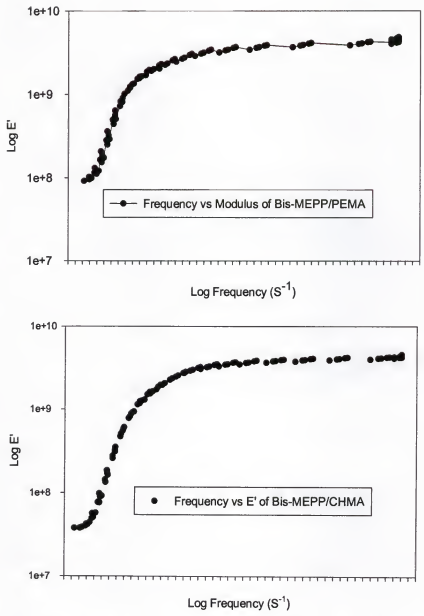

Figure 3.22: Master curve plots of the Bis-MEPP/PEMA (top) and Bis-MEPP/CHMA (bottom) formulated to glass transition temperatures of 135°C (the frequency range of the x-axis is 1e-16 to 1e32 s^{-1}.)

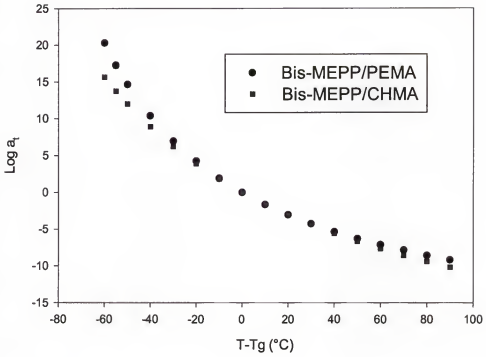

Figure 3.23: The plot of shift factors (a_t) calculated from the WLF equation for the Bis-MEPP/PEMA and Bis-MEPP/CHMA systems formulated to a Tg of 135°C

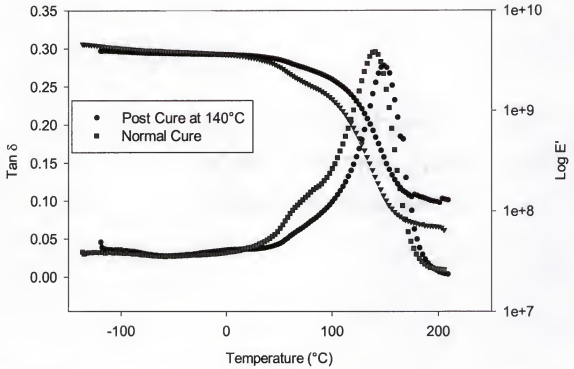

Figure 3.24: Log E' and tan δ response of dry Bis-MEPP/PEMA with normal cure and post cure at 140°C Bis-MEPP/CHMA

competing mechanisms of additional polymerization and plasticization by water dictate the properties of the wet samples. In the case of the EGDMA-modified resins, the quantity of water absorbed is not great enough to cause a reduction in the average modulus through plasticization ($P > 0.05$). In the more hydrophobic monofunctional resins the plasticization caused by the water is not great enough to reduce the modulus of the materials and generally there is an increase in the average modulus. This theory is supported by the larger amount of water absorbed by the Bis-MEPP/EDGMA-type systems.

There is not a significant difference between the Bis-MEPP/TEGDMA system and any of the monomethacrylates in the dry state ($P > 0.05$) except the Bis-MEPP/t-BCHMA system, which has a significantly lower ($P < 0.05$) modulus than all the other systems. The similarity in the modulus is surprising when the difference in cross-link densities is considered. The tan δ peaks are extremely broad in the Bis-MEPP/TEGDMA systems and the presence of the β-relaxations indicate a very heterogeneous network structure. The onset of the β-relaxation is at a lower temperature in the Bis-MEPP/TEGDMA systems than the monomethacrylate systems. As discussed earlier, the defective regions of the network and the incomplete cure of these systems, which is indicated by the shoulder in the tan δ peaks, mediate the modulus values and result in little difference in modulus values despite larger differences in cross-link density.

In the wet state the Bis-MEPP/CHMA system have significantly ($P < 0.05$) larger modulus values than Bis-MEPP/TEDGMA system. The modulus Bis-MEPP/t-BCHMA system is significantly ($P < 0.05$) lower than the other systems. The Bis-MEPP/PEMA and Bis-MEPP/CHMA systems are not significantly different ($P > 0.05$). The phenomena of plasticization by water and additional polymerization are responsible for

the higher modulus seen in the wet state of the Bis-MEPP/CHMA system. The difference seems to be in the amount of water absorbed by the Bis-MEPP/TEDGMA systems. The additional amount of water results in the reduction of modulus compared to the monomethacrylate systems, which absorbed less water. The low modulus values of the Bis-MEPP/t-BCHMA systems are due to the contamination present and may also be related to water uptake. It is difficult to make any conclusion about the properties of water uptake of the Bis-MEPP/t-BCHMA systems due to the possible leaching of material.

Tensile Strength and Fracture Toughness

The tensile strength (Figure 3.24) and fracture toughness (Figure 3.25) will be discussed simultaneously in this section. As might be expected from the flexure results, there is no difference ($P > 0.05$) in the fracture toughness or tensile strength for any of the Bis-MEPP/EDGMA-type systems in the wet or dry states. As discussed in the flexure testing results section, the differences in network structure are not great enough to result in changes in the mechanical properties. There is no significant difference ($P > 0.05$) in the dry tensile strength of the Bis-MEPP/t-BCHMA, Bis-MEPP/CHMA, and Bis-MEPP/TEDGMA polymers. The Bis-MEPP/t-BCHMA system has significantly lower tensile strength ($P < 0.05$) than all the other systems. The dry fracture toughness values of the Bis-MEPP/CHMA and Bis- MEPP/PEMA systems are significantly ($P < 0.05$) greater than the Bis-MEPP/t-BCHMA and Bis-MEPP/TEGDMA systems. There is no significant difference ($P > 0.05$) in the fracture toughness values of the Bis-MEPP/t-BCHMA and Bis-MEPP/TEDGMA systems. The differences in the tensile strength and the fracture toughness results can be attributed to the greater variability of the tensile

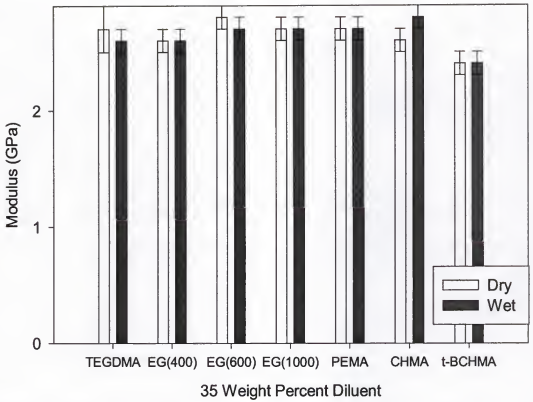

Figure 3.25: Flexure modulus values of wet and dry 65/35 weight percent Bis-MEPP/TEGDMA, Bis-MEPP/EGDMA multicomponent type, Bis-MEPP/CHMA, Bis-MEPP/PEMA, and Bis-MEPP/t-BCHMA polymers at 37°C. The legend represents the monomers used to dilute the Bis-MEPP monomer

strength due to its flaw sensitivity. The higher fracture toughness values of the Bis-MEPP/CHMA and Bis-MEPP/PEMA is surprising, considering the lower cross-link density of these systems compared to the Bis-MEPP/TEGDMA systems. It has been suggested that strength values in cross-linked acrylate polymers are dictated by the loose defective phase or a low cross-link density phase [34]. The decrease in fracture toughness of the Bis-MEPP/TEDGMA despite its high cross-link density suggests that the fracture properties are being dictated by the low cross-link density phase. The DMS spectra presented earlier in this work suggests that the Bis-MEPP/TEDGMA system is more heterogeneous than the Bis-MEPP/CHMA and Bis-MEPP/PEMA systems. This heterogeneity can be associated with a more defective network structure; hence, lower strength. Similar arguments were made for the increased compressive strength when n-butyl methacrylate was added to tertramethacrylate-(bis-trimethylolpropane)-adipate systems[34].

There is no difference in tensile strength ($P > 0.05$) in the wet state of the Bis-MEPP/CHMA, Bis-MEPP/PEMA, and Bis-MEPP/TEDGMA. The Bis-MEPP/t-BCHMA system is significantly weaker than the other wet systems. The Bis-MEPP/CHMA and Bis-MEPP/PEMA systems have higher ($P < 0.05$) fracture toughness values than the Bis-MEPP/t-BCHMA and Bis-MEPP/TEDGMA. The Bis-MEPP/t-BCHMA and Bis-MEPP/TEDGMA systems do not have significantly different ($P > 0.05$) fracture toughness values. The same claims for the higher fracture toughness values of the Bis-MEPP/CHMA and Bis-MEPP/PEMA systems in the dry state can be made for the wet state. The lower fracture toughness of the Bis-MEPP/t-BCHMA system is likely due to the network defects associated with the contamination present in the

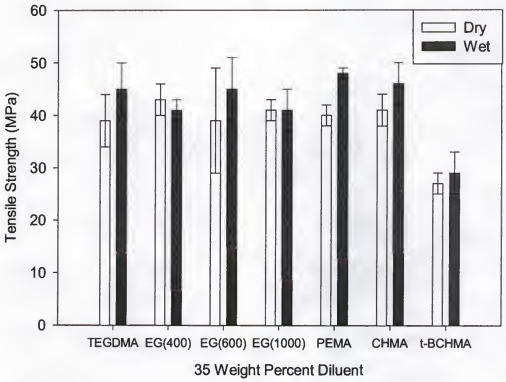

Figure 3.26: Tensile strength values of wet and dry 65/35 weight percent Bis-MEPP/TEGDMA, Bis-MEPP/EGDMA multicomponent type, Bis-MEPP/CHMA, Bis-MEPP/PEMA, and Bis-MEPP/t-BCHMA polymers at 37°C. The legend represents the monomers used to dilute the Bis-MEPP monomer

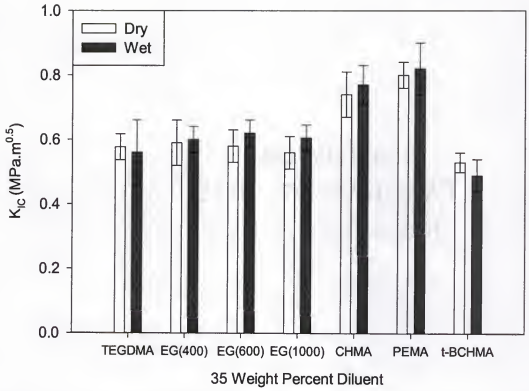

Figure 3.27: Fracture toughness values of wet and dry 65/35 weight percent Bis-MEPP/TEGDMA, Bis-MEPP/EGDMA multicomponent type, Bis-MEPP/CHMA, Bis-MEPP /PEMA, and Bis-MEPP/t-BCHMA polymers at 37°C. The legend represents the monomers used to dilute the Bis-MEPP monomer

t-BCHMA monomer. The fracture toughness of the pure system might be greater than the TEGDMA system, but it is unlikely that it would be much greater than the Bis-MEPP/PEMA and Bis-MEPP/CHMA systems due, to the high glass transition of the polymers it forms and the high viscosities of its monomers systems. The lack of difference in the fracture toughness of Bis-MEPP/CHMA and Bis-MEPP/PEMA, despite their difference cross-link density, suggests that there may be some threshold of cross-link density above which fracture toughness properties begin to degrade. The specifics of network structure such as cyclization, pendant groups, and inactive chain ends may also play a roll in dictating fracture properties.

Conclusions and Future Work

This work shows that monomethacrylates have potential as alternate comonomer systems for Bis-MEPP or Bis-GMA-type resin systems. PEMA and CHMA reduce viscosity more effectively than TEGDMA and yield polymers with lower quantities of remaining double bonds and less shrinkage. The lower viscosities will allow higher filler loadings; hence, composites with better properties. The higher fracture toughness values are also encouraging. The modulus values of these polymers are also comparable with those of Bis-MEPP/TEDGMA systems. The low water uptake of these systems is beneficial and may help reduce plasticization effects during long-term exposure to moisture. The low shrinkage values of Bis-MEPP/t-BCHMA systems are attractive; however, we cannot draw any conclusion about the mechanical properties due to the presence of contaminant. The higher viscosities of the Bis-MEPP/t-BCHMA monomer systems suggest they may not be effective as a viscosity modifying monomers. Again, it is difficult to say what the properties of the pure monomer would be. The Bis-

MEPP/CHMA and Bis-MEPP/PEMA systems have larger molar mass between cross-links than Bis-MEPP/TEDGMA systems. This may make them susceptible to creep in the oral environment. Long-term studies need to be performed to evaluate the properties of these systems and how they might change during long periods of time in the oral environment. Overall, these monomethacrylates are promising as alternate comonomers for Bis-GMA-type resins.

The addition of the monomethacrylates results in a more homogeneous network structure, as determined by the width of the tan δ peaks in DMS plots, compared to Bis-MEPP/TEGDMA systems. The β-relaxation in these systems is associated with a loose defective or low cross-link density phase (that is in large part due to the incomplete cure of these systems) strongly influences the properties of the polymers in this study. It results in normalization of the modulus values of all the systems in this work. When the monomethacrylates are compared to themselves there is very little difference in the strength properties despite differences in the glass transition temperature and cross-link density. The small amount of difference can also be attributed to low cross-link density phase of these materials dictating their strength properties. The more homogeneous network structure of the monomethacrylate-type systems correlates with improved fracture toughness values when they are compared to Bis-MEPP/TEDGMA systems. The similarity of the strength properties of the monomethacrylate type systems to themselves and their improvement over the Bis-MEPP/TEDGMA systems seems to indicate that there is some threshold of cross-link density above which strength properties begin to degrade. Studies with different cure cycles would elucidate whether there is an absolute threshold in dimethacrylates systems or if it is related to the conditions under which the polymers are formed. It would also be interesting to blend the

monomethacrylates with themselves as well as with TEGDMA to optimize the favorable properties of all the systems.

The relationship of the viscosity of the monomer systems to heterogeneity of the network structure formed is not direct but viscosity is an indicator of the heterogeneity that might be expected. Other factors such as the glass transition temperature of the polymer formed, the average functionality of the systems and the details of the network formation strongly affect the heterogeneity of the polymer formed. It was also shown that polymer based on different monomer systems can be formulated to the same glass transition temperature. Although, the polymers have the same glass transition temperature their properties vary across a range of temperature and frequencies due to different distribution of mobility and structures and chemical differences in the systems.

CHAPTER 4
CHARACTERIZING THE HETEROGENITY OF DIMETHACRYLATE POLYMERS

Relevant Background

It has been proposed that the weakest regions, those of low cross-link density, in the polymer determine the strength properties of dimethacrylates [34]. The heterogeneity of dimethacrylate polymers has been demonstrated experimentally using such techniques as dielectric spectroscopy [24, 25], dynamic mechanical spectroscopy [26-28], extraction and swelling experiments [29-31], photochromic [32], charge-recombination luminescence [33], paramagnetic probes [34], and CP/MAS NMR C^{13} spectroscopy [9, 35]. The heterogeneous network structure of dimethacrylates has been studied extensively but many questions still remain. Much of the structure and organization detail that occurs during cure still remains inaccessible to direct observation. The size and distribution of the low and high cross-link density phases, heterogeneity, has still not been determined. If the regions of low cross-link density are acting as flaws and failure is initiated in these regions then knowledge of the size of these regions may allow their correlation with fracture properties. This correlation may ultimately allow the tailoring of monomer selection and cure cycles for enhanced mechanical properties.

The purpose of this work is to combine TappingMode™ AFM (TMAFM) and Xenon-129 NMR methods to characterize the heterogeneity of dimethacrylate-type polymers as it develops during polymerization and in its final state. The heterogeneity of the fully cured polymers will be characterized using TMAFM with phase imaging

capability. TMAFM uses a sinusoidal frequency imposed on the tip. When the tip interacts with the sample the frequency that it oscillates at deviates from the imposed frequency. The phase image is a representation or map of the difference between these frequencies. Different tip-sample interactions will result in different phase shifts for the regions of different cross-link density.

The change in the NMR signal can provide information about how the different phases develop during cure [81]. ^{129}Xenon NMR was performed to further characterize the network structure and its formation. The xenon NMR signal is indicative of its chemical environment. The size of regions was estimated using Pulsed Field Gradient (PFG) NMR spectroscopy. The pulsed field gradient method allowed the calculation of the self-diffusion constant of xenon. With knowledge of the self-diffusion coefficient of xenon estimates were made of root mean square displacement in three dimensions via the following equations [86]:

$$r(t) = \sqrt{6Dt}$$

Where: "t" is the time over which the self-diffusion constant is measured. The self-diffusion constants "D" were calculated from the following relationship [90]:

$$\ln\left(\frac{A(G)}{A(G=0)}\right) = -\gamma^2\delta^2 D(\Delta - \frac{1}{3}\delta)G^2$$

A(G) stands for the echo amplitude in the presence of a field gradient with the strength G, γ is the gyromagnetic ratio of the considered nuclei, Δ is the time interval between the application of the field gradients and δ is the time interval during which the gradient is

applied. By varying the strength of G, D can be obtained from the slope of the resulting curve.

Xenon NMR studies were performed on dimethacrylate systems polymerized with an iniferter initiation system. Iniferter initiator systems were used to gain better control of the degree of conversion and to eliminate trapped radicals, which are detrimental to NMR signals. The iniferter initiation system is based on p-xylylene bis (N, N-diethyl dithiocarbamate) (XDT). Iniferters initiate polymerization when exposed to ultraviolet light. Unlike conventional initiators, iniferter systems form two types of radicals: a carbon radical and a sulfur-based dithiocarbamyl (DTC) radical [111]. The carbon radicals are reactive and capable of initiating polymerization, while the DTC radicals are less reactive and don't participate significantly in initiating polymerization. When the curing light is shut off, the DTC initiator fragments remain mobile and are able to combine with radicals remaining in the system, thus stopping polymerization. This prevents radical trapping and also halts polymerization in a more controlled fashion than a typical light-cured system. Another unique feature of XDT initiated systems is the ability of the DTC fragments to form "marcoiniferters" [111]. The DTC terminated polymer chains decay into radicals upon exposure to light and can reinitiate polymerization. Iniferter based systems are a valuable tool for studying network formation in dimethacrylate systems; however, the polymerization kinetics of XDT are slightly different from those of a conventional photoinitiator. This difference lies in the absence of the autoacceleration effect. Autoacceleration is due to an increase in the concentration of radicals because carbon-carbon radical termination becomes limited by diffusion. As previously mentioned, the DTC radicals remain mobile and thus are able to

terminate carbon radicals; hence, the concentration of radicals does not increase and autoaccelaration is not observed. Despite the differences, iniferter initiated systems form highly cross-linked heterogeneous networks that are analogous to systems polymerized with standard initiators [27].

Materials and Methods.

The xenon nmr samples were composed of 2,2'-bis-(4 - methacryloyloxyethoxyphenyl) propane Bis-MEPP monomer. The iniferter initiator system was 1.0 weight percent p–xylylene bis (N, N –diethyl dithiocarbamate) (XDT). The samples were created by placing the Bis-MEPP (XDT) solutions in 13 mm NMR tubes. The tubes were then placed on a vacuum line and evacuated at a 10^{-13} torr. Freeze-pump-thaw cycles were performed to aid in the removal of trapped air. The samples were then back-filled with xenon gas. A sufficient amount of gas to create a xenon pressure of approximately 10 atmospheres was then condensed into the tube using liquid nitrogen. While the xenon was condensed the tubes were flame sealed. The samples were then placed in a metal container where the xenon was allowed to sublimate. The samples were left in storage for 3 days to test the integrity of the flame seal and allow the xenon gas time to diffuse into the sample. The samples were polymerized in NMR tubes in the presence of xenon gas by exposing the samples to UV light for 10, 15, 20, and 30 seconds, and 5 minutes. The samples were irradiated with a UVP Model UVL-56 black ray lamp. The long wavelength on the black lamp is 366 nm.

Atomic force microscopy samples were prepared in two ways: fracturing and microtoming. Fractured samples were prepared from Bis-MEPP/ triethylene glycol dimethacrylate (TEGDMA) (60/40 wt%) polymers. The 70/30 Bis-MEPP/PEMA

samples, prepared as described in Chapter 3, were microtomed with an LKB/Bromma Ultratome to obtain a smooth surface for imaging. Bis-MEPP/TEGDMA samples were also microtomed. The post cured 70/30 Bis-MEPP/PEMA sample was prepared by placing it in an oven at 140°C for two hours immediately after the initial light curing. Bis-MEPP/TEGDMA samples were soaked in acetone for a period of 36 hours and then dried under vacuum to etch the sample to elucidate the morphology.

Atomic force microscopy was performed using a Digital Instruments NanoScope III in the Tapping Mode™. The phase and height image were recorded for each sample examined. The height images are a representation of the topography of the sample surface. The phase image is representation of the difference between the free oscillating frequency of the AFM tip and the phase of the tip as it interacts with the sample. A more in-depth discussion of sample-tip interactions will be provided in the results and discussion section. Table 4.1 is a compilation of the feed back parameters that were used to perform the scans. The scan sizes were 500 nm and 1000 nm or 1micron. Plane fitting and flattening were performed on all images using the Digital Instruments software.

Fourier Transform Infrared spectroscopy (FTIR) was performed after NMR was run on the samples. The samples were removed from their tubes and FTIR was then used

Table 4.1: Feedback parameters for Tapping Mode™ Atomic Force Microscopy

Parameter	Range of adjustment
Integral Gain	0.1 - 0.6 V
Proportion Gain	0.2 - 1.2 V
Tuning Set Point	0.4 - 2.0 V
Drive Frequency	300 ± 50KHz
Drive amplitude	100 - 700 mV

to measure the conversion of vinyl bonds. Caution was used to avoid exposure to ambient light because it could initiate polymerization in the samples. FTIR spectra were obtained using a Nicolet 20SXB FT-IR spectrometer. A Harrick attenuated total reflection (ATR) stage was used with a 30° KRS-5 parallelogram crystal. The spectra are a result of 64 scans with an instrument resolution of 4 cm^{-1}. The 5-minute cure sample was cryo-milled and then made into a KBr pellet. The pellet was measured in transmission. The quantity of vinyl bonds remaining or the degree of conversion was estimated using the equation given in Chapter 3.

Xenon NMR was performed using a Bruker Avance 400 Digital NMR spectrometer equipped with a triple resonance 10 mm high-resolution probe. The magnetic field strength used was 9.4 T/m. A Bruker imaging gradient stack was used to apply the field gradients. All spectra are referenced to a xenon thermal standard located at a frequency of 110.7 MHz. All experiments were performed at 25°C.

Standard xenon NMR spectra were collected from the samples prior to the diffusion measurements to locate the center frequency of the xenon signal in each sample. The parameters used to collect the spectra are located in Table 4.2.Pulsed gradient

Table 4.2: Parameters used to collect standard xenon spectra of Bis-MEPP(XDT) samples

Parameter	Value
Sweep Width	26455 Hz
Acquisition Time	0.4533 s
Dwell Time	18.9 μs
Relaxation Delay	40 s
Pulse Length	30 μs
Pulse Strength	3.0 dB
Number of FIDs Collected	16

experiments were performed using stimulated echo and Hahn echo sequences. The pulse schemes for a standard or Hahn echo pulsed field gradient and stimulated echo pulsed field gradient sequence are pictured in Figure 4.1. The linearity of the field gradient strengths was calibrated by measuring the self-diffusion coefficients of water. The calibration experiments were performed on de-ionized water doped with 5 μM manganese chloride salt. The Mn salt is paramagnetic and enhances T1 relaxation times from 5 to ~0.2 seconds. The first experiments were performed using a standard pulsed gradient sequence with the parameters described in Table 4.3. The experiments were performed with 64 gradient steps. The measured self-diffusion coefficient for water was determined to be $2.10 \pm 0.05 * 10^{-5}$ cm^2/s.

Table 4.3: Hahn echo sequence parameters used for water self-diffusion coefficient measurements

Parameter	Values
90° Pulse	29 μsec at 3 dB
180° Pulse	29 μsec at –3 dB
δ - Gradient Time	5 msec
G – Gradient Strength	5-900 mT/m
Δ - Time Between Gradient Pulses	20 msec

The self-diffusion coefficient of water was also measured using the stimulated echo sequence. The parameters used in the stimulated sequence were the same as the Hahn sequence with the exception of the absence of 180° pulse. In addition to the gradient strength range from 5 to 900 mT/m range experiments were also performed in the range 10 to 210 mT/m. The sequences were performed with 16 and 64 gradient steps. The diffusion values from the 16 step and 64 step experiments performed in 10 to 210mT/m

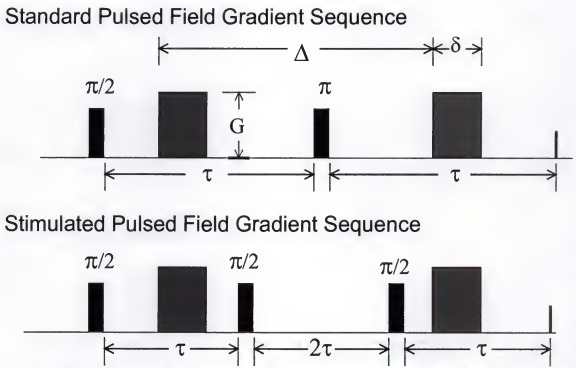

Figure 4.1: Pulse schemes of Hahn echo pulsed field gradient and stimulated echo pulsed field gradient sequence

gradient range were $2.18 \pm 0.18*10^{-5}$ cm^2/s and $2.04 \pm 0.13*10^{-5}$ cm^2/s, respectively. The diffusion values from the 16 step and 64 step experiments performed in 5 to 900mT/m gradient range were $2.27 \pm 0.12*10^{-5}$ cm^2/s and $2.15 \pm 0.06*10^{-5}$ cm^2/s. Values reported from other pulsed gradient diffusion studies are $2.34 \pm 0.08*10^{-5}$ cm^2/s [90]. The same authors reported a value of $2.23 \pm 0.05*10^{-5}$ cm^2/s with steady gradient experiments. Simpson and Carr reported a value of $2.13 \pm 0.15*10^{-5}$ cm^2/s [112].

Measurements were made on the Bis-MEPP(XDT) samples using the stimulated echo sequence. The parameters used in pulse sequence to measure the self-diffusion coefficient of xenon in the Bis-MEPP(XDT) systems are located in Table 4.4.

Table 4.4: Parameters used in pulse sequence to measure the self-diffusion coefficient of xenon in Bis-MEPP(XDT)

Parameter	0, 10, 15, and 20 Second cure	30 Second cure
90° Pulse	3 dB	3d B
Delay Time Between Scans	40 s	40 s
δ - Gradient Time	5 ms	0.5 ms
G – Gradient Strength	5-700 mT/m	5-700 mT/m
Δ - Time Between Gradient Pulses	0.5 s	1.0 s
Number of Gradient Steps	8	6
Number of FIDs Collected	64	256

Results and Discussion

Atomic Force Microscopy

Assigning phase and height components to atomic force microscopy (AFM) images is not a trivial task. The height and phase images depend on experimental parameters such as the free oscillation amplitude of the tip (A_0), the set-point amplitude (A_{sp}), the tip shape, the cantilever force constant, the compliance of the sample to the tip, and the frequency of the oscillation [113]. Correlating regions of different phase shifts

with the corresponding polymeric phases requires knowledge of type of sample-tip interaction that is occurring during imaging. In fact other experiments are often needed to correlate the polymeric components with the areas of different phase shift. The types of interactions that take place are partially controlled by the feedback parameters used to image the surface. Three regions of tip-sample interaction have been identified based on the ratio of the set-point amplitude (A_{sp}) to the free oscillation amplitude (A_o), $r_{sp} = (A_{sp}/A_o)$. The set-point amplitude is the amplitude that is maintained during scanning by adjustment of the vertical position of the tip. The free-oscillating amplitude is the amplitude of the AFM tip oscillation when it is not in contact with the surface. The regions are as follows: soft tapping ($r_{sp} > \sim 0.8$), moderate tapping ($r_{sp} = \sim 0.7 - 0.2$), and hard tapping ($r_{sp} < \sim 0.2$)[114]. Van der Waals and capillary forces govern the soft tapping regime tip-samples interactions, and negative phase shifts are observed. In the moderate and hard tapping regime repulsive forces govern tip-sample interactions, and positive phase shifts are observed. It should be noted that in all regimes the cantilever experiences both repulsive and attractive forces at various points in its oscillation cycle. However, the forces discussed above are the dominant forces in that regime. The magnitude of the free oscillation amplitude also has an effect on the tip-sample interactions [114, 115]. At small amplitudes, approximately 15 nm, attractive forces are dominant at all r_{sp} values. Larger amplitudes, approximately 45nm or greater, repulsive interactions dominate and positive phase shifts occur. Bar et al. have examined poly (ethene-co-styrene)/poly (2,6-dimethyl-1,4-phenylene oxide) blends by imaging samples in the soft, moderate and hard tapping regimes[114]. Contrast inversion occurred twice while the different regimes of tip-sample interaction were examined. In terms of the

images presented in this work, softer phases can be made to appear dark or light depending on the parameters selected. In the work by Bar et al. hard phases appear brighter, a greater positive phase shift, in the moderate tapping regime. Other work has also shown similar results [115-117]. In the moderate regime, the tip-sample interaction is dominated by sample stiffness; hence, the harder phases appear brighter. In the hard tapping regime soft phases appear brighter and hard phases appear darker. In the hard tapping regime the AFM tip spends a larger portion of its time in contract with the sample surface. Area effects result when the tip spends a significant portion of its oscillation in contact with the sample. A softer sample allows more material to come in contact with the tip of the sample. The larger sample area results in a larger effective stiffness. The higher stiffness results in increased repulsion forces thus a greater phase shift than the stiffer materials. Similar results have been demonstrated with poly (ethylene) blends composed to low and high density regions, and poly (diethyl siloxane) on silicon substrates [115].

Even with the knowledge of the different regimes of tip-sample interaction caution must be maintained when making assignments to regions of different contrast. Each polymer system must be treated individually. The response of known polymer systems in the different regimes of tapping should only be used as a guide for interpretation of images. As stated previously other experiments are often needed to correlate the polymeric components with the areas of different phase shifts. Two-studies on block copolymers illustrate these statements [113, 118]. The PMMA phase in a PMMA-b-PBD-b-PMMA polymer was identified as the component with less phase shift. This assignment was based on two correlations. First, a correlation was drawn between

the mass percent of phases and the image analysis. Second, a correlation was drawn between phase images and the corresponding height images. It was proposed that the softer domains, which correlate with regions of larger phase shift, appeared higher in the topography image. The increase in height is a result of softer phase polymer relaxing by protruding out of the surface of the material. The exact parameters of the tapping were not provided so the tapping regime that the image was recording in could not be ascertained. An assignment based on correlations between height and phase images alone is suspect because height artifacts are possible as a result of tip-sample interactions with materials of different stiffness [114]. In the moderate tapping regime stiff regions of a sample appear higher than the soft regions because they deform less during the tip-sample interaction. The feedback mechanism of the TMAFM adjusts the tip to sample distance so that constant amplitude is maintained. A hard material deforms less and results in the tip being adjusted higher relative to a soft sample to maintain the set-point amplitude. Conversely, a softer material allows the tip to indent more; therefore, the tip must be held at a lower height to maintain the same set-point amplitude. In a study of butadiene/styrene-co-butadiene rubber blends [113], the butadiene phase was identified as the phase with the greater phase shift. Although the styrene-co-butadiene phase is stiffer, area effects resulted in a greater phase shift for the butadiene phase. Frequency-sweep and force-probe measurements were performed to understand the factors affecting the images. Force-probe experiments indicated that at any given r_{sp} value the indention depth of the tip is greater in the butadiene phase. The more compliant sample allows a greater amount of materials to come in contact with the tip. This results in a greater phase shift. Correlation of indention depth to phase shift showed that at a constant

indention depth the styrene-co-butadiene phase had the greater phase shift due to its higher stiffness. Similar results were reported in poly (dimethylsiloxane) samples formulated with different cross-links densities [119, 120]. Despite the varying moduli there was not a significant difference in the phase shift for PDMS sample with different cross-link densities. This similarity was attributed to area effects.

Initially fracture surfaces were imaged to avoid surface and mold effects and to expose the bulk morphology. The images of the fracture surfaces of 60/40 Bis-MEPP/TEGDMA (Figures 4.2 and 4.3) indicate that the morphology is on the range of 25 to 150 nm. The light and dark areas represent the low and high cross-link density phases. Assignment of the regions of different contact will be addressed later in this work. The tortuous surface of the fractured samples prevented extensive imaging. Microtomed samples provided a less tortuous surface while still exposing the bulk morphology of the samples. Images taken of the microtomed surfaces show the same features as those samples prepared by fracture. The topographic and phase images of a microtomed 70/30 Bis-MEPP/PEMA sample at a 500 nm scale (Figure 4.4) was recorded with a free oscillating amplitude (A_o) of 3.0 V and set-point amplitude of approximately 1.0 V. These parameters correspond with what has been described previously as moderate tapping. The same sample at a 1micron scale (Figure 4.5) was recorded with an A_o value of 3.0 V and a set-point values of 0.78 V. These settings fall within the low end of r_{sp} values that have been defined as moderate tapping. The terms A_0 and A_{sp} have been discussed previously in terms of amplitudes. A_0 and A_{sp} are given in units of voltage by the AFM software. The voltages reported by the instrument are related to the

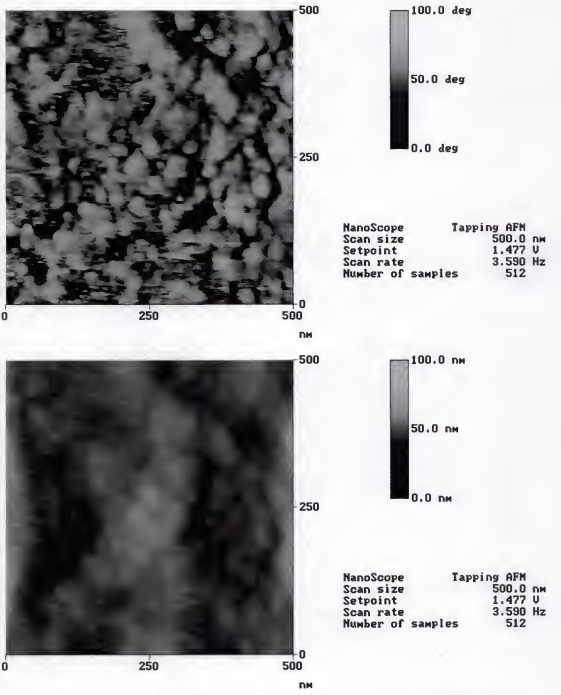

Figure 4.2: Phase and topographic AFM images of a fracture surface of a 60/40 Bis-MEPP/TEGDMA polymer at 500 nm scale

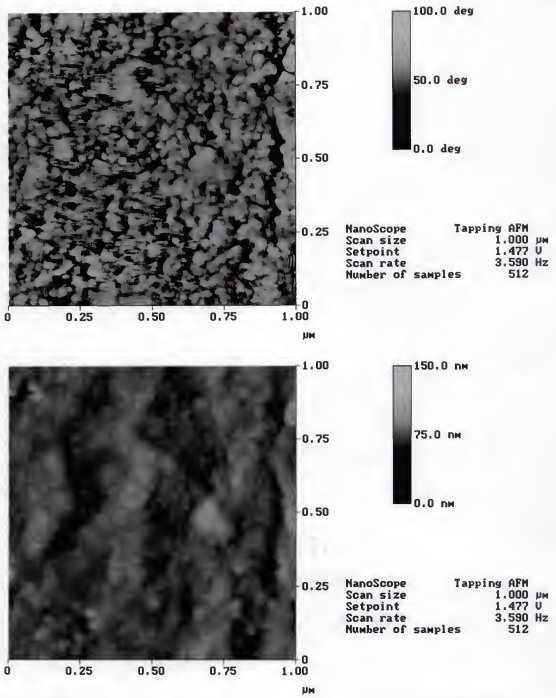

Figure 4.3: Phase and topographic AFM images of a fracture surface of a 60/40 Bis-MEPP/TEGDMA polymer at a 1 µm scale

amplitude of the tip oscillation; however, the actual amplitude of oscillation depends on the spring constant of the tip. A separate experiment is necessary to report the magnitude of the oscillation. The different regions of phase shift (Figure 4.4) represent the high and low cross-link density phases of the polymer. Examination of phase and topographic images shows that at a large scale, the height variation from the lower-left hand corner to the upper-right hand corner, the phase image is independent of the topographic features. At a smaller scale there is a correlation between the bright features and the local maximums in the topographic image. There is no sharp change in contrast between the light and dark regions and there also appears to be some regions with an intermediate contrast. The lack of sharp contrast change is most likely a result of domains that are partially located below the sample surface. Similarly, the regions of intermediate contrast are a result of phases that are located below the exposed surface. The 1000 nm image (Figure 4.5) has the same features as the 500 nm image (Figure 4.4) except the regions scale down with the size of the image. The size of the regions seen in the phase images correlates with the size of polymeric particles that have been isolated early in the cure cycle of ethylene glycol dimethacrylate[11]. The isolated particles had a biomodal size distribution with mean sizes in the range of 19 to 30 nm and 83 to 134 nm. It was proposed that larger particle sizes might be a result of the agglomeration of the primary particles. Strict comparison between the ethylene glycol dimethacrylate system and the ones examined this work is not possible because of the differences in the monomers structure and the initiator systems; however, the correlation between sizes of the isolated particles and the domains sizes seen in the phase images is encouraging. It should also be noted that it has been suggested that cross-linked polymers formed by chain

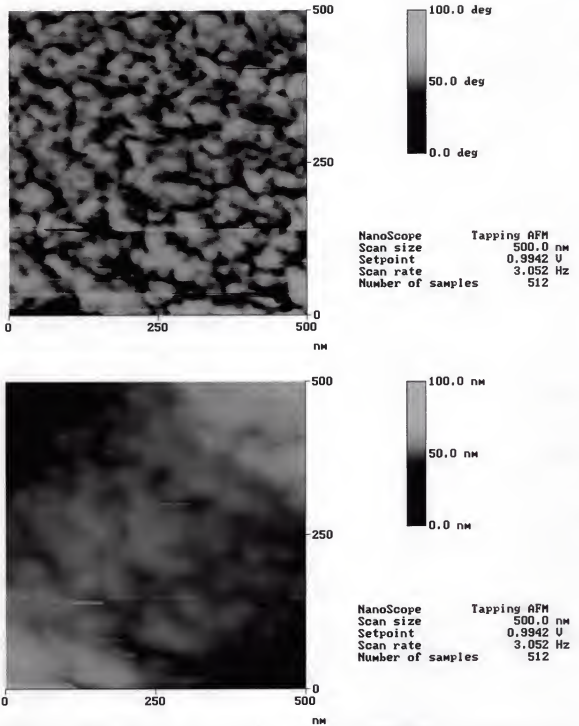

Figure 4.4: Phase and topographic AFM images of a microtomed surface of a 70/30 Bis-MEPP/PEMA polymer at 500 nm scale

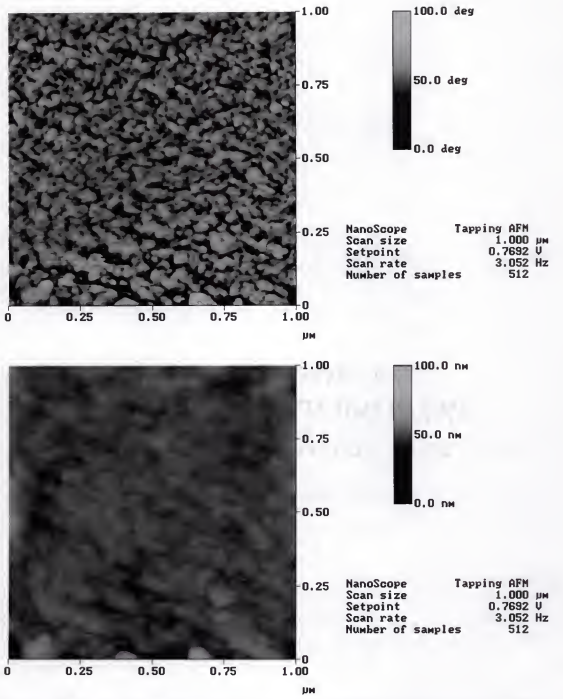

Figure 4.5: Phase and topographic AFM images of a microtomed surface of a 70/30 Bis-MEPP/PEMA polymer at 1 μm scale

polymerization have areas of low and high cross-link density with sizes on the order of 10 to 50 nm [110]. The variation in phase size is notable especially in the 1 micron images. This variation is expected due to the complex mechanism of formation of these polymers. As discussed early in this work heterogeneity in dimethacrylate polymers has it roots early in polymerization with the formation of microgel particles. Briefly, preferential polymerization around these particles and their eventual agglomeration results in the region of low and high cross-link density, heterogeneity. The variation in the domain sizes of the structures is a result of how the polymer particles agglomerate during polymerization.

As discussed previously, assigning regions of different contrast to specific morphological structures is a complex task and additional knowledge of the system in question is required to assign regions of different phase contrast to specific morphologies. To help make the assignments a microtomed sample was immersed in acetone for 36 hours, then removed and dried, and a post cured sample was also prepared. The phase and topographic images of the sample treated with acetone are contained in Figure 4.6. A 3-D perspective image of the phase image is provided in Figure 4.7 to elucidate morphology change induced by exposing the sample to acetone. Based on the images of the light-cured samples an assignment of specific morphological regions to area with different phase shift is not possible. The first factor considered was the relative amount of the different phases present. Based on the degree of conversion (~66%) of the 70/30 Bis-MEPP/PEMA, it might be expected that there would be a ratio of approximately 7 to 3 high cross-link density phase to the low cross-link density phase. However, it is not possible to make this assumption because the relative concentration of double bonds

within the different phases is not known. Chiu et al. have shown that the isolated microgels of ethylene glycol dimethacrylate, which is considered to be a region of high cross-link density, were found to have pedant double bonds [11]. One correlation that can be drawn from the images in Figures 4.2-4.5 is the relationship between local maxim in the height image and regions of bright contrast or large phase shifts. It has been proposed that a softer phase has the ability to relax by protruding out of the surface of a sample due to its higher mobility [118]. Based on this analysis it is temping to make the correlation between the regions of high phase shift and the low cross-link density phase. Two other factors must be considered that impede the assignment of the regions of high phase contrast to the low cross-link density phase. One, it has been shown that harder phases appear artificially high in topographic images due to reasons discussed earlier [114]. Two, examination of the images of samples exposed to acetone (Figures 4.6 and 4.7) shows that the regions of high phase shift correlate with higher topographic features. The exposure of the samples to acetone could result in the removal of the low cross-link density material or preferential swelling of the low cross-link density phase. Comparison of a post cured sample to a standard light-cured sample give another point of comparison to make the assignment. The phase and topographic images of a standard 70/30 Bis-MEPP/PEMA sample and the post cured 70/30 Bis-MEPP/PEMA (Figures 4.8 and 4.9) were both taken with the same tip and feedback parameters to minimize artifacts caused by differences in tip spring constants and imaging in different tapping regimes. The post cure should reduce the amount of volume of the low cross-linked density phase. The size of the region that represents that low cross-link density phase will be reduced in the images. In the images of the post cured sample (Figure 4.9), the lighter region (higher

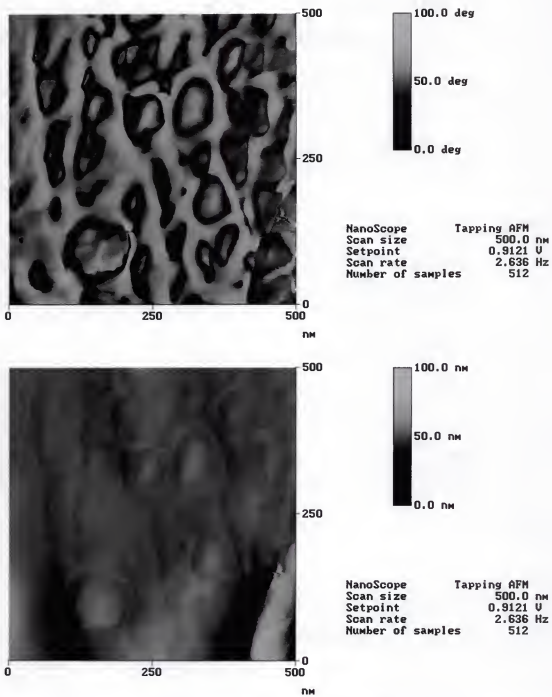

Figure 4.6: Phase and topographic AFM images of a microtomed surface of a 60/40 Bis-MEPP/TEGDMA polymer immersed in acetone and then dried

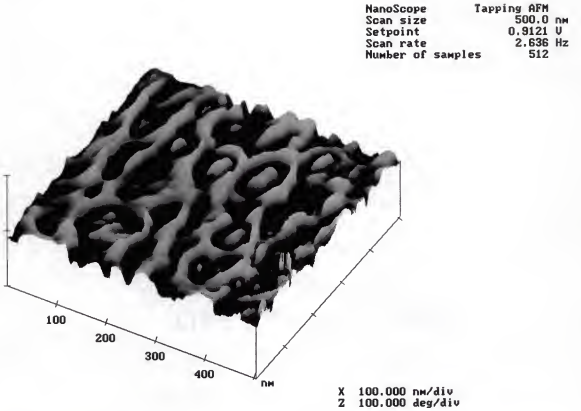

Figure 4.7: The 3-D perspective of an AFM phase image of a microtomed surface of a 60/40 Bis-MEPP/TEGDMA polymer immersed in acetone and then dried

phase shift) increases in size and the darker region (lower phase shift) decreases. This indicates that the brighter regions (higher phase contrast) represent the higher cross-link density phase. The growth of the bright regions (greater shift phase) upon post curing coupled with the apparent etching of dark phase (low phase contrast) in the samples exposed to acetone allows the brighter areas to be assigned to the high cross-link density phase. The assignment of the brighter regions to the high cross-link density phase correlates well with other studies, which showed that stiffer regions had a larger phase shift in the moderate tapping regime[114, 116].

It should be noted that there is some difference in appearance between the 70/30 images with a A_{sp} of 0.4 V (Figure 4.8) and the one imaged with a A_{sp} of ~ 1.0 V (Figure 4.4). The phase image taken at the higher set-point (Figure 4.8) appears to have more fine features than the image taken at the lower set-point (Figure 4.4). Some of the difference may be due to local variations in microstructure; however, the image in Figure 4.8 was taken in the hard tapping regime. The stronger sample tip interaction results in greater exposure of phases that are located beneath the surface of the sample. Phase inversion, the reversal in contrast between the different phases, has been reported when samples are imaged in different tapping regimes [114],[115]; however, phase inversion does not occur in all systems [113]. There were no signs of phase inversion observed in the images obtained in this work.

Xenon-129 NMR

The narrow peak of the xenon NMR spectra of the Bis-MEPP(XDT) monomer (Figure 4.10) is an indication that the xenon samples all the chemical environments in the monomer at a high frequency. The fast exchange results in a signal that is an average of

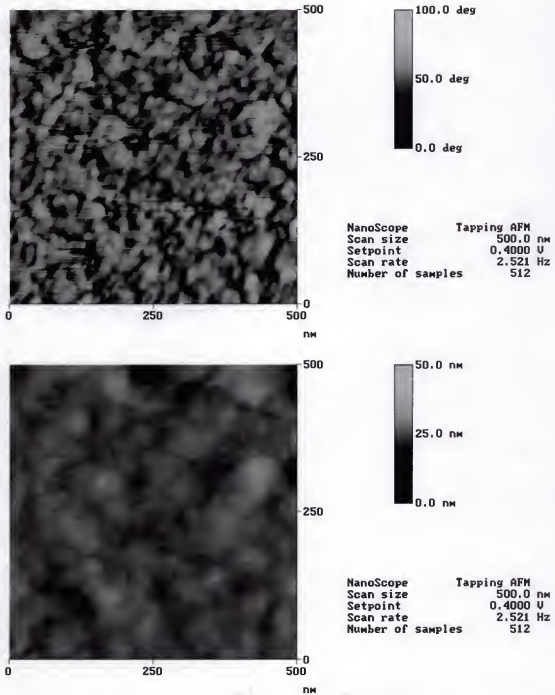

Figure 4.8: Phase and topographic AFM images of a microtomed surface of a 70/30 Bis-MEPP/PEMA polymer imaged with a set-point value of 0.40 volts at 500 nm scale

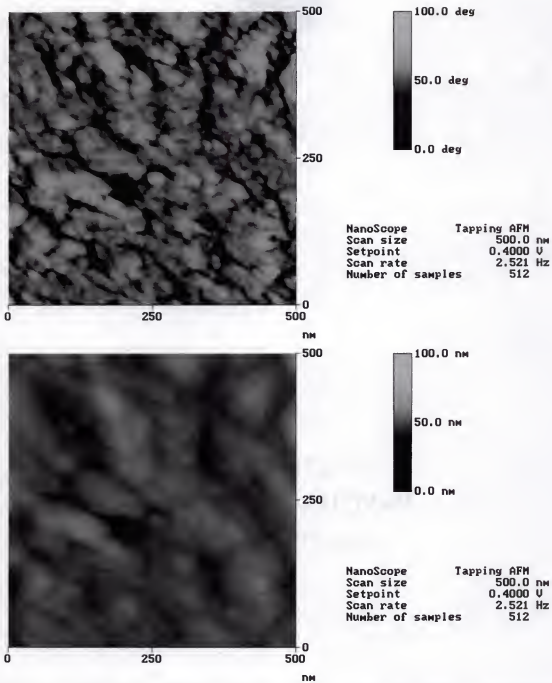

Figure 4.9: Phase and topographic AFM images of a microtomed surface of a 70/30 Bis-MEPP/PEMA polymer post cured for 2 hours at 140°C immediately after light-curing imaged with a set-point value of 0.40 volts at 500 nm scale

all the environments. It should be noted that a comparison of the relative magnitudes of the peaks is not possible for Figures 4.10-4.12. One can easily discern that the peak shifts further downfield as the degree of conversion is increased. The peak width increases and the intensity decreases with longer cure times. Similar behavior was reported when xenon NMR was used to follow the cross-linking reaction of poly (urethane) [81]. As the Bis-MEPP(XDT) system cures and becomes more dense and less uniform the exchange of xenon between the different environments slows down. The greater distribution of environments and the smaller

Table 4.5: Xenon NMR spectrum parameters for Bis-MEPP(XDT) at various stages of cure

Sample	Chemical Shift (ppm)	Line Width (Hz)	Intensity (AU)
Monomer	190.0	22	3,530,106
30	195.3	274.5	941,252
5 minutes	198.9	545.8	298,921

amount of signal averaging result in a broader peak. Similarly, the intensity of the peaks decreases from 3,530,106 for the monomer to 298,921 for the sample cured for 5 minutes. As the Bis-MEPP cures the high cross-link density phases compose more volume fraction of the sample and the xenon is expelled from the sample. The smaller amount of xenon present in the sample results in lower signal intensity.

The sample cured for 5 minutes has attained the maximum degree of conversion possible by light curing at room temperature. A Bis-MEPP sample cured using the camphorquinone/di-methyl-p-toluidine initiator described elsewhere in this work attained roughly the same degree of conversion. Upon removal from the NMR tube the sample

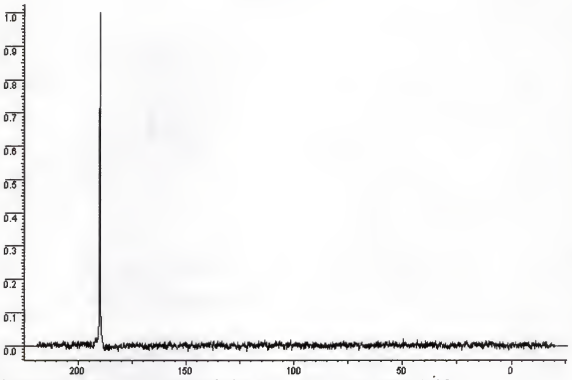

Figure 4.10: Xenon-129 spectra of Bis-MEPP(XDT) monomer at 25°C

appeared to be glassy. The xenon spectra of glassy polymers are generally weak and very broad. The line width of polycarbonate was reported at 500 Hz in a 4.7 tesla magnetic field strength [77]. The line width of PMMA was reported at 2000 Hz at 4.7 tesla magnetic field strength. The full width half maximum line width of the 5-minute cure sample was 545.76 at 9.4 tesla magnetic field. Assuming a rapid exchange limit is reached the change in line-width is proportional to the square root of the magnetic field strength [77]. This approximation estimates the line width of the 5-minute cure sample at 385 Hz in a 4.7 tesla magnetic field. The smaller line width, line shape, and intensity of the spectrum indicate a portion of the material in this sample is not in a fully vitrified state and has a pore structure that accommodates more xenon than a fully glassy structure. The existence of a bimodal distribution of pore structures is corroborated by the bimodal phase distribution seen in the AFM images presented earlier in this chapter.

The lack of two clearly resolved peaks in the spectra of the samples cured for 30 seconds and 5 minutes is not necessarily an indication of a material consisting of a single phase. As mentioned earlier the solubility of xenon in the glassy highly cross-linked phase is small compared to that of the monomer and the low cross-link density phase. The high density results in the low xenon solubility and a broad weak signal. The contribution of the highly cross-linked phase to the signal is minor; therefore, the signal of the highly cross-link phase cannot be easily resolved from that of the low cross-linked phase. Depending on the rate of the diffusion of xenon in the various phases and the size of the phases, the single peak might be the result of signal averaging from the different phases. Similar behavior has been reported in PEO/PMMA blends [87]. PMMA, a glassy polymer, was referred to as a "hidden exchange partner" because its contribution

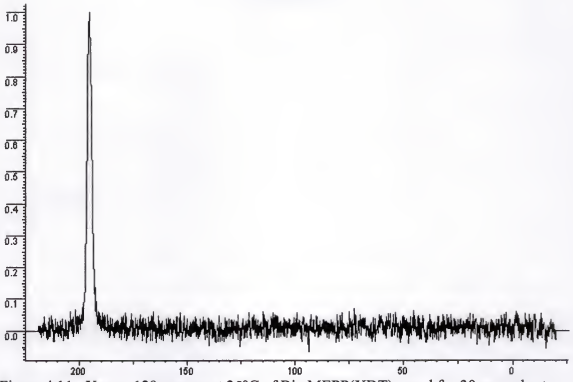

Figure 4.11: Xenon-129 spectra at 25°C of Bis-MEPP(XDT) cured for 30 seconds at 25°C

to the signal in the blends was difficult to resolve. As mentioned earlier, PMMA has a broad weak signal.

If two assumptions are made, an estimation of the volume fraction of the phases that are present can be made based on the difference in intensity of the monomer spectrum and the spectrum of the sample cured for 5 minutes. The first assumption is that the differences in pressures between the xenon samples in negligible and does not affect the intensity of the signal. The second assumption is that the two phases formed are a highly cross-linked phase, in which gas solubility is negligible compared to the monomer phase, and a monomer like phase. The volume fraction of monomer like phase, calculated using these assumptions, is approximately 8.5 volume percent. A more accurate description of the monomer phase is one of low cross-link density with higher mobility than the highly cross-linked phase. The solubility of xenon in this phase is lower than that of the monomer. This indicates that the volume fraction of the low cross-link density phase is greater than 8.5 percent.

As might be expected the self-diffusion coefficients of xenon decrease with increasing conversions (Table 4.6). The diffusion coefficients in the Bis-MEPP(XDT) samples were not measurable in the 30-second and 5-minute cure samples for reasons that will be discussed later. 15 μm is the maximum domain size measurable as indicated by the results in the monomer system. In the system cured for 20 seconds that value has been reduced to approximately 12 μm. This is due to the shorter mean free path in the monomer like environment due to the formation of high cross-link density phases and the increased density of the systems. The samples cured 10, 15, and 20 seconds all had gel-like physical properties upon removal from NMR tubes. The sample cured for 30

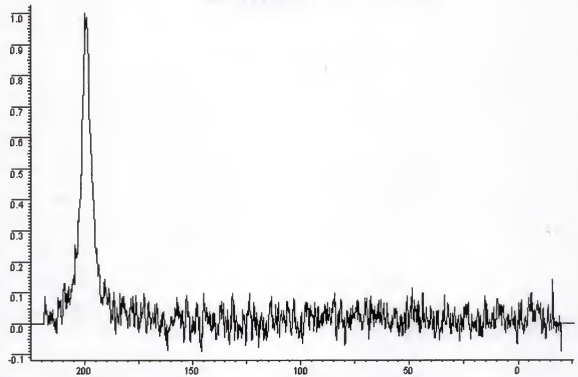

Figure 4.12: Xenon-129 spectra at 25°C of Bis-MEPP(XDT) cured for 5 minutes

seconds can be described as leathery. The physical properties of the sample cured for 5 minutes appeared to be glassy. The critical conversion for gelation in tetrafunctional systems predicted with the following equation based on percolation theory is approximately 33 percent [121]:

$$p_c = \frac{1}{(f-1)}$$

Where: P_c = critical conversion to gelation

f = average functionality of the system

The sample cured for 30 seconds had a degree of conversion of approximately 26 percent. The ability to make pulsed field gradient measurements ceased and the physical properties of the sample changed from gel-like to leathery in the 30-second cure samples. This suggests the gel formation is related to these changes in properties. The similarity of the values for the systems cured for 10, 15, and 20 seconds may be due to some depth of cure issues. Initially, there is probably a higher concentration of radicals in the monomer near the external region of the sample than in the center. After 30 seconds of curing the radical concentration may be more uniform. This may account for the jump in conversion between the sample cured for 20 seconds and the sample cured for 30 seconds.

Diffusion coefficients were not measurable in the systems cured for 30 seconds and 5 minutes. A signal was not observed using the original parameters of the stimulated echo sequence. A modified sequence as described in the materials and methods section

Table 4.6: Degree of conversion values, diffusion coefficients, and domain sizes of Bis-MEPP(XDT) at various stages of cure

Cure Time (Seconds)	Degree of Conversion (%)	Diffusion Coefficient (M^2/S)	Domain Size Measured (μm)
Monomer	0	$7.0 \pm 0.53 \times 10^{-11}$	15 ± 0.6
10	3.3 ± 1.7	$5.4 \pm 0.18 \times 10^{-11}$	13 ± 0.3
15	5.5 ± 2.6	$5.2 \pm 0.16 \times 10^{-11}$	13 ± 0.2
20	7.6 ± 2.4	$5.1 \pm 0.21 \times 10^{-11}$	12 ± 0.3
30	26 ± 3.0	N/A	N/A
5 min	54.1 ± 3.4	N/A	N/A

was used. The time between the pulses and the length of gradient pulses was decreased to prevent loss of signal due to T2 or spin-spin relaxation. A signal was observed, but no attenuation occurred within the noise of the spectrum. Similar difficulty was encountered with the sample cured for 5 minutes. The root of the problem is signal attenuation due to rapid T2 relaxation. Assuming that only homogeneous signal broadening is occurring, the T2 relaxation time of a system can be estimated using the following equation [122]:

$$\delta\omega_{1/2} = \frac{2}{T_2}$$

Where $\delta\omega_{1/2}$ = the spectrum width and half-maximum in hertz.

The T2 relaxations times of the systems cured for 30 seconds and 5 minutes are 7.3 and 3.7 milliseconds, respectively. For comparison, the T2 of the monomer systems is 90 milliseconds. In the second pulse sequence described for the 30-second cure sample (Table 4.5) the time elapsed between the first $\pi/2$ pulse and the second is nearly 3 milliseconds. During that period a large portion of the signal has been lost for the 30-second cure sample and nearly all of the signal has been lost for the 5-minute cure

sample. As mention early, there was no resolvable signal attenuation for 30-second cure sample. This is due to the short duration of the gradient pulses (0.5 ms). In other studies where gradient pulses of this duration were used, gradient strengths of nearly an order of magnitude greater were required to attain measurable signal attenuation [86]. Unfortunately, our gradient strength is already at its maximum; however, this does suggest that these measurements can be pushed further into the cure cycle with the appropriate equipment.

Conclusions and Future Work

Tapping Mode™AFM measurements using phase imaging demonstrated that there are variations in the cross-link density of dimethacrylate-type polymers on the order of 25-150 nm. The spectrum of Bis-MEPP in its fully cured state corroborates the AFM results. The spectrum indicates that there are lower cross-link density regions present with a pore structure that accommodates xenon despite having a macroscopic glassy appearance. The presence of a structure with a bimodal distribution of cross-link densities is also indicated by the DMS data presented in Chapter 3. These results all show that dimethacrylate polymers are heterogeneous materials composed of regions of low and high cross-link density rather than a continuum-type structure.

Further refinement of the AFM techniques may allow relationships between the sizes of the different regions and mechanical properties to be established. The local variation in domain sizes in the images makes it difficult to determine their average size by casual observation. Image analysis software would be useful to determine the average size of the domains as well as their volume fractions and to establish relationships between mechanical properties and domain sizes.

Pulsed field gradient xenon NMR was used to measure the change in domain sizes with cure in dimethacrylate systems. Unfortunately, measurements could only be made at conversions less than 26 percent. Equipment in which stronger field gradients can be applied would allow the measurement to be pushed further into the cure cycle. In polymer blends where peaks of the different phases are resolved, changes in the exchange rate can observed by 2D experiments as well as changes in the 1D spectra such as coalescence of the peaks. If the xenon self-diffusion coefficient of the system is known, then the exchange rate can be used to calculate domain sizes. This type of analysis is not possible when one of the phases is acting as a hidden exchange partner. This means that the alterations in the signal due to different exchange rates are not visible. Schantz and Veeman have measured domain sized on the order of 50 nm in systems where one phase is acting as a hidden exchange partner by modeling the one-dimensional spectra of the system using the exchange rate as a variable. A similar analysis might be applied to dimethacrylate systems to estimate domain sizes to corroborate those observed by AFM.

CHAPTER 5
EVALUATION OF THE EFFICIENCY OF THE INCORPORATION OF NADIC METHYL ANHYDRIDE, NORBORNENE BASED COMPOUNDS AND MALEIC ANHYDRIDE INTO METHACRYLATE-BASED DENTAL RESINS

Relevant Background

Monomers that introduce cyclic groups into the methacrylate backbone of dental polymers, such as maleic anhydride, methylene lactone, and norbornene-type monomers, have been studied with mixed results. This chapter will investigate the mechanistic and structural behavior of nadic methyl anhydride and maleic anhydride polymerized with 2-phenyl ethyl methacrylate. The properties of methylene lactone monomers, described as cyclic analogs of methyl methacrylate, lead to their study as coreactants with dental monomers [123]. Poly (α-methylene-γ-butyrolactone) (MBL) (Figure 5.1) has a glass transition temperature of 195 °C as compared to MMA, which is approximately 105 °C. MBL is also more polar than MMA and is considered more reactive as determined by copolymerization studies with MMA. The addition of up to 20 weight percent MBL to Bis-GMA resins increased the diametral tensile strength of the polymer, which was conditioned for 24 hours at 37°C in water. The increase in properties is attributed to the lower viscosity of MBL as well as the incorporation of the rigid lactone rings into the methacrylate backbone. FTIR studies revealed that the addition of 30 weight percent MBL to Bis-GMA resins increased the conversion of vinyl bonds to 71% compared to 32% for pure Bis-GMA. The addition of 10 weight percent MBL to Bis-GMA/TEGDMA resins increased the conversion of double bonds from 57 to 71

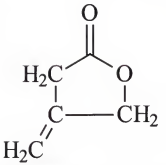

Figure 5.1: The structure of α-methylene-γ-butyrolactone

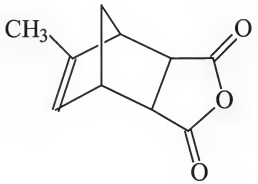

Figure 5.2: The structure of nadic methyl anhydride (NMA)(methyl-5-norbornene-2,3 dicarboxylic acid anhydride)

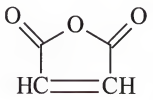

Figure 5.3: The structure of maleic anhydride (MA)

percent compared to Bis-GMA/TEGDMA systems. A 10 percent increase in strength values also occurred; however, the increase was not statistically significant at $\alpha = 0.05$. The increase in conversion could be a result of the higher reactivity of the MBL. The lower initial viscosity and average functionality of MBL containing mixtures are factors as well. Improved mechanical properties have been reported in Bis-MEPP/TEGDMA systems in which 10 wt.% nadic methyl anhydride (NMA) was added. Despite its rigid ring structure, the addition of 20 wt. % nadic methyl anhydride (NMA) to Bis-MEPP/TEGDMA systems (60/40 weight percent) lowered the glass transition temperature by 42 °C) (Figure 5.2)[99] compared to the Bis-MEPP/TEGDMA (60/40 weight percent) systems. Similarly, MLB may lower the glass transition temperature of the systems in which it is incorporated by lowering the cross-link density; although, its incorporation probably stiffens the methacrylate backbone of the polymer. Maleic anhydride (MA) (Figure 5.3) incorporated into urethane dimethacrylate/TEGDMA composites at 30 mol.% lowered the flexure strength and modulus by 49 MPa and 2.0 Gpa, respectively. [64]. The incorporation of maleic anhydride into 2-phenylethyl methacrylate polymers resulted in higher glass transition temperatures [124]. One might expect similar results from the MBL and NMA systems as from the MA systems. The incorporation of MA into these 2-phenylethyl methacrylates was shown to be inefficient by FTIR and DSC, indicating a low reactivity of MA with methacrylates. NMA is also assumed to be less reactive due to steric considerations. The extractable sol fraction of Bis-MEPP/TEGDMA/NMA polymers increased with increasing NMA concentration, which indicates a lower reactivity of NMA with MEPP/TEGDMA. This could be a result of the lower functionality of NMA.

This work will attempt to understand the findings in nadic methyl anhydride modified methacrylate systems by determining the efficiency of its incorporation along with other norbornene-based monomers and maleic anhydride. The model compounds were based on the monomers 2-phenyethyl methacrylate (PMA), nadic methyl anhydride, and maleic anhydride. PMA is model compound for aromatic dimethacrylates such as ethoxylated bis-phenol dimethacyrate and Bis-GMA. PMA forms linear polymers that are more easily characterized than cross-linked systems. The compounds were characterized using FTIR, GPC, DSC and ^{1}H NMR. The effect of anhydride feed concentration on their incorporation into the PMA based polymers was determined. The incorporation of maleic anhydride and nadic methyl anhydride through a reaction in the vinyl bond was also confirmed.

Materials and Methods

Model compounds were made by polymerizing various norbornenes with 2-phenylethyl methacrylate (PMA) (Figure 5.4). The norbornene compounds that were examined were methyl-5-norbornene-2,3 dicarboxylic acid anhydride or nadic methyl anhydride (NMA) (Figure 5.2), 5-norbornene-2,3 dicarboxylic acid anhydride (Figure 5.4), 5-norbornene-2-carboxaldehyde (Figure 5.5), and 5-norbornene-2-butane (Figure 5.6). Norbornene monomers were added at 10, 20, 30, and 40 mol.% concentrations to PMA. Model compounds that contained nadic methyl anhydride and maleic anhydride (MA) were also formulated (Table 5.1). PMA was vacuum distilled prior to use at 72 °C under a vacuum (< 1mmHg). Maleic anhydride was recrystallized from benzene. The compounds were polymerized in bulk using 0.4 weight percent AIBN as an initiator. The monomer/initiator mixtures were purged with dry nitrogen, sealed, and then polymerized

at 75°C for 4 hours. The polymer was then dissolved in chloroform and precipitated in methanol. Samples were filtered and then dried under vacuum (28 in Hg) at 40°C.

Table 5.1: 2-phenylethyl methacrylate/nadic methyl anhydride/maleic anhydride monomer compositions in mol.%

Sample	PMA	NMA	MA
PNM1	70	22.5	7.5
PNM2	70	15	15
PNM3	70	7.5	22.5

The molar masses were determined by GPC using a Waters HPLC system composed of a Waters 600 Fluid Delivery System, a Waters 717 Auto sampler, a Waters 410 Differential Refractometer, and a Waters 996 Photodiode Array Detector. Four Phenomenex cross-linked polystyrene columns with pore sizes of 10^5,10^4, 500, and 100 Å were used in series at a flow rate of 0.4 ml/min. The injection volume was 50 µl of each sample, which were approximately 0.25 weight percent in HPLC grade THF. Anionically polymerized polystyrene standards obtained from Polymer Laboratories were used for calibration. The samples and standards were also randomized.

A Seiko DSC 220C Differential Scanning Calorimeter interfaced with a Seiko SDM/5600h Rheostation was used to determine the glass transition temperatures of the model compounds. The temperature of the sample and an inert alumina reference are monitored with thermocouples. Samples were heated at a rate of 10°C/min. under a nitrogen purge of 100 ml/min. Samples were scanned from -50°C to 150°C three times. A baseline thermogram was run with an empty pan and subtracted from the sample thermograms. Three runs were made on all of the compositions tested.

The polymers prepared with nadic methyl and maleic anhydrides were examined with Fourier Transform InfraRed spectroscopy (FTIR) to determine the concentration of anhydride in the various polymers. Calibration standards for the anhydride groups were made from the infrared spectra of the monomer mixtures prior to the addition of catalysts. Peaks at 1781 cm^{-1} and 1853 cm^{-1} due to the asymmetric and symmetric carbonyl stretches identify the anhydride functionality. The aromatic double bonds at 1608 cm^{-1} were used to identify the 2-phenylethyl methacrylate. Peak fitting software was used to deconvolute and measure the areas of these peaks (PeakFit v4 by SPSS Inc.).

The specific site of NMA incorporation into the polymer was investigated with ^{1}H Nuclear Magnetic Resonance Spectroscopy (NMR) of the model compounds to determine if the norbornenes incorporated via reaction through the double bond. The NMR spectroscopy was performed on a Gemini 300 NMR system composed of a 7 Tesla Oxford magnet and 5mm Varian broadband probe. The spectra were referenced to tetramethylsilane (TMS). The model compounds and base monomers were dissolved in deuterated-dimethylformamide deuterated at 2.5 weight percent. The solutions were made in a dry environment (less then 20% relative humidity) to avoid water uptake in the DMF.

Results and Discussion

A full study was only performed on the model compounds based on 2-phenylethyl methacrylate/nadic methyl anhydride and 2-phenylethyl methacrylate/nadic methyl anhydride/maleic anhydride compounds. Solubility issues were encountered with the other compounds preventing further analysis. The aliphatic norbornene compounds were soluble in the 2-phenylethyl methacrylate monomer; however, as the polymerization

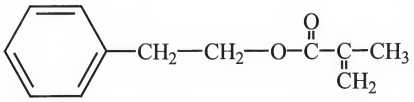

Figure 5.4: The structure of 2-phenylethyl methacrylate

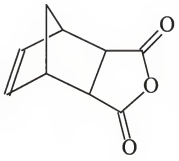

Figure 5.5: The structure of 5-norbornene-2,3 dicarboxylic acid anhydride

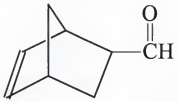

Figure 5.6: The structure of 5-norbornene-2-carboxaldehyde

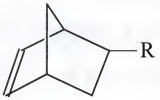

R= $(CH_2)_3CH_3$ or $(CH_2)_5CH_3$

Figure 5.7: The structures of 5-norbornene-2-butane and 5-norbornene-2-hexane

progressed, phase segregation occurred. 5-norbornene-2,3 dicarboxylic acid anhydride (Figure 5.4) and 5-norbornene-2-carboxaldehyde (Figure 5.5) were not soluble in 2-phenylethyl methacrylate monomer. It should also be noted that 2-phenoxy ethyl methacrylate, the original monomer planned for this study, was discarded due to difficulties obtaining compounds which were soluble.

The FTIR and DSC data collected from 2-phenylethyl methacrylate/nadic methyl anhydride type polymers indicates a low incorporation efficiency of NMA with PMA, i.e., less than 2 weight percent. The amount of NMA in the 2-phenylethyl methacrylate polymers is not sensitive to the concentration of NMA in the monomer feed (Table 5.2). Examples of FTIR from various systems are shown in Figure 5.8. As might be expected from the FTIR results, the glass transition temperature of the polymers was also not affected by the feed concentration of the monomers. The glass transition temperature of poly (norbornene) is in the range of 350°C [125]. Incorporation of NMA into the polymer at an amount greater than 2 percent would increase the glass transition temperature of the polymers formed. The increase in the feed concentrations of NMA resulted in no detectable difference in glass transition temperatures.

The small amount of NMA incorporated does not change the molar mass of the PMA polymer, which implies that it does not alter the polymerization kinetics of the PMA. It should be noted that there is large batch-to-batch variability in bulk polymerization processes. This variability is illustrated by the differences in molar mass between the original samples and their replicates. The high amount of scatter may obscure any trends in molar mass or polydispersity that the presence of NMA might induce.

Table 5.2: FTIR and DSC results from 2-phenylethyl methacrylate/nadic methyl anhydride based model compounds

Polymer	Tg (°C)	Anhydride content (mol.%)
Poly (PMA)	31 ± 4	0
Poly (PMA-co-10%NMA)	32 ± 2	Less than 2
Poly (PMA-co-20%NMA)	29 ± 1	Less than 2
Poly (PMA-co-30-%NMA)	33 ± 6	Less than 2
Poly (PMA-co-40%NMA)	31 ± 4	Less than 2

Table 5.3: Molar mass averages from GPC for 2-phenylethyl methacrylate-nadic methyl anhydride copolymers

Polymer	Mn (kg/mol)	PDI
Poly (PMA)	42.6	3.6
Poly (PMA) repeat	58.9	4.8
Poly (PMA–co-10%NMA)	41.2	4.9
Poly (PMA–co-10%NMA) repeat	29.5	4.4
Poly (PMA-co-20%NMA)	47.8	4.7
Poly (PMA-co-20%NMA) repeat	48.3	4.1
Poly (PMA-co-30-%NMA)	55.1	4.5
Poly (PMA-co-30-%NMA) repeat	64.1	4.1
Poly (PMA-co-40%NMA)	48.0	4.8
Poly (PMA-co-40%NMA) repeat	50.6	4.2

NMA, maleic anhydride (MA), and 2-phenylethyl methacrylate were blended with the idea that a synergistic effect between the maleic anhydride and the NMA would increase concentration of both anhydrides in the copolymer. Maleic anhydride/norbornene polymerizations have been reported that produced alternating copolymers with yields ranging from 60-76% [126]. In the same studies, it was

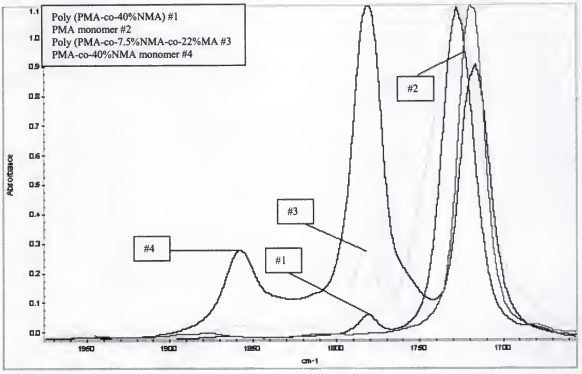

Figure 5.8: FTIR spectra of PMA-co-40%NMA, PMA, poly (PMA-co-40%NMA), and poly (PMA-co-7.5%NMA-co-22.5%MA)

determined that tert-butyl acrylate concentration in the copolymers, i.e., tert-butyl acrylate/MA/NB, increased linearly with its monomer feed concentration, up to a maximum mole fraction of 0.2. There was no reduction in either the number average molar mass or polydispersity.

The concentration of anhydride functionalities increases with an increase in the feed concentration of MA in poly (PMA-co-NMA-co-MA), which indicates that MA is more reactive with PMA than NMA. The incorporation is confirmed by a concurrent increase in the glass transition temperature of the polymers. Previous studies on 2-phenylethyl methacrylate-co-maleic anhydride polymers showed that maleic anhydride incorporated at roughly 45% of its feed in the monomer system [124]. In the poly (PMA-co-22.5 mol.% NMA-co-7.5 mol.% MA) system there is 4.6 mol.% anhydride. The feed concentration of MA was 7.5 mol.%. Based on the results from PMA-co-MA systems, the amount expected would be approximately 3.4 percent. It is not possible to determine the ratios at which maleic anhydride or NMA are incorporated by FTIR only that the presence of NMA results in increased amounts of anhydride in the polymer compared to what would be expected due to MA by itself. In the poly (PMA-co-7.5mol.%NMA-co-22.5mol.%MA) system, the total amount of anhydride incorporation is 7.7 mol.%. The amount of MA incorporated estimated by comparison with poly (PMA-co-MA) systems should be approximately 10.1%. This indicates some inhibition of the incorporation of MA by the NMA. The exact nature of the incorporation of NMA and MA cannot be discerned. These results indicate that MA and NMA do not copolymerize efficiently with PMA at any concentration.

As mentioned previously polymers of norbornene, maleic anhydride (MA), t-butyl acrylate (TBA) reported yields as high as 76%[126]. The difference between the cited study and the present study could be due to the polymerization methods, solubility differences, reactivity differences, and ratios of feed monomers. It should also be noted that PMA is a methacrylate and TBA is an acrylate, which also might result in differences in reactivity. The norbornene, maleic anhydride, t-butyl acrylate copolymers were prepared by polymerization in a THF solution at 65°C for 24 hours. Both the PMA/MA/NMA and the Norbornene/MA/TBA systems used AIBN as an initiator. The PMA/MA/NMA were polymerized in bulk at 75°C for 4 hours. The long reacting time may have allowed additional reaction of the MA and norbornene. In the same work Houlihan et al. [126] explored other cycloelfinic-maleic anhydride copolymers. A norbornene-based monomer with a bulky side group did not polymerize with maleic anhydride. In the absence of an explanation for the lack of polymerization, it may be reasonable to attribute it to steric hindrance. The anhydride ring in NMA might also cause steric hindrance and reduce the reactivity of NMA with maleic anhydride (MA) and PMA.

Table 5.5 contains the GPC data from the PMA/NMA/MA systems. At the low concentrations of anhydride incorporation seen in this study the average molar mass of the PMA polymers is not affected by the incorporation of the anhydrides enough to see a trend within the scatter of the measurement.

Table 5.4: FTIR data and DSC from 2-phenylethyl methacrylate/nadic methyl anhydride/maleic anhydride based model compounds

Polymer	Tg (°C)	Anhydride Content (mol.%)
Poly (PMA-co-7.5%NMA-co-22.5%MA)	37 ± 4	7.7 ± 1.1
Poly (PMA-co-15%NMA-co-15%MA)	35 ± 7	5.1 ± 0.9
Poly (PMA-co-22.5%NMA-co-7.5%MA)	31 ± 3	4.6 ± 0.6

Proton NMR was performed to confirm that the anhydrides are incorporating through the polymerization of the vinyl functionality. It should be noted that in all spectra the peaks located at 8.03, 2.92, and 2.75 ppm are due to the DMF solvent.

Table 5.5: Molar mass averages from GPC for 2-phenylethyl methacrylate-nadic methyl anhydride-maleic anhydride copolymers

Polymer	Mn (Kg/mol)	PDI
Poly (PMA-co-7.5%NMA-co-22.5%MA)	38.7	5.0
Poly (PMA-co-7.5%NMA-co-22.5%MA) Repeat	50.8	4.6
Poly (PMA-co-15%NMA-co-15%MA)	39.2	5.2
Poly (PMA-co-15%NMA-co-15%MA) Repeat	48.0	4.8
Poly (PMA-co-22.5%NMA-co-7.5%MA)	39.6	5.0
Poly (PMA-co-22.5%NMA-co-7.5%MA) Repeat	44.0	4.9

The spectrum of PMA (Figure 5.9) contains six major peaks associated with the different chemical environments of protons Table 5.6. There is a small peak located at 3.5 ppm. This peak is due to contamination in one of the vials of deuterated DMF solvent used to make samples. The contaminant does not show up in all the systems because it was only in one of the vials. Figure 5.14 contains the spectra of the contaminated solvent.

Table 5.6: Summary of the 1H NMR Spectra from phenylethyl methacrylate

Chemical Group	Shift (ppm)
Aromatic-H	7.2 Singlet
C=CH_2	5.1,5.7 Singlet
COO-CH_2-C	4.4 Triplet
Aromatic-CH_2	3.0 Triplet
CH_2=C-CH_3	1.9 Singlet
Contaminant in d-DMF	3.5 Singlet

The spectrum of nadic methyl anhydride (Figure 5.10) has three major regions where peaks occur. The most identifiable are the peaks located at 5.8 ppm that are associated with protons in vinyl bonds. This peak is split into a doublet by the single proton on the adjacent carbon. The second group of peaks is located between 3 and 4 ppm. The doublet peak with the largest integration is located at 3.2 ppm. This peak is due to protons located on carbon atoms adjacent to carbonyl groups in the anhydride linkages. The third group of peaks is associated with the carbons in the aliphatic linkages and the methyl group adjacent to the vinyl bonds. Exact peak assignments are difficult due to the large amount of spin couplings and complex chemical environments. There are also some notable peaks in the 3 to 4 ppm range. These peaks along with the low integration values of the vinyl proton indicate that there is some contamination in the NMA monomer. The normalized integration values indicate that the vinyl functionality is present at 38 percent of what would be expected based on the structure of NMA. The chemical structure of maleic anhydride indicates that there should only be a single proton environment (Figure 5.11). There are 4 peaks in maleic anhydride spectra. The peak that occurs at 6.4 is due to the protons in the vinyl group. The other three peaks are due to DMF.

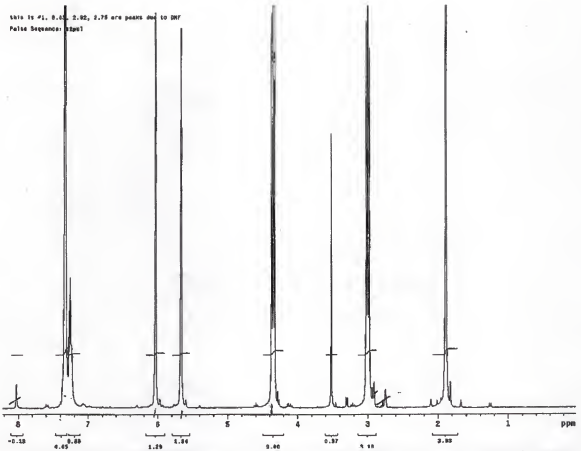

Figure 5.9: The proton NMR spectra of 2-phenylethyl methacrylate in deuterated DMF referenced to TMS

The peaks in the spectrum of poly (PMA-co-40%NMA) are broader than those of the corresponding monomers (Figure 5.12). The broadening is due to the reduced mobility of the chemical groups in the polymer structure. The peaks previously identified in the PMA spectra at 7.3, 4.2, and 3.0 are present. The peak at 3.5 is due to contamination in DMF solvent. The peaks at 1.8 and 0.8 ppm are due to the protons located along the aliphatic backbone and the α-methyl group, respectively. The α-methyl peak was previously located at 1.9 ppm; however, reaction of the vinyl bond changed the chemical environment and resulted in an upfield shift. The values of the integration, which normalize to 2.86, confirm this assignment. There are no peaks present in the 5.8 ppm range confirming that NMA incorporates through a reaction of the vinyl bonds; however, there are no resolved peaks that allow quantification of concentration of NMA. This might be expected based on the lower percentages of incorporation, i.e. 2 wt.%, which is below the detection level.

The spectrum of the poly (PMA-co-7.5%NMA-co-22.5%MA) (Figure 5.13) is very similar to the spectrum from poly (PMA-co-40%NMA). The only notable difference is the magnitude of the peak at 3.5 ppm. There are no vinyl proton peaks (6.4 ppm), which indicates that the anhydrides are incorporating through a reaction of the vinyl bonds. The peak 3.5 ppm is notably strong and may be due to protons of maleic anhydride that have been incorporated into the polymer backbone; however, proton NMR spectrum of poly (norbornene-co-MA) report no peaks at a chemical shift greater than 3.15 [126]. As mentioned earlier, the peak at 3.5 is due to contamination in the DMF solvent (Figure 5.14). Although there is no single peak that identifies NMA or maleic

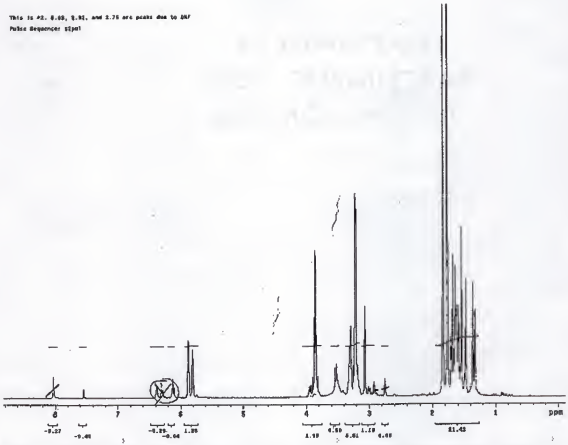

Figure 5.10: The proton NMR spectra of nadic methyl anhydride in deuterated DMF referenced to TMS

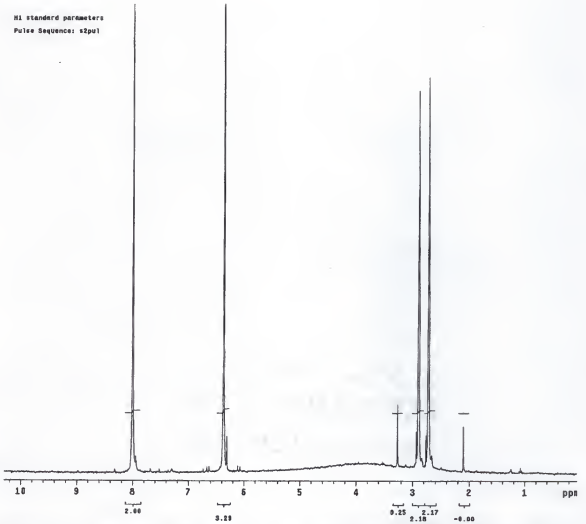

Figure 5.11: The proton NMR spectra of maleic anhydride in DMF referenced to TMS

anhydride in these NMR spectra, the possibility of maleic anhydride being incorporated into the polymer backbone cannot be ruled out based on this data. The peaks representing NMA and MA that has been incorporated into poly (PMA) are not resolvable from the peaks due to poly (PMA). The possibility that NMA and MA are incorporating through some mechanism other than polymerization through the vinyl bond can be ruled out using this data.

Conclusions

FTIR and DSC data indicate that anhydrides are incorporating into the polymer backbone. NMR data confirms that incorporation is through a polymerization of the vinyl group. Nadic methyl anhydride (NMA) does not incorporate at levels higher than 2% irrespective of its feed composition in the monomer. A higher concentration of MA in the feed results in larger amounts of anhydrides in the polymers; however, the exact ratio of NMA to MA in the polymer was not determined. There also does not appear to be a synergistic or copolymerization effect when MA and NMA are present together in the monomer feed. The incorporation efficiency is less than 30% of the feed concentration for all systems studied in this work. This indicates that the maleic anhydride and nadic methyl anhydride may not be good candidates for incorporating anhydride moieties into methacrylate-based materials.

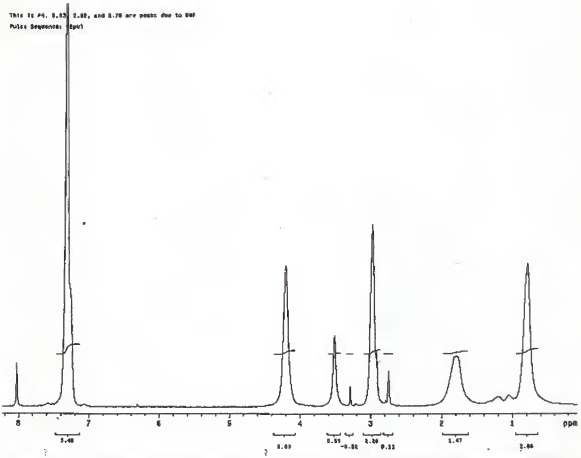

Figure 5.12: The proton NMR spectra of poly (PMA-co-40%NMA) in deuterated DMF referenced to TMS

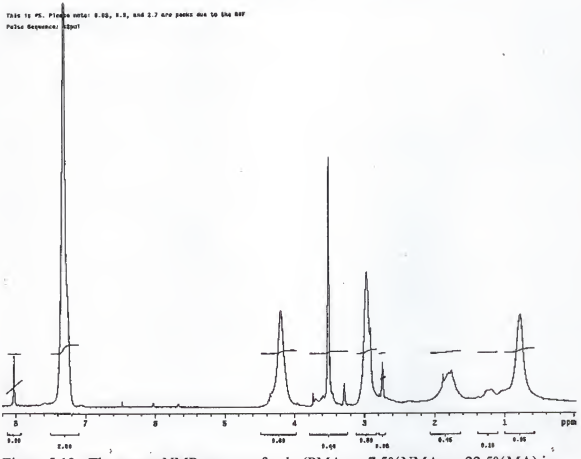

Figure 5.13: The proton NMR spectra of poly (PMA-co-7.5%NMA-co-22.5%MA) in deuterated DMF referenced to TMS

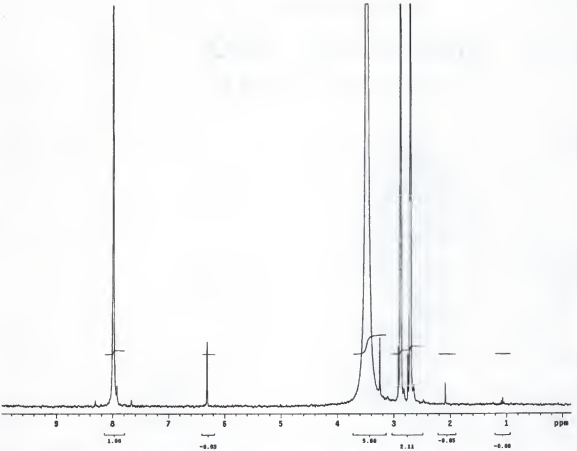

Figure 5.14: The proton NMR spectra of deuterated DMF referenced to TMS

CHAPTER 6
CLOSING REMARKS

In Chapter 3, the monofunctional methacrylates cyclohexyl methacrylate (CHMA), phenyloxyethyl methacrylate (PEMA), and tert-butylcyclohexyl methacrylate (t-BCHMA) were introduced as alternate diluent systems for Bis-MEPP-type monomers for dental applications. The monofuctional methacrylates reduced polymerization shrinkage by 10 to 20 percent when compared to Bis-MEPP/TEGDMA systems. The reduction in shrinkage is due to the higher specific volume per methacrylate group of monomethacrylates compared to TEGDMA. CHMA and PEMA reduced the viscosity of Bis-MEPP more effectively than TEGDMA, while t-BCHMA did not. The Bis-MEPP/CHMA and Bis-MEPP/PEMA systems had similar moduli, 2.8 ± 0.1 and 2.7 ± 0.1 GPa for the Bis-MEPP/CHMA and Bis-MEPP/PEMA systems in wet state at 37°C, respectively, to the Bis-MEPP/TEGDMA systems (2.6 ± 0.1 GPa). Quantitative fractography was applied to measure fracture toughness. To the author's knowledge, this is the first time this technique has been used to measure fracture toughness in dental polymers. The fracture toughness of the Bis-MEPP/PEMA and Bis-MEPP/CHMA systems was an average of 0.2 $MPa.m^{0.5}$ greater than the Bis-MEPP/TEGDMA systems. The modulus and fracture toughness were lower in the Bis-MEPP/t-BCHMA systems than in the Bis-MEPP/TEDGMA systems. The reduced properties might in part be due to the high glass transition temperatures and viscosities of the Bis-MEPP/t-BCHMA monomer systems. A non-reactive contaminant was also present that might result in the reduction of the mechanical properties of these systems. Multicomponent diluent

systems based on variable molar mass analogs of ethylene glycol dimethacrylate were also explored as alternate diluent systems. The modulus and strength properties of the multicomponent systems did not vary greatly from those of the Bis-MEPP/TEGDMA polymers. The similarity of the properties of all the systems examined in Chapter 3 is attributed to the heterogeneous network structure that results from the incomplete cure as well as the mechanisms of network formation. The dimethacrylate polymers are composed of regions of high and low cross-link density. This structure is indicated by the DMS data presented later in Chapter 3 as well as the work presented in Chapter 4.

Monomer systems based on Bis-MEPP/CHMA Bis-MEPP/PEMA and Bis-MEPP/t-BCHMA were formulated to produce polymers with the same glass transition temperature. Formulating the polymers to the same Tg allows the isolation of the effect of initial viscosity on vitrification and heterogeneity of these systems. Initial viscosity was shown to be an indicator of heterogeneity of the polymers formed rather than a primary factor. The details of network formation, phase segregation, and isomeric forms of the monomers have strong effects on the heterogeneity of the polymers formed.

The heterogeneity of dimethacrylate polymers was elucidated by ^{129}xenon NMR, Tapping Mode™AFM measurements using phase imaging, and dynamic mechanical spectroscopy. Xenon spectra of a Bis-MEPP(XDT) polymer cured for 5 minutes with UV light showed a peak indicative of a polymer that is not fully glassy. The width and intensity of the peak suggest that a portion of the polymer has a pore structure that is not representative of a fully glassy polymer. Pulsed Field Gradient ^{129}xenon NMR was used to measure the change in domain sizes of the sol phase with cure in the Bis-MEPP(XDT) systems. It is thought that heterogeneity has its roots early in the cure cycle. Measuring

how the sol phase changes with cure would lead to a better understanding of the mechanisms that yield a heterogeneous structure. Unfortunately, measurements could only be made at low conversions. Equipment in which stronger field gradients can be applied would allow the measurement to be pushed further into the cure cycle. Variations in the cross-link density of dimethacrylate type polymers on the order of 25-150 nm was demonstrated using Tapping Mode™AFM measurements using phase imaging. Samples were etched in acetone and post cured to help make the assignment of different regions of phase contrast to the low and high cross-link density phases. In these systems the high cross-link density phases have a greater phase shift than the low cross-link density phase. The presence of the low temperature shoulder on the main transition in the tan δ plots of the polymers tested in Chapter 3 is also indicative of a bimodal distribution of cross-link density.

Characterization of the size and distribution of the low and high cross-link density phases is important because the low cross-link density phases of these polymers dictate their mechanical properties. Further quantification of the size of these structures with image analysis techniques might allow correlations to be drawn between their distribution and mechanical properties. These correlations may ultimately allow the tailoring of monomer selection and cure cycles to improve mechanical properties.

The efficiency of the incorporation of nadic methyl anhydride (NMA) and maleic (MA) anhydride into 2-phenyl ethyl methacrylate polymers was determined using FTIR, GPC, DSC, and ^{1}H NMR. This study was performed to glean information about how NMA and MA incorporate into aromatic dimethacrylate polymers such as Bis-GMA and Bis-MEPP. The results indicate that nadic methyl anhydride does not incorporate at

amounts greater than 2 mol.% regardless of the feed concentrations. The amount of anhydride present in the polymers increased as the concentration of maleic anhydride was increased in the monomer feed. The exact ratios of the MA and NMA were not determined. The incorporation efficiency of all the anhydrides in this study was less than 30 mol.% of the feed concentration, thus indicating that these anhydrides may not be good candidates for comonomers in methacrylate based dental polymers. The incorporation of anhydride groups into methacrylate dental polymers might be better facilitated by monomers that have a methacrylate functionality or a functionality that is known to polymerize with methacrylates.

LIST OF REFERENCES

1. Holter, D., et al. *Branched Bismethacrylates Based on Bis-GMA - A Systematic Route to Low Shrinkage Composites*. in *Proceedings of the 1997 Las Vegas ACS Meeting*. 1997. Las Vegas, NV, USA: Division of Polymer Chemistry, American Chemical Society.

2. Sankarapandian, M., et al. *Synthesis of New Dental Composite Matrix Dimethacrylates*. in *Proceedings of the 1997 Las Vegas ACS Meeting*. 1997. Las Vegas, NV, USA: Division of Polymer Chemistry, American Chemical Society.

3. Ferracane, J.L. and E.H. Greener, *The Effect of Resin Formulation on the Degree of Conversion and Mechanical Properties of Dental Restorative Resins.* Journal of Biomedical Materials Research, 1986. **20**: p. 121-131.

4. Shobha, H.K., et al., *Structure property relationship among novel dental composite matrix resins.* Journal of Materials Science: Materials in Medicine, 1997. **8**: p. 385-389.

5. Kalachandra, S., *Glassy Polymers as Dental Materials*, in *Encylopedia Handbook of Biomaterials and Bioengineering*, D.J.T. D. L. Wise, D. E. Antobelli, M. J. Yaszemski, J. D. Gresser, and E. R. Schwartz, Editor. 1995, Marcel Dekker, Inc.: New York. p. 1545-1556.

6. Liu, C.-F., C.M. Collard, and C.D. Armeniades, *Constant -volume polymerization of composites by addition of ammonia-modified montmorillonite.* American Journal of Dentistry, 1990. **3(2)**(April): p. 44-50.

7. Stansbury, J.W., *Synthesis and Evaluation of New Oxaspiro Monomers for Double Ring-opening Polymerization.* Journal of Dental Research, 1991. **71(7)**(July): p. 1408-1412.

8. Peutzfeldt, A. and E. Asmussen, *Influence of Carboxylic Anhydrides on Selected Mechanical Properties of Heat-cured Resin Composites.* Journal of Dental Research, 1991. **70(12)**(December): p. 1537-1541.

9. Simon, G.P., et al., *Nature of Residual Unsaturation during Cure of Dimethacrylates Examined by CPPEMAS ^{13} C and Simulation Using a Kinetic Gelation Model.* Macromolecules, 1989. **22**: p. 3555-3561.

10. Chiu, Y.Y. and L.J. Lee, *Microgel Formation in the Free Radical Crosslinking Polymerization of Ethylene Glycol Dimethacrylate (EDGMA). II. Simulation.* Journal of Polymer Science: Part A: Polymer Chemistry, 1995. **33**: p. 269-283.

11. Chiu, Y.Y. and L.J. Lee, *Microgel Formation in the Free Radical Crosslinking Polymerization of Ethylene Glycol Dimethacrylate (EGDMA). I. Experimental.* Journal of Polymer Science: Part A: Polymer Chemistry, 1995. **33**: p. 257-267.

12. Watts, D.C., *Filling the Gaps.* Chemistry in Britain, 1992. **28**(3): p. 235 - 238.

13. Peutzfeldt, A., *Resin composites in dentistry: the monomer systems.* European Journal of Oral Sciences, 1997. **105**: p. 97-116.

14. Jones, D.W., *Synthesis and evaluation of ceramic, polymer, and composite biomaterials*, in *Encylopedia Handbook of Biomaterials and Bioengineering*, D.J.T. D. L. Wise, D. E. Antobelli, M. J. Yaszemski, J. D. Gresser, and E. R. Schwartz, Editor. 1995, Marcel Dekker, Inc.: New York. p. 187 - 202.

15. Prati, C., et al., *Dental Composite Resin Porosity and Effect on Water Absorption.* Boll. Soc. It. Biol. Sper., 1991. **LXVII**(4).

16. Phillips, R.W., *Elements of Dental Materials*. Fourth ed. 1984, Philadelphia: Saunders.

17. Yamaguchi, R., J.M. Powers, and J.P. Dennison, *Thermal Expansion of visible-light-cured composite resins.* Operative Dentistry, 1989. **14**: p. 64-67.

18. Taylor, D.F., et al., *Relationship between filler and matrix resin characteristics and the properties of uncured composite pastes.* Biomaterials, 1998. **19**: p. 197-204.

19. Shobha, H.K., et al., *Effect of dilution on the kinetics of cross-linking thermal polymerization of dental composite matrix resins.* Journal of Materials Science: Materials in Medicine, 1997. **8**: p. 583-586.

20. Venhoven, B.A.M., et al., *Influence of filler parameters on the mechanical coherence of dental restorative resin composites.* Biomaterials, 1996. **17**(7): p. 735-740.

21. Jones, D.W. and A.S. Rizkalla, *Characterization of Experimental Composite Biomaterials.* Journal of Biomedical Materials Research, 1996. **33**: p. 89-100.

22. Willems, G.P., et al., *A classification of dental composites according to their morphological and mechanical characteristics.* Dental Materials, 1992. **8**(September): p. 310-319.

23. Craig, R.G., W. J. O'Brien, and J. M. Powers, *Dental Materials:Properties and Manipulation*. 6th ed. 1996, St. Louis: Mosby. 55 - 75.

24. Chernova, Z.D., et al., *Densely Crosslinked Polymer Compositions Based on Various Types of Dimethacrylates.* Polymer Science U.S.S.R., 1981. **23**(10): p. 2438-2445.

25. Kannurpatti, A.R. and C.N. Bowman, *Structural Evolution of Dimethacrylate Networks Studied by Dielectric Spectoscopy.* Macromolecules, 1998. **31**(10): p. 3311-3316.

26. Kannurpatti, A.R., J.W. Anseth, and C.N. Bowman, *A study of the evolution of mechanical properties and structural hertogeneity of polymer networks formed by photopolymerizations of multifunctional (meth)acrylates.* Polymer, 1998. **39**(12): p. 2507-2513.

27. Kannurpatti, A.R., et al., *Use of "Living" Radical Polymerizations to Study the Structural Evolution and Properites of Highly Crosslinked Polymer Networks.* Journal of Polymer Science: Part B: Polymer Physics, 1997. **35**: p. 2297-2307.

28. Simon, G.P., P.E.M. Allen, and D.R.G. Williams, *Properties of dimethacrylate copolymers of varying crosslink density.* Polymer, 1991. **32**(14): p. 2577-2587.

29. Ferracane, J.L. and J.R. Condon, *Rate of Elution of Leachable Components from composite.* Dental Materials, 1990. **6**: p. 282-287.

30. Simon, G.P., P.E.M. Allen, and D.R.G. Williams, *Examination of Dimethacrylate Inhomogeneity by Solvent Swelling Tehcniques.* Polymer Engineering and Science, 1991. **31**(20): p. 1483-1492.

31. Spahl, W., H. Budzikiewicz, and W. Geurtsen, *Determination of leachable components from four commercial dental composites by gas and liquid chromatography/mass spectrometry.* Journal of Dentistry, 1998. **26**(2): p. 137-145.

32. Anseth, K.S., M.D. Rothenberg, and C.N. Bowman, *A Photochromic Technique To Study Polymer Network Volume Distributions and Microstructure during Photopolymerizations.* Macromolecules, 1994. **27**(10): p. 2890-2892.

33. Lange, J., R. Ekelof, and G.A. George, *Indications of Micro-vitrification during chainwise cross-linking poymerisation.* Polymer, 1999. **40**: p. 3595-3598.

34. Golikov, I.V., et al., *Formation of the Microstructure and Strength Properties of Oligoester Acrylate Polymers.* Polymer Science U.S.S.R., 1979. **21**(8): p. 2013-2022.

35. Baidin, I.S., et al., *Effect of the Structure of a Three-Demensional Network of the Polymer Triethylene Glycol Dimethacrylate on the Kinetics of its Radical Polymerization.* Polymer Science USSR, 1989. **31**(7): p. 1525-1529.

36. Erath, E.H. and R.A. Spur, *Occurrence of Globular Formation in Thermosetting Resins.* Journal of Polymer Science, 1959. **35**: p. 391-399.

37. Kannurpatti, A.R., et al. *Polymerization Behavior and Properties of Networks formed by Dimethacrylate Dental Resins.* in *Proceedings of the 1997 Las Vegas ACS Meeting.* 1997. Las Vegas, NV, USA: Division of Polymer Chemistry, American Chemical Society.

38. Sandner, B., et al., *Synthesis of BISGMA derivatives, properties of their polymers and composites.* Journal of Materials Science: Materials in Medicine, 1997. **8**: p. 39-44.

39. Kalachandra, S., et al., *Polymer Materials for Composite Matrices in Biological Environment.* Polymer, 1993. **34(4)**: p. 778-782.

40. Stansbury, J.W., M.C. Kyung, and J.M. Antonucci. *Consideration in the Development of Semi-fluorinated Methacrylate Dental Resins and Composites.* in *Proceedings of the 1997 Las Vegas ACS Meeting.* 1997. Las Vegas, NV, USA: Division of Polymer Chemistry, American Chemical Society.

41. Kawaguchi, M., T. Fukushima, and T. Horibe, *Effect of Monomer Structure on the Mechanical Properties of Light-cured Unfilled Resins.* Dental Materials Journal, 1988. **7(2)**: p. 174-181.

42. Chowdhury, N.A., et al., *Dental application of binary urethane monomer mixtures: strengthened resin matrix.* Journal of Materials Science: Materials in Medicine, 1997. **8**: p. 149-155.

43. Mitra, S.B. *Dental Composites Prepared from Resin Matrices Containing Ethylenically Unsaturated Carbamoyl Isocyanurates.* in *Proceedings of the 1997 Las Vegas ACS Meeting.* 1997. Las Vegas, NV, USA: Division of Polymer Chemistry, American Chemical Society.

44. Culbertson, B.M., Q. Wan, and Y. Tong. *Synthesis, Characterization and Evaluation of New BPA Based Multi-Methacrylates for Dental Composites.* in *Proceedings of the 1997 Las Vegas ACS Meeting.* 1997. Las Vegas, NV, USA: Division of Polymer Chemistry, American Chemical Society.

45. Dulik, D., R. Bernier, and G.M. Brauer, *Effect of Diluent Monomer on the Physical Properties of Bis-GMA-based Composites.* Journal of Dental Research, 1981. **60**(6): p. 983-989.

46. Davy, K.W.M. and M. Braden, *Study of polymeric systems based on 2,2 bis-4(2-hydroxy-3-methacyloyl-oxypropoxy) phenyl propane.* Biomaterials, 1991. **12**(May): p. 406-410.

47. Labella, R., et al., *THFMA in dental monomer systems.* Biomaterials, 1996. **17**(4): p. 431-436.

48. Labella, R., et al., *Monomethacrylate co-monomers for dental resins.* European Journal of Oral Sciences, 1998. **106**: p. 816-824.

49. Patel, M.P. and M. Braden, *Heterocyclic Methacrylates for clinical applications I. Mechanical properties.* Biomaterials, 1991. **12**(September): p. 645-648.

50. Cowperthwaite, G.F., J.J. Foy, and M.A. Malloy, *The Nature of the Cross-linking Matrix Found in Dental composite Filling Materials and Sealants*, in *Biomedical and Dental Applications of Polymers*, C.G. Gebelein and F.F. Koblitz, Editors. 1981, Plenum Press: New York. p. 379.

51. Patel, M.P., M. Braden, and K.W.M. Davy, *Polymerization Shrinkage of Methacrylate Esters.* Biomaterials, 1987. **8**: p. 53-56.

52. Loshaek, S. and T.G. Fox, *Cross-linked Polymers. I. Factors Influencing the Efficiency of Cross-linking in Copolymers on Methyl Methacrylate and Glycol Dimethacrylates.* Journal of the American Chemical Society, 1953. **75**: p. 3544-3550.

53. Bowen, R.L. *Preparation of a Beta-Cyclodextrin Methacrylate.* in *Proceedings of the 1997 Las Vegas ACS Meeting.* 1997. Las Vegas, NV: Division of Polymer Chemistry, American Chemical Society.

54. Kalachandra, S., et al., *Influence of Hydrogen Bonding on Properties of BIS-GMA Analogues.* Journal of Materials Science: Materials in Medicine, 1997. **8**: p. 283-286.

55. Rawls, H.R., et al. *Low Shrinkage Resins From Liquid Crystal Diacrylate Monomers.* in *Proceedings of the 1997 Las Vegas ACS Meeting.* 1997. Las Vegas, NV, USA: Division of Polymer Chemistry, American Chemical Society.

56. Byerley, T.J., et al., *Synthesis and Polymerization of New Expanding Dental Monomers.* Dental Materials, 1992. **8**: p. 345-350.

57. Chappelow, C.C., et al. *Photocured Epoxy/SOC Matrix Resin Systems for Dental Composites.* in *Proceedings of the 1997 Las Vegas ACS Meeting.* 1997. Las Vegas, NV, USA: Division of Polymer Chemistry, American Chemical Society.

58. Millich, F., et al., *Elements of Light-Cured Epoxy-based Dental Polymer Systems.* Journal of Dental Research, 1998. **77**(4): p. 603-608.

59. Moszner, N. and T. Volkel. *Radical Ring-Opening Monomers for Dental Composites*. in *Proceedings of the 1997 Las Vegas ACS Meeting*. 1997. Las Vegas, NV, USA: Division of Polymer Chemistry, American Chemical Society.

60. Miyazaki, K., et al. *Synthesis and Polymerization of Acrylic Monomers with Pendant Spiro Ortho Ester and Cyclic Carbonate Groups*. in *Proceedings of the 1997 Las Vegas ACS Meeting*. 1997. Las Vegas, NV, USA: Division of Polymer Chemistry, American Chemical Society.

61. Yoshida, K., H. Matsumura, and M. Atsuta, *Monomer Composition and Bond Strength of Light Cured 4-META Opaque Resin.* Journal of Dental Research, 1990. **69(3)**(March): p. 849-851.

62. Peutzfeldt, A. and E. Asmussen, *Effect of temperature and duration of post-cure on selected mechanical properties of resin composites containing carboxylic anhydrides.* Scandinavian Journal of Dental Research, 1992. **100**: p. 296-298.

63. Peutzfeldt, A., *Effect of Temperature and Duration of Postcure On in-Vitro Wear and Quantity of Remaining Double-Bonds of Resins Containing Carboxylic Anhydride.* European Journal of Oral Sciences, 1995. **103**(4): p. 259-263.

64. Asmussen, E. and A. Peutzfeldt, *The role of maleic anhydride in adhesive resin cements.* European Journal of Oral Sciences, 1998. **106**: p. 882-886.

65. Ishihara, K. and N. Nakabayashi, *Adhesive bone cement both to bone and metals:4-META in MMA with tri-n-butyl borane.* Journal of Biomedical Materials Research, 1989. **23**: p. 1475-1482.

66. Ishihara, K., et al., *Adhesive bone cement containing hydroxyapatite particle as bone compatible filler.* Journal of Biomedical Materials Research, 1992. **26**: p. 937-945.

67. West, J.K., et al., *Cyclic anhydride ring opening reactions: Theory and application.* Journal of Biomedical Materials Research, 1998. **41**(1): p. 8-17.

68. Zamora, M.P., *Poly(Amide-Grafi-Acrylate) Interfacial Compounds*, in *Materials Science and Engineering*. 1997, University of Florida: Gainesville. p. 185.

69. Bowen, R.L., E.N. Cobb, and J.E. Rapson, *Adhesive Bonding of Various Monomers to Hard Tooth Tissues Improvement in Bond Strength to Dentin.* Journal of Dental Research, 1982. **61**(9): p. 1070-1076.

70. Bowen, R.L., et al., *New Surface-active comonomer for Adhesive Bonding.* Journal of Dental Research, 1996. **75**(1): p. 606-610.

71. Kalachandra, S. and R.P. Kusy, *Comparison of water sorption by methacrylate and dimethacrylate monomers and their corresponding polymers.* Polymer, 1991. **32**(13): p. 2428-2434.

72. Soderholm, K.-J., *Water sorption in a bis(GMA)/TEGDMA resin.* Journal of Biomedical Materials Research, 1984. **18**: p. 271-279.

73. Turner, D.T. and A.K. Abell, *Water sorption of Poyl(methyl methacrylate): 2. Effects of crosslinks.* Polymer, 1987. **28**: p. 297-302.

74. Miller, J.B., J.H. Walton, and C.M. Roland, *The NMR Chemical Shift of Xenon-129 Dissolved in Polymers.* Macromolecules, 1993. **26**(21): p. 5602-5610.

75. Sefcik, M.D., et al. *Effects of Sorbed Gases on the Molecular Dynamics and Structure of Glassy Polymers.* in *Polymer Preprints.* 1983: American Chemical Society, Divsion of Polymer Chemistry.

76. Stengle, T.R. and K.L. Williamson, *Nuclear Magnetic Resonance of Xenon Absorbed in Solid Polymers: A Probe of the Amorphous State.* Macromolecules, 1987. **20**: p. 1428-1430.

77. Kentgens, A.P.M., et al., *Line-Broading Effects for ^{129}Xe Absorbed in the Amorphous State of Solid Polymers.* Macromolecules, 1991. **24**: p. 3712-3714.

78. Kennedy, G.J., *^{129}Xe NMR as a probe of the effect of crosslinking on the amorphous phase structure of solid polymer.* Polymer Bulletin, 1990. **23**: p. 605-608.

79. Walton, J.H., *A Review of ^{129}Xe NMR as a Probe of Polymer Morphology.* Polymers and Polymer Composites, 1994. **2**(1): p. 35-41.

80. Chu, P.J., et al. . in *International Symposium on Solid State NMR Spectroscopy of Polymers.* 1993. Keystone, CO.

81. Morgan, D.R., E.O. Stejskal, and A.L. Andrady, *^{129}Xe NMR Investigation of the Free Volume in Dendritic and Cross-Linked Polymers.* Macromolecules, 1999. **32**(6): p. 1897-1903.

82. Tomaselli, M., et al., *Probing Microheterogeneity in Polymer Systems Via Two-Dimensional $^{129}Xenon$ NMR Spy Detection. A Heterogeneous Model Blend System.* Chemical Physics Letters, 1993. **205**(2,3): p. 145-152.

83. Mansfeld, M. and W.S. Veeman, *^{1}H-^{129}Xe double resonance NMR in a polymer blend.* Chemical Physics Letters, 1994. **222**(27 May): p. 422-424.

84. Walton, J.H., J.B. Miller, and C.M. Roland, *^{129}Xe NMR as a Probe of Polymer Blends.* Journal of Applied Polymer : Part B: Polymer Physics, 1992. **30**: p. 527-532.

85. Mirabella, F.M.J. and D.C. McFaddin, *^{129}Xe NMR Spectroscopic Characterization of Multiphase Polypropylene Copolymers.* Polymer, 1996. **37**(6): p. 931-938.

86. Junker, F. and W.S. Veeman, *Xenon Self-Diffusion on Organic Polymers by Pulsed Field Gradient NMR Spectroscopy.* Macromolecules, 1998. **31**: p. 7010-7013.

87. Schantz, S. and W.S. Veeman, *NanoHeterogeneity in PEO/PMMA Blends Probed.* Journal of Polymer Science, Part B: Polymer Physics, 1997. **35**: p. 2681-2688.

88. Walton, J.H., et al., *Phase Transitions in Polymer Blends via ^{129}Xe NMR Spectroscopy.* Macromolecules, 1993. **26**(15): p. 4052-4054.

89. Brownstein, S.K., J.E.L. Roovers, and D.J. Worsfold, *^{129}Xe Line widths in Block Copolymers.* Magnetic Resonance in Chemistry, 1988. **26**: p. 392-393.

90. Stejskal, E.O. and J.E. Tanner, *Spin Diffusion Measurements: Spin Echoes in the Presence of a Time-Dependent Field Gradient.* Journal of Chemical Physics, 1965. **42**(1): p. 288-292.

91. Whiting, R. and P.H. Jacobsen, *Dynamic Mechanical Properties of Resin-based Filling Materials.* Journal of Dental Research, 1980. **59(1)**(January): p. 55-60.

92. Wilson, T.W. and D.T. Turner, *Characterization of Polydimethacrylates and Their Composites by Dynamic Mechanical Analysis.* Journal of Dental Research, 1987. **66(5)**: p. 1032-1035.

93. Clarke, R.L., *Dynamic mechanical thermal analysis of dental polymers II. Bis-phenol A-related resins.* Biomaterials, 1989. **10**(October): p. 549-552.

94. Wilson, T.W., *Multiple Transitions in a Dimethacrylate Network.* Journal of Applied Polymer Science, 1990. **40**: p. 1195-1208.

95. Allen, P.E.M., et al., *Dynamic-Mechanical Properties and Cross-Polarized, Proton-Enhanced, Magic Angle Spinning ^{13}C NMR Time Constants of*

Poly[oligo(ethylene glycol) dimethacrylates]. Macromolecules, 1989. **22**: p. 809-816.

96. McCrum, N.G., B.E. Read, and G. Williams, *Anelastic and Dielectric Effects in Polymeric Solids*. 1991, New York: Dover Publications Inc. 617.

97. Nichetti, D. and I. Manas-Zloczower, *Viscosity model for polydisperse polymer melts*. Journal of Rheology, 1998. **42**(4): p. 951-969.

98. Plangsangmas, L., *Determination of Fracture Toughness of Epoxy Using Fractography*. Journal of Applied Polymer Science, 1998. **72**: p. 257-268.

99. Mehlem, J.J., *The Influence of Nadic Methyl Anydride on Mechanical and Thermomechanical Properties of Dental Resins and Composites*, in *Materials Science and Engineering*. 1999, University of Florida: Gainesville. p. 115.

100. Nomoto, R. and T. Hirasawa, *Residual Monomer and Pendant Methacryloyl Group in Light-cured Composite Resins*. Dental Materials Journal, 1992. **11(2)**: p. 177-188.

101. Allcock, H.R. and F.W. Lampe, *Contemporary Polymer Chemistry*. Second ed. 1990, Englewood Cliffs: Prentice-Hall, Inc. 624.

102. Ferracane, J.L., *Fourier Transform Infrared Analysis of Degree of Polymerization in Unfilled Resins-Methods Comparison*. Journal of Dental Research, 1984. **63(8)**(August): p. 1093-1095.

103. Asmussen, E., *Factors affecting the quantity of remaining double bonds in restorative resin polymers*. Scandinavian Journal of Dental Research, 1982. **90**: p. 490-496.

104. Ruyter, E.I. and S.A. Svendsen, *Remaining methacrylate groups in composite restorative materials*. Acta Odontol. Scand., 1977. **36**: p. 75-82.

105. Rueggeberg, F.A., D.T. Hashinger, and C.W. Fairhurst, *Calibration of FTIR conversion analysis of contemporary dental resin composites*. Dental Materials, 1990. **6**(October): p. 241-249.

106. Bastioli, C., G. Romano, and C. Migliaresi, *Water sorption and mechanical properties of dental composites*. Biomaterials, 1990. **11**(April): p. 219-223.

107. Soderholm, K.-J.M. and M.J. Roberts, *Influence of Water Exposure on the Tensile Strength of Composites*. Journal of Dental Research, 1989. **69(12)**: p. 1812-1816.

108. Kloosterboer, J.G. and G.F.C.M. Lijten, *Photopolymers exhibiting a large difference between glass transition and curing temperatures.* Polymer, 1990. **31**(January): p. 95-101.

109. Floudas, G., G. Fytas, and E.W. Fischer, *Relaxation Porcesses in a Poly(cyclohexyl methacrylate)/Additive System As Studied by Photon Correlation, Dielectric Relaxation, and Mechanical Relaxation Spectroscopy.* Macromolecules, 1991. **24**(8): p. 1955-1961.

110. Sperling, L.H., *Introduction to Physical Polymer Science.* Second ed. 1992, New York: John Wiley & Sons. 594.

111. Kannurpatti, A.R., et al., *Kinetic and Mechanistic Studies of Iniferter Photopolymerizations.* Macromolecules, 1996. **29**(23): p. 7310-7315.

112. Simpson, J.H. and H.Y. Carr, *Diffusion and Nuclear Spin Relaxation in Water.* The Physical Review, 1958. **111**(5): p. 1201-1202.

113. Bar, G., et al., *Examination of Butadiene/Styrene-co-butadience Rubber Blends by Tapping Mode Atomic Force Microscopy. Tip-Sample Energy Dissipation in Tapping Mode Atomic Force Microscopy study of Elastomers.* Langmuir, 2000. **16**(13): p. 5702-5711.

114. Bar, G., et al., *Factors Affecting the Height and Phase Images in Tapping Mode Atomic Force Microscopy. Study of Phase-Separated Polymer Blends of Poly(Ethene-co-Styrene) and Poly(2,6-dimethyl-1,4-phenylene oxide).* Langmuir, 1997. **13**(14): p. 3807-3812.

115. Magonov, S.N., V. Elings, and M.-H. Whangbo, *Phase imaging and stiffness in tapping-mode atomic force microscopy.* Surface Science, 1997. **375**: p. L385-L391.

116. Thomann, Y., et al., *Investigation of Morphologies of One- and Two-Phase Belnds of Isotactic Poly(propene) with Random Poly(ethene-co-1-butene).* Macromolecules, 1998. **31**(16): p. 5441-5449.

117. Kajiyama, T., et al., *Imaging of Dynamic Viscoelastic Properties of a Phase-Separated Polymer Surface by Forced Oscillation Atomic Force Microscopy.* Macromolecules, 1994. **227**(26): p. 7932-7934.

118. Leclere, P., et al., *Microdomain Morphology Analysis of Block Copolymers by Atomic Force Microscoy with Phase Detection Imaging.* Langmuir, 1996. **12**(18): p. 4317-4320.

119. Bar, G., et al., *Examination of the relationship between phase shift and energy dissipation in tapping mode atomic force microscopy by frequency-sweep and force probe measurements.* Surface Science, 2000. **444**: p. L11-L16.

120. Bar, G., et al., *Improtance of the indentation depth in tapping-mode atomic force microscopy study of compliant materials.* Applied Physics Letters, 1999. **75**(26): p. 4198-4200.

121. Rosen, S.L., *Fundamental Principles of Polymeric Materials*. 1993, New York: John Wiley and Sons. 420.

122. Stejskal, E.O. and J.D. Memory, *High Resolution NMR in the Solid State*. 1994, New York: Oxford University Press. 189.

123. Stansbury, J.W. and J.M. Antonucci, *Evaluation of Methylene lactone monomers in dental resins.* Dental Materials, 1992. **8**: p. 270-273.

124. Zamora, M., K.B. Wagener, and A.B. Brennan. *Copolymer composites designed to offset polymerization shrinkage in dental composites: I. maleic anhydride*. 1994: Division of Polymer Chemistry, American Chemical Society.

125. Dorkenoo, K.D., P.H. Pfromm, and M.E. Rezac, *Gas Transport Porperties of a Series of High Tg Polynorbornenes with Aliphatic Pendant Groups.* Journal of Polymer Science: Part B: Polymer Physics, 1998. **36**: p. 797-803.

126. Houlihan, F.M., et al., *Synthesis of Cycloolefin-Maleic Anhydride Alternating Copolymer for 193nm Imaging.* Macromolecules, 1997. **30**(21): p. 6517-6524.

BIOGRAPHICAL SKETCH

Jeremy Mehlem was born to John and Sheila Mehlem on the afternoon of October 30, 1972, in Phoenix, Arizona. He grew up in Arizona, with an occasional summer escape to New Jersey to visit relatives. During high school Mehlem was involved in extracurricular activities such as swimming and tennis. While in high school, he also developed interests in mountain biking and windsurfing, despite the desert's arid climate.

After graduating from high school in 1990, Mehlem attended the University of Arizona, in Tucson, graduating with a Bachelor of Science degree in materials science and engineering in December of 1994.

After travel in Mexico and the Pacific Northwest, Mehlem began graduate studies at the University of Florida in 1995. Unaware that Mehlem's father was a dentist, Dr. Anthony Brennan introduced Mehlem to research in dental materials, the subject of his master's thesis and this dissertation. He married Ms. Kacy Gapinski in November of 1999. Upon graduating he will begin work with Michelin in Greenville, South Carolina.

I certify that I have read this study and that in my opinion it conforms to acceptable standards of scholarly presentation and is fully adequate, in scope and quality, as a dissertation for the degree of Doctor of Philosophy.

Dr. Anthony Brennan, Chairman
Associate Professor of Materials Science and Engineering

I certify that I have read this study and that in my opinion it conforms to acceptable standards of scholarly presentation and is fully adequate, in scope and quality, as a dissertation for the degree of Doctor of Philosophy

Dr. Christopher Batich
Professor of Materials Science and Engineering

I certify that I have read this study and that in my opinion it conforms to acceptable standards of scholarly presentation and is fully adequate, in scope and quality, as a dissertation for the degree of Doctor of Philosophy.

Dr. Elliot Douglas
Assistant Professor of Materials Science and Engineering

I certify that I have read this study and that in my opinion it conforms to acceptable standards of scholarly presentation and is fully adequate, in scope and quality, as a dissertation for the degree of Doctor of Philosophy.

Dr. Ronald Baney
Associate Engineer of Materials Science and Engineering

I certify that I have read this study and that in my opinion it conforms to acceptable standards of scholarly presentation and is fully adequate, in scope and quality, as a dissertation for the degree of Doctor of Philosophy.

Dr. Kenneth Wagener
Professor of Chemistry

This dissertation was submitted to the Graduate Faculty of the College of Engineering and to the Graduate School and was accepted as partial fulfillment of the requirements for the degree of Doctor of Philosophy.

May 2001

M. J. Ohanian
Dean, College of Engineering

Winfred M. Phillips
Dean, Graduate School